



# UNIVERSITAT DE BARCELONA

Final Degree Project

**Biomedical Engineering Degree**

**Design of colon phantoms and a colon phantom motorized measuring system to verify the operation of a microwave-based diagnostic device**

Barcelona, 7th June 2023

Author: Júlia Torras Amat

Director/s: Marta Guardiola

Tutor: Gloria Fernández



---

## Abstract

Microwave imaging (MWI) is an emerging medical imaging technique with promising biomedical applications. In line with this research area, MiWEndo Solutions is a spinoff devoted to the development of a MWI device for colorectal cancer diagnosis called MiWEndo, which is attached to the regular colonoscope. Before its actual commercialization, a fundamental step towards the validation of the MiWEndo prototype is the design of realistic colon tissue-mimicking phantoms. Such phantoms allow the assessment of the imaging system performance under well controlled and reproducible conditions.

In this thesis, a new, simple, and highly reproducible phantom recipe based on polyvinylpyrrolidone (PVP) has been developed to mimic healthy colon mucosa. Moreover, a comparative study between the currently used oil-based phantom recipe and the new PVP phantom has been conducted to assess the lifespan and stability of each type of fabricated phantom. It has been concluded that PVP phantoms must be conserved in the fridge for increased stability. With this conservation protocol, the PVP recipe shows a similar lifespan as the oil-based one. Nevertheless, due to both the limited number of samples and time, further studies must be carried out to conclusively determine the recipe with larger stability.

Furthermore, a colon phantom motorized measuring system has been designed to improve repeatability and reliability in the measurements of the phantoms. The system consists of an XYZ motorized positioning system, an Arduino Nano, stepper motor drivers and Arduino IDE firmware. Even though further improvements will be required once implemented, a first conception of a system that fulfils the established requirements has been obtained, based on reasonable-cost and simple-implementation components. Besides, a successful proof of concept of the measuring system has been carried out, concluding that a further implementation of the system seems viable.

**Keywords:** Microwave imaging, colorectal cancer, imaging phantoms, polyvinylpyrrolidone, phantom motorized measuring system.

## Acknowledgments

I would like to express my deepest gratitude to all those who have supported me throughout the journey of completing this bachelor thesis.

First and foremost, I am immensely grateful to my director, Dr. Marta Guardiola. Her guidance, expertise, and invaluable insights throughout the research process have been crucial for the elaboration of this thesis. I specially thank her constant encouragement, and constructive feedback.

Furthermore, I would also like to extend my gratitude to my tutor, Dr. Gloria Fernandez, along with all the members of MiWEndo Solutions' team, which have offered me help and advice during the elaboration of the project. They have created a supportive and conducive work environment, which has not only eased my research but also enhanced my overall professional growth.

Finally, I want to express my gratitude to my friends and family for their unwavering belief in me and their encouragement throughout all these four years. Their words of support and motivation have been a constant source of strength during moments of doubt and fatigue.

## List of figures

Figure 1. Flux diagram of the general methodology followed to develop the project .....	13
Figure 2. MiWEndo's microwave endoscopy system is composed by an accessory attachable at the distal tip of a standard colonoscope .....	17
Figure 3. MiWEndo prototype setup .....	18
Figure 4. Dielectric properties (relative permittivity and conductivity) of colon tissues.....	18
Figure 5. Table of the dielectric properties (relative permittivity and conductivity) of colon tissues: adenocarcinoma (ACA), adenoma with high-grade dysplasia (A-HGD), adenoma with low-grade dysplasia (A-LGD), and hyperplastic polyps (HP), for different frequencies .....	19
Figure 6. Evolution of a breast oil-in-water mixture phantom versus time: the day of its manufacturing (left) and 3 months later (right).....	21
Figure 7. Homogeneous anthropomorphic head phantom (left); heterogeneous anthropomorphic breast phantom (right) .....	22
Figure 8. Summary of some breast microwave imaging systems with their main features .....	23
Figure 9. MiWEndo measurements set-up.....	25
Figure 10. Incidence of colorectal cancer in 2017-2031 in the seven leading market countries .....	26
Figure 11. Plot of the growth of the medical imaging phantoms market during 2017-2027 .....	27
Figure 12. Number of imaging phantom publications in PubMed during 1970-2020. ....	28
Figure 13. Colonoscope Training Model from Kyoto Kagaku (left) and Kroton Kolono Colonoscopy Trainer from Kroton Medical Technology (right).....	28
Figure 14. First successful endoscope, Lichtleiter, (left); first gastroscope (right) .....	29
Figure 15. Colonoscopy historical milestones.....	30
Figure 16. Imaging phantom's historical evolution .....	31
Figure 17. Arduino UNO board .....	39
Figure 18. Arduino Nano board.....	40
Figure 19. FMC4030 controller .....	40
Figure 20. Arduino IDE software layout .....	41
Figure 21. FMC4030 Software layout .....	41
Figure 22. Simplified schematic of the implemented automated measuring system with the selected components .....	43
Figure 23. The 3 produced phantoms, from left to right: PVP phantom left at room T, PVP phantom preserved at the fridge and oil-based phantom. ....	47
Figure 24. Setup for dielectric properties measurements .....	48
Figure 25. Automated measuring system design with AutoCAD .....	49
Figure 26. Electronics schematics of the automated measuring system .....	50
Figure 27. Pinout configuration of Arduino Nano for Grbl firmware.....	51
Figure 28. Header file to tune pinout configuration in the Arduino Nano .....	51
Figure 29. Example of some of the parameters that may be used to configure Grbl for the proposed system. ....	52
Figure 30. Diagram of the sent signals between the firmware and the hardware of the automated measuring system .....	52
Figure 31. Plots of the relative permittivity (top) and conductivity (bottom) measurements throughout time of the three phantoms.....	56
Figure 32. Plot of the hardness measurements evolution for the 3 phantoms .....	57
Figure 33. Images of the oil-based phantom (left), Room T PVP phantom (middle) and Fridge PVP phantom (right), after the first measurement.....	57

---

Figure 34. Images of the oil-based phantom (left), Room T PVP phantom (middle) and Fridge PVP phantom (right), after the last measurement. ....	58
Figure 35. Water formation under oil-based phantom on day 25/05/2023. ....	58
Figure 36. Schematic of the proof of concept. ....	59
Figure 37. Proof of concept setup. ....	60
Figure 38. WBS of the project. ....	65
Figure 39. PERT-CPM diagram. ....	71
Figure 40. GANTT diagram. ....	72
Figure 41. Schematic of a medical device's lifecycle. ....	73

## List of tables

Table 1. CRC five-year survival rates, by stage at diagnosis.....	16
Table 2. Summary of some phantoms used at MiWEndo Solutions for MiWEndo device validation. ....	24
Table 3. Main advantages and disadvantages of liquid and gel phantom consistencies .....	34
Table 4. Main advantages and disadvantages of simple-shaped and anthropomorphic phantom geometries .....	35
Table 5. Main advantages and disadvantages of homogeneous and heterogeneous phantoms. ....	36
Table 6. Main characteristics of the Iqus, Fuyu and Toseastars XYZ motorized positioning systems. ....	38
Table 7. Main characteristics of the stepper motor drivers considered.....	39
Table 8. Dielectric properties of water and PVP mixtures for increasing PVP concentrations.....	44
Table 9. Dielectric properties of water, PVP and agar mixtures for increasing 25, 30 and 35% PVP concentrations. ....	45
Table 10. Plots of the relative permittivity measurements (left axis) and temperature (right axis) throughout time of the oil-based phantom (top), room T-conserved PVP phantom (middle), and fridge-conserved PVP phantom (bottom).....	53
Table 11. Plots of the conductivity measurements (left axis) and temperature (right axis) throughout time of the oil-based phantom (top), room T-conserved PVP phantom (middle), and fridge-conserved PVP phantom (bottom). ....	55
Table 12. SWOT analysis of the project .....	61
Table 13. Direct costs of the project. ....	63
Table 14. Approximation of the total cost of the project.....	64
Table 15. WBS dictionary of the task 1.Documentation.....	66
Table 16. WBS dictionary of the task 2.Photoms.....	67
Table 17. WBS dictionary of the task 3.Automated measuring system.....	68
Table 18. WBS dictionary of the task 4.Experimental validation.....	69
Table 19. WBS dictionary of the task 5.Completion of the project.....	70
Table 20. Collection of the chronological dependencies of the activities with their respective ID and duration .....	70

---

## Glossary of abbreviations

CRC	Colorectal cancer
MWI	Microwave imaging
PVP	Polyvinylpyrrolidone
AI	Artificial Intelligence
VNA	Vector network analyzer
CNC	Computer numerical control
WBS	Work Breakdown Structure
PERT-CPM	Program Evaluation and Review Technique with its Critical Path Method
SWOT	Strengths, Weaknesses, Opportunities and Threats
MDR	Medical device regulation
QMS	Quality management system
EMA	European Medicines Agency



## Table of contents

<b>1. INTRODUCTION</b> .....	11
<b>1.1. Motivation and aim of the project</b> .....	11
<b>1.2. Objectives</b> .....	12
<b>1.3. Structure and methodology</b> .....	12
<b>1.4. Limitations and scope</b> .....	14
<b>1.5. Location of the project</b> .....	15
<b>2. BACKGROUND</b> .....	16
<b>2.1. General concepts</b> .....	16
2.1.1. <i>Colorectal cancer</i> .....	16
2.1.2. <i>MiWEndo Solutions</i> .....	17
2.1.3. <i>Dielectric properties of biological tissues</i> .....	19
2.1.4. <i>Imaging phantoms</i> .....	20
<b>2.2. State of the art</b> .....	21
2.2.1. <i>Phantoms for MWI</i> .....	21
2.2.2. <i>Motorized MWI systems</i> .....	22
<b>2.3. State of the situation</b> .....	24
<b>3. MARKET ANALYSIS</b> .....	26
<b>3.1. Market sector</b> .....	26
3.1.1. <i>Colonoscopy tools market</i> .....	26
3.1.2. <i>Imaging phantoms market</i> .....	27
<b>3.2. Historical evolution</b> .....	28
3.2.1. <i>Historical evolution of colonoscopy</i> .....	28
3.2.2. <i>Historical evolution of imaging phantoms</i> .....	30
<b>3.3. Future perspectives</b> .....	31
3.3.1. <i>Future perspectives of the colonoscopy market</i> .....	31
3.3.2. <i>Future perspectives of the imaging phantoms market</i> .....	32
3.3.3. <i>Future applications of the technology developed in this project</i> .....	32
<b>4. CONCEPTION ENGINEERING</b> .....	34
<b>4.1. Phantom recipe</b> .....	34
4.1.1. <i>Consistency</i> .....	34
4.1.2. <i>Geometry</i> .....	35
4.1.3. <i>Homogeneity</i> .....	36
<b>4.2. Automated measuring system</b> .....	37
4.2.1. <i>XYZ motorized positioning system</i> .....	37

---

4.2.2. Stepper motor driver .....	38
4.2.3. Controller.....	39
4.2.4. Firmware .....	40
<b>4.3. Selected solution.....</b>	<b>41</b>
4.3.1. Phantoms .....	41
4.3.2. Automated measuring system.....	42
<b>5. DETAILED ENGINEERING .....</b>	<b>44</b>
<b>5.1. Phantoms .....</b>	<b>44</b>
5.1.1. Ingredient concentration assessment.....	44
5.1.2. New developed phantom recipe.....	46
5.1.3. Phantom experimental work.....	47
<b>5.2. Automated measuring system .....</b>	<b>48</b>
5.2.1. CAD design .....	48
5.2.2. Electronics.....	49
5.2.3. Firmware .....	51
<b>5.3. Results and discussion .....</b>	<b>52</b>
5.3.1. Phantoms comparative study.....	53
5.3.2. Proof of concept of the automated measuring system .....	59
<b>6. TECHNICAL VIABILITY: SWOT ANALYSIS.....</b>	<b>61</b>
<b>7. ECONOMIC VIABILITY .....</b>	<b>63</b>
<b>8. EXECUTION SCHEDULE .....</b>	<b>65</b>
8.1. Work Breakdown Structure (WBS).....	65
8.2. PERT-CPM diagram.....	70
8.3. GANTT diagram .....	72
<b>9. LEGISLATION AND REGULATION .....</b>	<b>73</b>
<b>10. CONCLUSIONS .....</b>	<b>75</b>
10.1. Future work.....	76
<b>11. BIBLIOGRAPHY .....</b>	<b>77</b>
<b>ANNEXES .....</b>	<b>82</b>

---

---

## 1. INTRODUCTION

This first introductory section presents the purpose of the thesis and the motivation that has led to its development. Other essential aspects of the work are also included, such as the methodology used, the structure of the report, as well as the scope and limitations of the project itself.

### 1.1. Motivation and aim of the project

With almost 2 million new cases and 1 million deaths globally in 2020, colorectal cancer (CRC) is the third most commonly diagnosed and the second most lethal malignancy. Thus, CRC has become a huge burden to global health, especially in countries with a westernized lifestyle. [1, 2]

The tumor stage at the time of diagnosis plays a major role in patient survival. The overall 5-year survival of CRC patients is close to 65%; 5-year survival rates range from 90% for patients with localized disease to 70% and 13% for regional and distant stages, respectively. Furthermore, differently from many cancers, CRC can be prevented and potentially cured if early-stage tumors and high-risk adenomas are removed. Thus, since CRC is mostly asymptomatic until it progresses to advanced stages, the implementation of screening programs for early detection is essential to reduce incidence and mortality rates. [3]

There are several screening tests for CRC but, as of now, colonoscopy is considered the most effective method for detecting CRC, even allowing the retrieval of tissue samples (e.g. polyps) for posterior histological analysis. Nonetheless, visual limitations of the optical camera located at the end of the endoscope result in an estimated 22% of polyps going undetected [4]. Besides, inadequate bowel preparation before the examination or the fact that colonoscopy is a technique where the degree of expertise of the endoscopist plays a significant role, are other causes of polyp misdiagnosis. All these limitations of the technique result in an 8% of the CRCs getting detected after a negative colonoscopy. [5]

This context has urged the development of new approaches to solve the drawbacks of colonoscopy. Microwave imaging seems promising as a complementary technique to conventional colonoscopy, as it can enhance both the detection rate of polyps and the classification of tissue in situ. Unlike conventional colonoscopy, microwaves can generate images without any limitation of the field of view (360°) and offer a reasonable balance between resolution and penetration through light opaque tissue. Consequently, it may potentially overcome the visualization difficulties encountered in conventional colonoscopy. Moreover, focusing on their dielectric properties, microwaves can quantitatively distinguish between normal and abnormal tissues. [6, 7]

MiWEndo Solutions is a spinoff that aims to combine conventional optical endoscopy with microwave imaging (MWI). To do so, it has developed MiWEndo, a medical device that integrates microwave technology with colonoscopy in order to improve the prevention and diagnosis of CRC. [8] A fundamental step towards the development and testing of the MiWEndo prototype is the design of realistic colon tissue-mimicking phantoms. Such phantoms allow the assessment of the imaging system performance under well controlled and reproducible conditions. [9]

Thereby, this project aims to test a new, easy to produce, non-toxic and stable-over-time recipe for colon phantoms and compare it to the current used one [9]. At the same time, an automatic setup to perform repeatable measurements of the phantom with the MiWEndo prototype will be designed, detailing all its different components, and characterizing their implementation.

## 1.2. Objectives

The main objective of this bachelor final thesis is to design colon phantoms and a colon phantom motorized measuring system to verify the operation of a microwave-based diagnostic device by performing repeatable measurements. To achieve this final goal, the project has been divided into two parts with their own principal objectives.

The first subproject will aim to design and test a new, easy to produce and stable-over-time recipe for colon phantoms. To achieve this, the following secondary objectives have to be fulfilled:

1. Develop the new colon phantom recipe by studying the most suitable concentrations of each component and establishing the correct fabrication protocol.
2. Define several parameters to monitor its stability over time.
3. Measure and register periodically the different established parameters to monitor the stability over time.
4. Compare the stability and conservation of the new and the currently-used phantom recipes.

In parallel, the second part of the project has the final goal of designing and implementing an automated phantom measurement system with motors to move the MiWEndo device, so that stable and repeatable measurements can be obtained. To do so, several objectives have been established:

1. Determine the appropriate technical requirements that the automated system must have.
2. Design the automatized measurement system that fulfills the established requirements.
3. Identify and purchase the required and most optimal elements for the equipment.
4. Characterize the implementation and integration of the different components of the automated system including the software to control it.
5. Perform a proof of concept of the designed measuring system.

## 1.3. Structure and methodology

In this section, the strategy followed by the author in order to achieve the final goal of the project has been detailed in the following diagram:

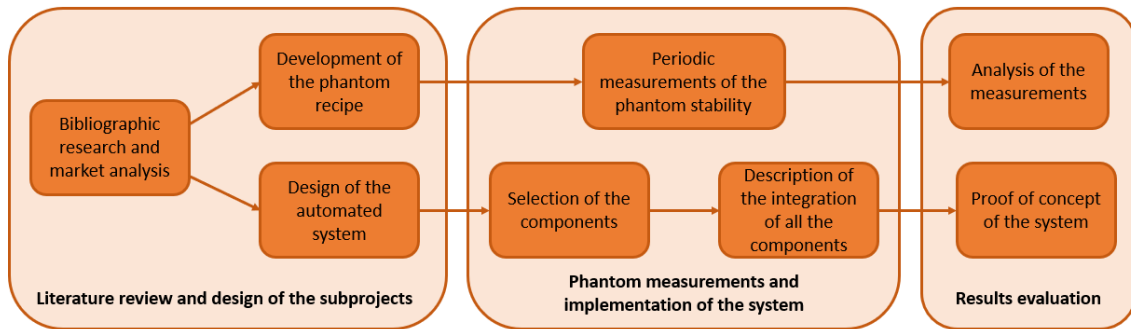


Figure 1. Flux diagram of the general methodology followed to develop the project.

The project consists of three main phases. Initially, a comprehensive review of existing literature and state-of-the-art research was conducted to provide a foundation for designing the new phantom recipe and the automated MWI measuring system. Subsequently, periodic measurements of phantoms were performed to gather data on their preservation and stability. Simultaneously, the selection of the most adequate components for the measuring system was performed, along with the detailed description of the implementation of the measuring setup, including both hardware and software components, was carried out. Finally, the data obtained from the different phantoms will be analyzed to draw up conclusions, and a proof of concept of the system will be performed.

The whole project has been executed between January 2023 and June 2023. The initial phase encompassed literature research, analysis of the state of the art, and market assessment, which was conducted in January and February. Subsequently, laboratory work and report writing were conducted in parallel throughout the remaining months.

A further and more detailed explanation on the execution plan and timeline of the project can be checked at section 8. *Execution schedule*.

In terms of the report of this final bachelor project, it has been divided into eleven main sections. The first one is the introduction devoted to explaining the context in which the project is embedded and its motivation, as well as describing the main objectives, scope and limitations. Section 2 includes the primary concepts surrounding microwave imaging and phantoms, the state of the art on advanced colonoscopy methods, MWI phantoms and automated measuring systems, along with the state of the situation of the processes conducted at MiWEndo that the author aims to improve with her project. A market analysis and a study of the possible solutions to be developed are also performed in sections 3 and 4, respectively. The methodology of the lab work performed has been described in the detailed engineering section (section 5), with the main obtained results displayed and discussed in the last subsection. To ascertain its feasibility, sections 6 and 7 have been written in which both the project's technical and economic viability have been assessed. With the aim of studying the timeline and organizing the project, the WBS and GANTT diagram have been elaborated upon chapter 8. An assessment of the legislative and regulatory framework pertaining to the impact of in vitro chips has been conducted in section 9. The conclusions of the project have been discussed in chapter 10, where the future work has also been commented on. Finally, a bibliographic section has been added where all the sources of information are displayed.

---

## 1.4. Limitations and scope

The scope of this final degree project includes the following stages:

- Conducting a literature review on automated microwave imaging (MWI) measurement setups and MWI phantoms.
- Formulating a recipe based on the polymer polyvinylpyrrolidone (PVP) for fabricating phantoms with the desired dielectric properties.
- Monitoring the preservation of the newly developed phantoms and comparing them to the currently utilized recipe.
- Analyzing the obtained results to determine the recipe that exhibits more stability over time.
- Designing, procuring, and selecting the necessary components for an automated MWI system, incorporating motors.
- Describing the implementation and integration of the different components of the automated measuring system.
- Studying the capability of the setup to perform automated and reproducible measurements and performing a proof of concept of the final design.

Nevertheless, owing to the intrinsic characteristics of the final degree project and the author's resource constraints, this work exhibits noteworthy limitations that must be contemplated and discussed:

- Time is the most notorious limitation since the duration of the totality of the project is less than 6 months. Thus, this has posed a significant limitation across various aspects of the project. Primarily, in terms of evaluating the monitored variables of the phantoms, the measurements have only been conducted during two months. In order to obtain more meaningful and conclusive results, these features should be studied over a more extensive timeframe, such as 6 months.

Concerning the acquisition of the various electronic components for the automated setup, the delivery times from different providers are significantly long and, unfortunately, beyond the author's control. Furthermore, due to their elevated cost, the decision to procure these components necessitates approval from the responsible parties of the spin-off. Consequently, this bachelor thesis only focuses on the theoretical conception and implementation of the automated measuring system's hardware and software, since its actual implementation would require a larger time span than six months.

- Furthermore, there is a limitation in evaluating the monitored variables of the phantoms, as the assessment will be carried out using the available resources. This implies that standardized tests like the Rockwell hardness test, which necessitate specialized testing services and entail additional time and cost, will not be utilized to measure the hardness

evolution of the phantoms. Instead, tests will be conducted using the resources accessible for this purpose.

- Due to the lack of information on how to develop polyvinylpyrrolidone-based phantoms with the dielectric properties of colon tissue, a learning curve and several proofs of concept are needed. This has substantially reduced the available time to perform measurements.
- Finally, the elevated cost of CNC-like motorized systems, capable of maneuvering in 3D axes (X, Y and Z) and able to accommodate substantial payloads, pose a significant limitation in the equipment's design and the quest for optimal components.

### 1.5. Location of the project

The entire experimental work pertaining to the presented project was conducted at the MiWEndo Solutions office, located in the center of Barcelona. Regular project development meetings have been carried out periodically with Dr. Marta Guardiola, co-founder of MiWEndo Solutions, both online and in-person at the office. Additionally, remote supervision has been diligently provided by Dr. Glòria Fernández.

## 2. BACKGROUND

Before carrying out the market analysis, it is crucial to provide a comprehensive description of the theoretical framework that underpins this project. That is, acquiring an understanding of colorectal cancer (CRC), comprehending the significance of dielectric properties of biological tissues in the field of microwave imaging (MWI) for medical applications, and recognizing the role of phantoms in validating medical imaging devices such as the one developed by MiWEndo Solutions. In addition, it is also important to study the state of the art of these technologies and the state of the situation, to properly contextualize this work.

### 2.1. General concepts

#### 2.1.1. Colorectal cancer

Colorectal cancer (CRC) refers to cancerous malignancies of the colon and rectum. These cancers are grouped because they are anatomically close, are associated with the same risk factors, share similar etiology and symptoms, and are treated with similar approaches [10]. CRC is the third most common cancer and the second leading cause of cancer-related deaths worldwide. Furthermore, the incidence and mortality of CRC increase with age, with most cases diagnosed in people over the age of 50. The incidence of colorectal cancer also varies by region, with higher rates observed in developed countries. [11]

CRC often arises from polyps, beginning with an aberrant crypt, evolving into a neoplastic precursor lesion (a polyp), and eventually progressing to CRC over an estimated 10-15-year period. Polyps are small tumors that form in the lining of the colon or rectum and can become cancer if left untreated. Although typically asymptomatic, polyps can be detected and removed during routine screening procedures, such as a colonoscopy [11]. Without intervention, CRC can grow and spread to other parts of the body, such as the liver, lungs, or lymph nodes, which can be life-threatening. This progression is typically slow, and at early stages it might not cause noticeable symptoms. Symptoms of CRC may include changes in bowel habits, blood in the stool, abdominal pain, and unintentional weight loss. These symptoms are highly unspecific and may be indicative of other digestive or health issues, which is one cause of misdiagnosis. [11,12]

Regarding the prognosis, the overall five-year survival rate of CRC is approximately 65% [13]. Patient's survival depends on stage at diagnosis, meaning that the sooner it is detected, the higher the survival rate, as it is shown in the table below.

Table 1. CRC five-year survival rates, by stage at diagnosis. [13]

Stage at diagnosis	Description of the stage	Five-year relative survival rate (%)
I-II	Localized (confined to primary site)	89.9
III	Regional (spread to regional lymph nodes)	71.3
IV	Distant (cancer has metastasized)	13.9
n/a	Unknown (unstaged)	35.4



Hence, prevention of CRC is primarily focused on early detection through routine screening and the removal of polyps before they become cancerous. Other preventative measures include maintaining a healthy diet and lifestyle, such as consuming a diet rich in fruits, vegetables, limiting red and processed meats, maintaining a healthy weight, engaging in regular physical activity, avoiding tobacco and excessive alcohol consumption. [11]

For diagnosing colorectal cancer, colonoscopy is the gold standard method. Colonoscopic identification of advanced lesions is relatively straightforward, but early colorectal cancers might appear as very subtle mucosal lesions. It is estimated that 20% of polyps go undetected after an examination [4]. This situation has prompted the development of complementary diagnostic techniques to improve colonoscopy performance, which include improvements in endoscopes and accessory devices that increase mucosal visualization and the implementation of artificial intelligence (AI) algorithms. [5]

### 2.1.2. MiWEndo Solutions

Microwave imaging (MWI) is a technology that uses electromagnetic radiation in the microwave range (most applications employ frequencies between 0.5 and 10 GHz) to gather anatomical and functional data from targets based on changes in their dielectric properties. Due to the non-ionizing nature, low cost, and portability of the device, microwave imaging is arousing a great deal of interest for biomedical applications. Currently, MWI is being used or it is in ongoing research for image-based diagnosis in an extensive number of applications: acute ischemia or cerebral hemorrhage, pulmonary edema, urinary incontinence, osteoporosis, and breast cancer detection. [14]

The purpose of the MiWEndo Solutions spinoff is to integrate microwave imaging with traditional optical endoscopy, specifically with colonoscopy. Dielectric properties, i.e., relative permittivity and conductivity, are biomarkers for a number of diseases, including cancerous tumors. Thus, MiWEndo Solutions aims to use MWI for CRC cancer diagnosis. This is an innovative approach since MWI has never been proposed before for endoscopic applications. [14]

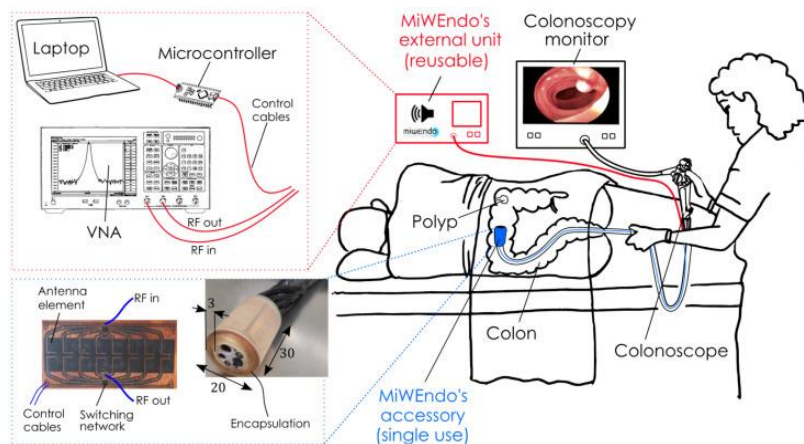


Figure 2. MiWEndo's microwave endoscopy system is composed by an accessory attachable at the distal tip of a standard colonoscope. [15]

A first prototype that integrates MWI into conventional colonoscopy has been developed called MiWEndo. MiWEndo is a class IIa medical device and its technology consists in a ring-shaped switchable antenna array accessory that might be attached to the distal tip of a standard colonoscope and it is connected to an external processing unit (Figure 2, left). During a colonoscopy exploration, MiWEndo provides a field of view inside the colon of 360° and emits an acoustic signal to warn the endoscopist when a polyp is detected (Figure 2, right). This system allows the generation of cross-sectional images of the colon thanks to a frequency-domain microwave imaging reconstruction scheme. [14,15]

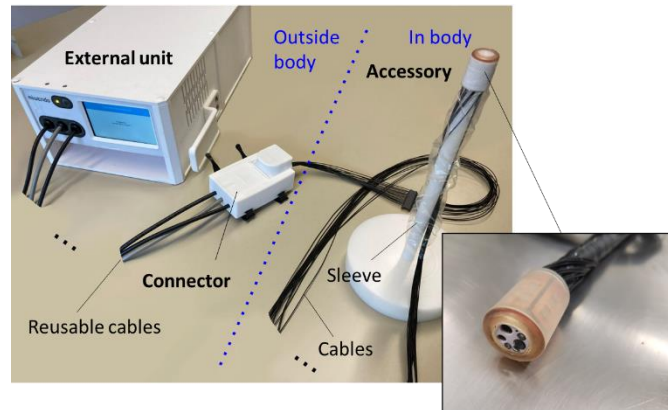


Figure 3. MiWEndo prototype setup. [15]

In addition, MiWEndo prototype generates an external electric field at a frequency of 7.5 GHz, because at this value of frequency the contrast between healthy colon mucosa and colorectal cancer is 30% and 90% for the relative permittivity and conductivity, respectively [14]. This excellent discriminating capabilities might be observed in the graphs of Figure 4: permittivity and conductivity values show the largest difference between benign and malignant tissues at the range of 5-10 GHz.

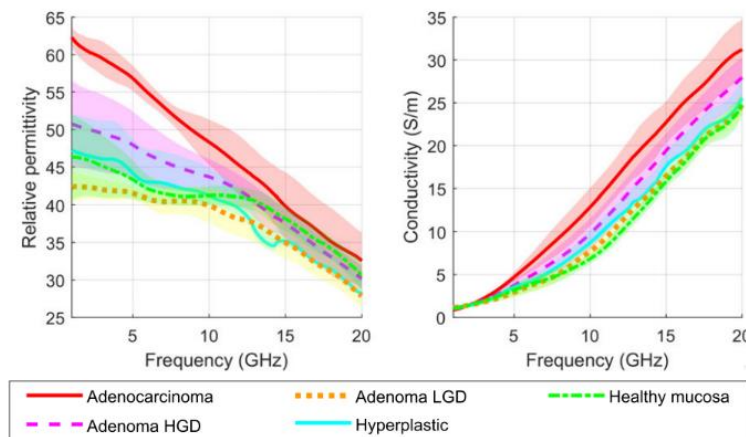


Figure 4. Dielectric properties (relative permittivity and conductivity) of colon tissues. [14]

Before being able to test the MiWEndo prototype with patients, several previous steps of preclinical validation have been performed. Firstly, computational models have been developed for *in silico* validation. Then, a further step has been the development of phantoms with the anatomical and dielectric properties of a human colon with polyps, which allow the realization of reproducible measurements over time, and the obtention of controlled and stable quantifications. Thus, it is of

vital importance the production of easy-to-make, repeatable and stable-in-time colon phantoms that present the desired dielectric properties. [15]

### 2.1.3. Dielectric properties of biological tissues

The dielectric properties or more specifically, the complex permittivity,  $\epsilon(\omega)^*$ , defines how a dielectric material, in this case a tissue, interacts with an external electric field. In the tissue, most of the electrons are bound to the nuclear. When an external electric field is applied, the bound electrons of an atom are displaced such that the centroid of the electronic cloud is separated from the centroid of the nucleus. Hence, an electric dipole is created, and the atom is said to be polarized. This phenomenon is known as **polarization**. The complex permittivity is composed of a real part ( $\epsilon'(\omega)$ ) called the relative permittivity of dielectric constant, and an imaginary part ( $\epsilon''(\omega)$ ). These terms are related in the following way:

$$\epsilon'(\omega)^* = \epsilon'(\omega) - j\epsilon''(\omega) = \epsilon'(\omega) - j \frac{\epsilon''(\omega)}{\omega\epsilon_0} \quad (1)$$

where  $\omega$  is the angular frequency,  $\omega = 2\pi f$ , and  $f$  is the frequency in Hz of the applied external electric field. The relative permittivity expresses the ability of the tissue to store energy from an external electric field, while the imaginary part englobes the dissipative nature of the tissue (absorbs the energy and partially transforms it into heat). This imaginary part is normally expressed in terms of conductivity,  $\sigma(\omega) = \epsilon_0\epsilon''\omega$ , being  $\epsilon_0 = 8.85 \text{ F/m}$  the free space permittivity. [14,16]

The dielectric properties of a biological tissue can be affected by a number of factors, including temperature, pressure, and the frequency of the electric field. In general, the permittivity of a material decreases with increasing frequency, while the conductivity of a material increases with increasing frequency [16]. Furthermore, it has been shown that tumoral processes affect the dielectric properties of the tissue, so that cancerous tissues exhibit different dielectric properties than healthy ones. Such fact allows non-invasive detection and monitoring of the disease, which is the basis of microwave imaging for oncologic applications. [17]

Tissue	4 GHz				5 GHz				6 GHz			
	$\epsilon'_{Sn}$	$\epsilon'_{Sp}$	$\sigma_{Sn}$	$\sigma_{Sp}$	$\epsilon'_{Sn}$	$\epsilon'_{Sp}$	$\sigma_{Sn}$	$\sigma_{Sp}$	$\epsilon'_{Sn}$	$\epsilon'_{Sp}$	$\sigma_{Sn}$	$\sigma_{Sp}$
ACA	100	92.68	100	80.49	100	95.12	100	78.05	100	92.68	100	75.61
A-HGD	81.28	61.76	72.73	58.82	90.91	55.88	72.73	58.82	81.82	55.88	90.91	58.82
A-LGD	90.76	60.61	75.00	39.39	100	60.61	83.33	42.42	91.67	60.61	75.00	39.39
HP	71.43	52.63	100	10.53	100	13.16	100	10.53	100	7.89	100	10.53
Tissue	7 GHz				8 GHz				9 GHz			
	$\epsilon'_{Sn}$	$\epsilon'_{Sp}$	$\sigma_{Sn}$	$\sigma_{Sp}$	$\epsilon'_{Sn}$	$\epsilon'_{Sp}$	$\sigma_{Sn}$	$\sigma_{Sp}$	$\epsilon'_{Sn}$	$\epsilon'_{Sp}$	$\sigma_{Sn}$	$\sigma_{Sp}$
ACA	100	95.12	100	85.37	100	95.12	100	85.37	100	92.68	100	90.24
A-HGD	72.73	61.76	90.91	58.82	81.82	58.82	90.91	58.82	81.81	53.87	90.91	61.76
A-LGD	66.67	60.61	66.67	42.42	91.67	39.39	75.00	45.45	91.67	39.39	66.67	51.52
HP	42.86	26.32	100	10.53	57.14	21.05	100	15.03	57.14	73.68	100	15.03

Figure 5. Table of the dielectric properties (relative permittivity and conductivity) of colon tissues: adenocarcinoma (ACA), adenoma with high-grade dysplasia (A-HGD), adenoma with low-grade dysplasia (A-LGD), and hyperplastic polyps (HP), for different frequencies. [14]

In the specific case of CRC, it has been seen that non-malignant tissues (healthy mucosa, adenomas with low grade dysplasia and hyperplastic polyps) show both lower permittivity and

conductivity than adenomas with HGD, which might be observed in the table from Fig. 5. Hence, the higher the dielectric properties of the tissue, the higher the probability of malignancy. This is consistent with the observation that the water content affects the dielectric characteristics, which rises when the angiogenic switch (increase in vascularization) occurs at an adenoma stage. [14]

#### 2.1.4. *Imaging phantoms*

Imaging phantoms, or simply phantoms, are specially designed objects used to mimic human tissue or organs that are scanned or imaged in the field of medical imaging to validate, analyze, and calibrate the performance of imaging equipment and techniques. Phantom tests instead of in vivo tests with patients, animals or ex vivo tests with cadavers or resected tissues, is more practical and readily available, yields more controlled results, and prevents exposing a live subject to potentially harmful radiation or other imaging-related risks. [18,19]

Phantoms can be made from materials with similar physical, electrical or chemical properties to human tissue, or they can be computer-generated models. The material of choice for building phantoms is crucial to the success of its application, because a phantom used to test a given imaging device should respond similarly to how human tissues and organs would in that particular imaging modality. For instance, phantoms manufactured for 2D radiography may contain different quantities of X-ray contrast agents with characteristics similar to those of normal tissue in terms of X-ray absorption, but the radiography phantom would not necessarily need to have comparable textures or mechanical properties, since these factors are not relevant in X-ray imaging modalities. [18,20]

For the particular case of microwave imaging phantoms, the object of study of this project, their anatomical structure must be close to that of the targeted human body part, and the dielectric properties of their constitutive materials must be similar to that of the biological. Additionally, their shape and dielectric properties must remain stable over time so that the phantom can be used as a benchmark and repeatable measurements can be obtained. [21]

Currently, there is a lack of commercially available phantoms for MWI in the market thus, making it difficult for companies like MiWEndo Solutions to validate their MWI medical devices. As a result, they need to fabricate their own phantoms that mimic the dielectric properties of the specific tissue of study, based on published papers.

Finally, it must be highlighted that phantoms play a vital role in quality assurance and regulatory compliance of medical devices. They provide a means of testing and validating the accuracy and precision of imaging systems, which is critical for ensuring the safety and efficacy of medical imaging in the preclinical validation phase. They also enable the development of new imaging techniques and technologies, as well as the optimization of already existing ones. [22]

## 2.2. State of the art

### 2.2.1. Phantoms for MWI

As aforementioned, when validating, analyzing, or calibrating the performance of MWI equipment or reconstruction algorithms, a controlled, repeatable, economical, and representative assessment procedure must be implemented. Hence, phantoms for MWI are usually the testing method of choice. A realistic tissue-mimicking phantom for MWI has to satisfy mainly three requirements: first, it has to mimic the shape and the dielectric properties of target tissues in a certain frequency range; second, its electromagnetic properties must remain unaltered over time; and third, it is preferable that neither its production nor its preservation require expensive or toxic materials [9,23].

There is a limited number of papers discussing MWI phantom recipes and none of them refer to colonoscopy applications; instead, the majority of the studies try to mimic breast or head tissues. The state of the art in MWI phantoms is reviewed below.

The most commonly used recipes are the oil-in-gelatin-based mixtures. They involve combining gelatin or agar (to solidify the mixture), water and oil (to adjust the dielectric properties), and detergent (to mix water and oil since they are immiscible). The dielectric properties can be fine-tuned by adding other components such as salts so that higher conductivities can be obtained. Furthermore, the amount of jellifying agent can be increased to produce more solid materials that are more suitable to mimic complex-shaped organs. Utilizing molds is an excellent strategy for getting a fair geometrical representation of the body. [9,23,24] Oil-in-gelatin dispersions that have been developed exhibit stable dielectric characteristics for at least 8 weeks. [25] Nevertheless, they are extremely susceptible to environmental exposure, and if they are not properly conserved and sealed, they will desiccate. Besides, a significant variation of the dielectric properties of such mixtures has been observed after a 6-month time lapse. [26]

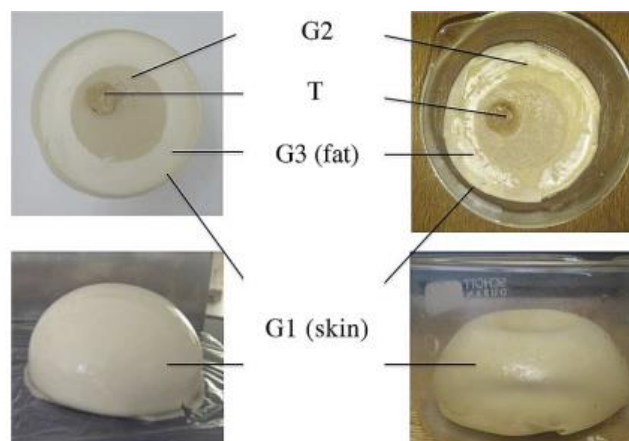


Figure 6. Evolution of a breast oil-in-water mixture phantom versus time: the day of its manufacturing (left) and 3 months later (right). [26]

Other papers [24,27] have developed similar recipes but using polymers such as polyvinylpyrrolidone (PVP) powder or polyvinyl alcohol cryogel, instead of oil and detergent. In some phantoms, they also add formalin as a conservation method. The resulting polymer-based phantoms have high structural rigidity, indefinite longevity, since they are inorganic, and are more

resistant to crack formation in comparison to gelatin-based phantoms. Nonetheless, they are prone to dry out.

Apart from gels, there are liquid phantoms that use liquid mixtures based upon surfactants such as Triton X-100 and salted water solutions. Liquid phantom preparation is simple because the dielectric properties only depend on the proportion of 2 materials, Triton X-100 and salt. Nevertheless, liquid phantoms are contained in molds that simulate geometries of the target organ, but this container cannot be removed unlike gel phantoms; hence, the overall dielectric properties are affected by the presence of the mold. [23,28]

In terms of geometries, phantoms might be molded into simple structures like cylinders, spheres or cubes for preliminary validations, or they can be the so-called anthropomorphic phantoms: phantoms designed to replicate the shape and size of human organs or tissues to simulate realistic imaging scenarios. Additionally, the widespread use of 3D printers has made the creation of molds considerably simpler. By utilizing 3D scans, provided by magnetic resonance imaging or X-ray computed tomography, of actual patients from hospitals, realistic models can be obtained. [23,29]

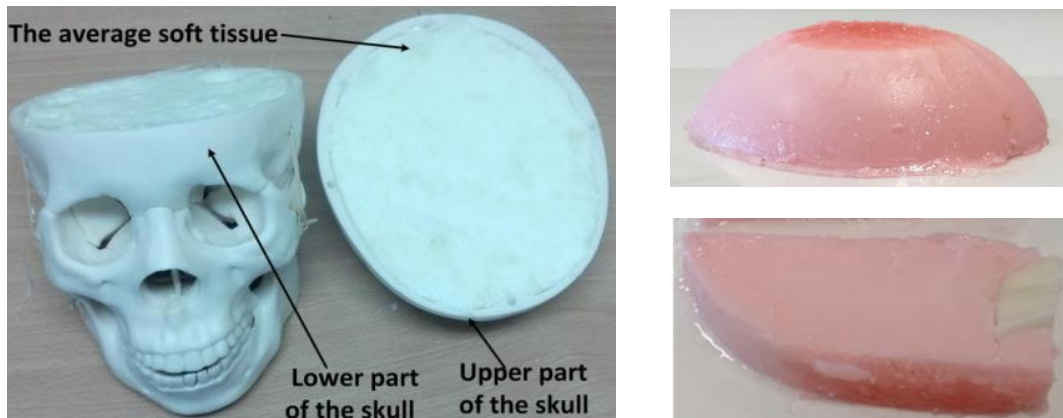


Figure 7. Homogeneous anthropomorphic head phantom (left); heterogeneous anthropomorphic breast phantom (right). [9,30]

Finally, in terms of composition, phantoms might be homogeneous, made of materials with uniform dielectric properties, they are easy to manufacture and can be used to validate the performance of imaging systems; however, they do not provide realistic measurements and do not accurately reflect the behavior of human tissues. On the other hand, heterogeneous phantoms are made of materials that mimic the dielectric properties of different tissues, they are more realistic and can be used to test the imaging systems' ability to distinguish between different tissue types. [9]

Each type of phantom has its advantages and limitations and may be more suitable for certain applications than others. The choice of phantom will depend on the specific requirements of the imaging system being tested and the clinical application for which it is intended.

### 2.2.2. Motorized MWI systems

In the field of MWI, the sector with more on-going research and development is breast cancer imaging. Different systems have been developed that present different solutions in terms of scan

time, position in which the patient is examined, type of antenna used... In MWI systems, motorized solutions can be used for two purposes: for creating a synthetic array or for moving the object under test. Three different kinds of MWI arrays exist:

- *Hardware arrays*, which do not involve moving individual antennas but allow the entire array to be rotated for repeated scanning and artifact removal.
- *Stationary arrays*, which have no moving parts, simplifying the system mechanically.
- *Synthetic arrays*, which involve moving the transmitting antennas, receiving antennas, or both during the patient scan to create a complete synthetic array. To perform the movement of the antennas these systems usually incorporate motors, thus, they will be called motorized MWI systems from now on [31]. A MWI system with a synthetic antenna array is able to scan body parts from different angles. This scanning process generates multiple sets of data that might be used to construct a 3D image of the internal structures, providing greater detail than 2D images.

Down below, some motorized MWI systems (DC, TSAR, HU, and SUST) are displayed with their main features:



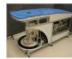




	DC [15]–[19]	MARIA© [20]–[26]	TSAR [27]–[30]	HU [33]	SUST [34]	MU [35], [36]	SU [37], [38]
							
<b>Largest trial:</b>	150	223	8 patients	5 patients	11 patients	13 volunteers	2 patients
<b>Scan time:</b>	5 min	10 s	30 min	14 min	4 min	5 min	3 min
<b>Position:</b>	prone	prone	prone	supine	prone	seated	prone
<b>Coupling:</b>	medium	shell	medium	shell	medium	shell	shell
<b>Table:</b>	✓	✓	✓	✗	✓	✗	✓
<b>Array type:</b>	synthetic	hardware	synthetic	synthetic	synthetic	stationary	hardware
<b>Acquisition:</b>	frequency	frequency	frequency	time	frequency	time	frequency
<b>Antenna:</b>	monopole	slot	vivaldi	planar slot	horn	microstrip	stacked patch
<b>Multistatic:</b>	✓	✓	✗	✓	✓	✓	✓
<b>Artefact:</b>	—	rotation	neighbour-based	averaging	adaptive filtering	differential	rotation
<b>Imaging:</b>	tomography	IDAS	DAS	DAS	DAS	DAS	DAS

Figure 8. Summary of some breast microwave imaging systems with their main features. [31]

Another approach for motorized MWI systems is proposed by Kibria et al for breast phantom imaging. They developed a microwave imaging system of a nine-antenna array, one transmitting (Tx) and eight receiving (Rx), incorporated in a turntable platform that rotated the antenna array in a complete revolution around the breast phantom using a stepper motor. This system allowed the obtention of measurement in 50 rotated positions and provided repeatable results. [32]

In the case of MiWEndo, it is composed of a stationary array where the antennas are electronically multiplexed with a switch. In this way the antenna array can be miniaturized to be introduced into the patient's colon. Nonetheless, in the case of MiWEndo, a motorized setup is needed to move the accessory through the phantoms' lumen simulating a colonoscopy. This procedure can be done manually, without motors, but it would be less accurate, less comfortable, and more time consuming.





### 2.3. State of the situation

The aim of this project is the development of a new stable MWI phantom recipe, and the design and implementation of an automatic setup based on motors to perform repeatable measurements of phantoms. These new strategies will assist in the validation stage of the MiWEndo endoscopic device. Therefore, in this section, we will discuss the existing methodologies currently employed for this validation, along with their significant limitations. By doing so, we aim to establish the need for improvement in these methodologies.

At MiWEndo Solutions, they currently utilize an oil-in-gelatin mixture for validating their MWI phantoms. The ingredients used in the recipe are deionized water, agar, sunflower oil, and dishwashing liquid. To finely tune the dielectric properties of the resulting phantom, the proportions of these materials are adjusted depending on the tissue that is aimed to mimic. To create the phantom, the ingredients are heated and dissolved in deionized water, while being continuously stirred with an electric stirrer. Once a uniform mixture is achieved, it is poured into a cylindrical mold and refrigerated. After 24 hours, the mixture solidifies, resulting in the phantom.

Using this protocol, different phantoms have been developed at MiWEndo Solutions with numerous shapes (curved, cylindrical, with folds...), and tissue-mimicking dielectric properties to perform different validation assessments with MiWEndo medical device. A summary of some of these produced phantoms is displayed below.

Table 2. Summary of some phantoms used at MiWEndo Solutions for MiWEndo device validation. [33-36]

Name	Image	Shape	Tissue
Phantom 3		Curved colon lumen phantom model derived from patient's virtual colonoscopy, with and without different sorts and shapes of polyps.	Healthy mucosa of the colon with and without polyps of adenocarcinoma, LGD and HGD adenoma.
Phantom 4		Cylindrical colon lumen phantom without folds. It may have different types of pedunculated polyps.	Healthy mucosa of the colon with and without polyps of adenocarcinoma or HGD adenoma.
Phantom 5		Cylindrical phantom molded with a straight section of a 3D colon model obtained from a real computed tomography (CT) colonography.	Healthy mucosa of the colon with and without polyps of adenocarcinoma or HGD adenoma.
Phantom 8		Realistic model of the entire lower gastrointestinal tract with folds.	Healthy mucosa of the colon with and without polyps of adenocarcinoma or HGD adenoma.



These oil-in-gelatin based phantoms are stored in the refrigerator with film placed on top of the phantom surface. They maintain their integrity for a period of 4 to 6 months. However, during this period of time, phantoms dehydrate, and water appears at the bottom part of the container. This causes the gradual alteration of their dielectric properties, as well as the appearance of mold and unpleasant odors. Consequently, despite being a well-studied recipe that enables the production of phantoms that effectively mimic different colon tissues, their conservation poses significant challenges.

To perform measurements of such phantoms for MiWEndo device validation, a manual measurement setup has been manufactured, displayed in Figure 9. The MiWEndo accessory is attached to the tip of a millimetric bar, with the phantom placed underneath this system. With this bar, the accessory is moved downwards and upwards along the lumen of the colon phantom to take the measurements. The basis of the phantom is placed on a platform that allows it to move along the x and y axis. These movements are controlled with integrated rulers. These movements of the device are performed manually by an operator; hence, the repeatability and precision of such measurements are subjected to human error.

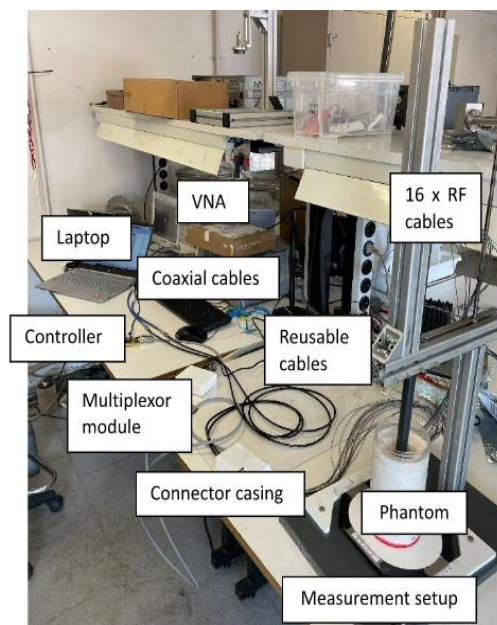


Figure 9. MiWEndo measurements set-up. [33]

As for the reference coordinate system considered to perform the measurements, the Z axis is established as the reference point ( $z=0$ ) when the center of the two antenna rings of the MiWEndo aligns with the top of the colon phantom. The relative positioning of the MiWEndo with the colon lumen model is determined through the millimetric bar. Then, for the XY axes, the coordinate center of the XY-plane ( $x=0$ ,  $y=0$ ) is the center of the cross-section plane of the colon lumen model. To ensure stability during measurements, a PVC millimeter-scale bar is employed to prevent any rotation of the setup. Thus, the reference coordinate system might be somehow arbitrary and susceptible to small variations during measurements. [33]

### 3. MARKET ANALYSIS

This project focuses on the validation stage of a MWI endoscopy system integrated into conventional colonoscopes. The final target market of the project is the colonoscopy market. Therefore, the current trends, the historical evolution and the future perspectives of the colonoscopy market will be further analyzed in this section, as well as the role of imaging phantoms in this context.

#### 3.1. Market sector

##### 3.1.1. Colonoscopy tools market

According to a report by InsightAce Analytic, the global colonoscopy market was valued at approximately \$3.72 billion in 2022 [37]. The market for colonoscopy has been growing steadily over the years. The key market drivers of such growth are the rising prevalence of colorectal disease, especially of CRC due to the aging population and westernized-lifestyle, along with the growing awareness and organized screening programs, such as Government initiatives for early detection of CRC. Thus, nowadays the demand for colonoscopy procedures continues to experience sustained growth. [37,38]

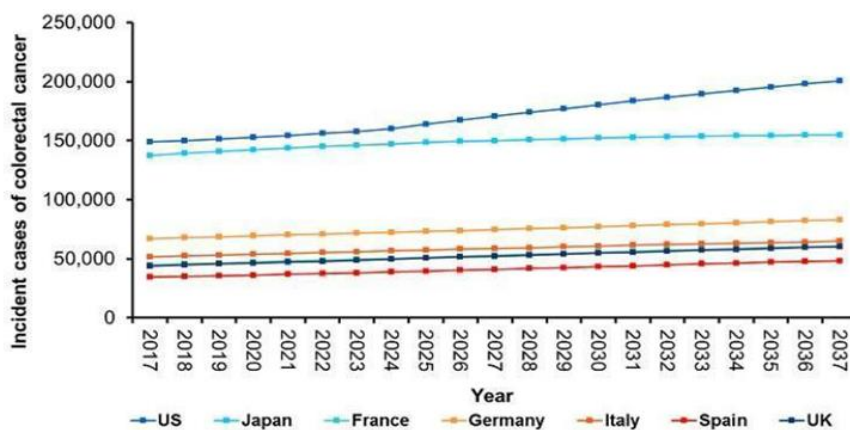


Figure 10. Incidence of colorectal cancer in 2017-2031 in the seven leading market countries. [39]

The colonoscopy market is characterized by intense competition and is composed of numerous global players, being the major markets the US, Japan, UK, France, Italy, Germany and Spain. Furthermore, the leading market players currently include Boston Scientific Corporation, Fujifilm Corporation, Olympus Corporation, PENTAX Medical, Medtronic, and Slim Colonoscopes. As the market continues to advance, all these companies are working to achieve distinct differentiators in their colonoscopy systems, primarily based on their application. Diverse client groups are moving toward optimal visualization systems that include a colonoscope and camera due to the demands of high-quality imaging. [40]

Furthermore, technological advances have also played a key role in the development of the colonoscopy market. High-definition imaging, narrow-band imaging, and virtual chromoendoscopy, have enhanced the accuracy and effectiveness of the procedure, and increased the detection polyp rate. Even robotic applications have been developed in colonoscopy, which improve the safety and

the whole performance of the procedure providing precision and reliability. All these technological innovations are driving market growth by improving patient outcomes and increasing the effectiveness of colonoscopy procedures. [38,41]

### 3.1.2. Imaging phantoms market

The medical imaging phantoms market is valued at \$212.4 million by 2027 and it is expected to experience a compound annual growth rate (CAGR) of 5.2% during 2020-2027. The rising prevalence of lifestyle-associated disorders such as cardiac failure, several types of cancer, or Chronic Obstructive Pulmonary Disease (COPD), along with the escalating demand for in-house accurate calibration techniques to ensure effective diagnostic imaging procedures, are significant drivers of market growth. Furthermore, the increasing demand for early diagnostic methods, as well as the growing emphasis on patient safety and quality control are also key factors contributing to the market's expansion. [42]

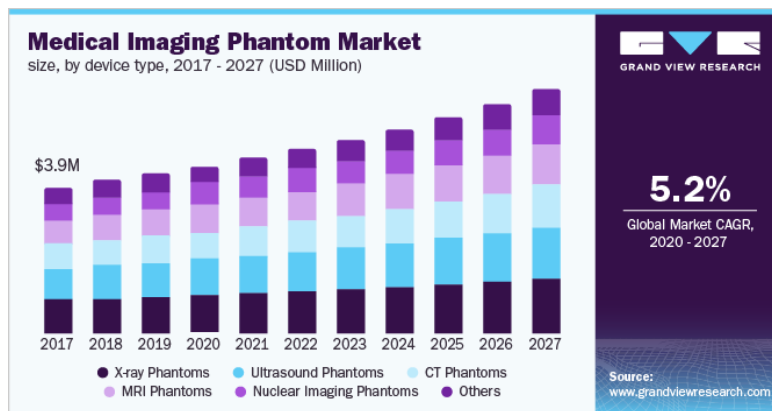


Figure 11. Plot of the growth of the medical imaging phantoms market during 2017-2027. [42]

Imaging phantoms are essential tools utilized across various imaging applications, including radiography, computed tomography (CT), magnetic resonance imaging (MRI) and nuclear medicine. With the rapid advancement in medical imaging technologies and the need for non-invasive and radiation-free imaging techniques, other applications are expected to gain importance in this phantom imaging sector like ultrasound or microwave imaging. Currently, the market for MWI phantoms is still relatively niche and centered in research-like applications. [42]

The principal end users of the medical imaging phantoms market are hospitals for the calibration of their medical imaging equipment and for training of physicians and nurses in specific procedures; medical device companies in the preclinical trials and validation stages of the technology; and academic research, in which is specially rising the usage of phantoms to perform the training and test of artificial intelligence and reconstruction algorithms in imaging. For instance, in PubMed, with a history of more than 40 years, there is a significant rise in the number of publications investigating Tissue-Mimicking and Anthropomorphic phantoms. [42,43]

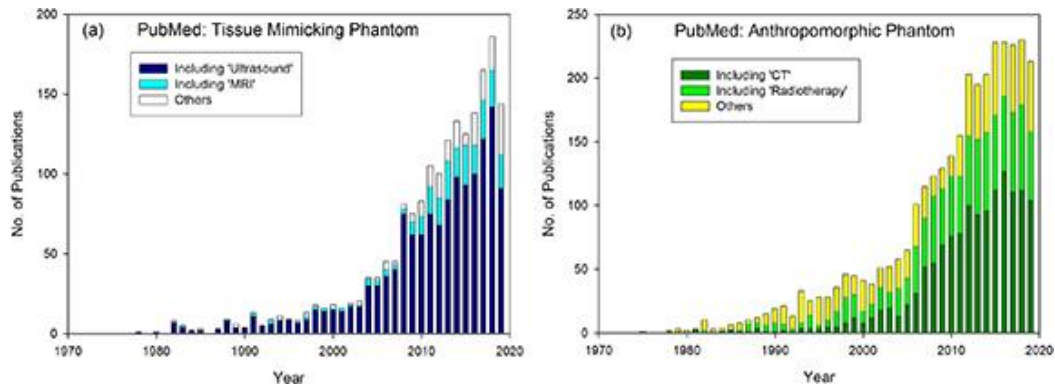


Figure 12. Number of imaging phantom publications in PubMed during 1970-2020. [43]

The global market for medical imaging phantoms exhibits a slightly fragmented structure, characterized by a moderate level of competition among various players. Key participants in the market include Gold Standard Phantoms, Kyoto Kagaku Co. Ltd., Dielectric Corporation, Pure Imaging Phantoms, and several others. [44]

Finally, in terms of colonoscopy phantoms, Kyoto Kagaku is commercializing the *Colonoscope Training Model*. It comprises a life-size molded plastic torso with a soft and flexible colon tube mounted inside. The colon is tethered to the torso by a series of rubber rings connected to Velcro-backed fixtures, which allows the configuration of 6 different scenarios from simple to complex cases [45]. Another example of this technology is the *Kroton Kolono Colonoscopy Trainer* from Kroton Medical Technology. It is a training phantom device for colonoscopy that allows endoscopists to practice both on a healthy colon, and on a colon with lesions. This resin-based phantom has 15 ports which allows for the development of interesting and different training scenarios. [46]

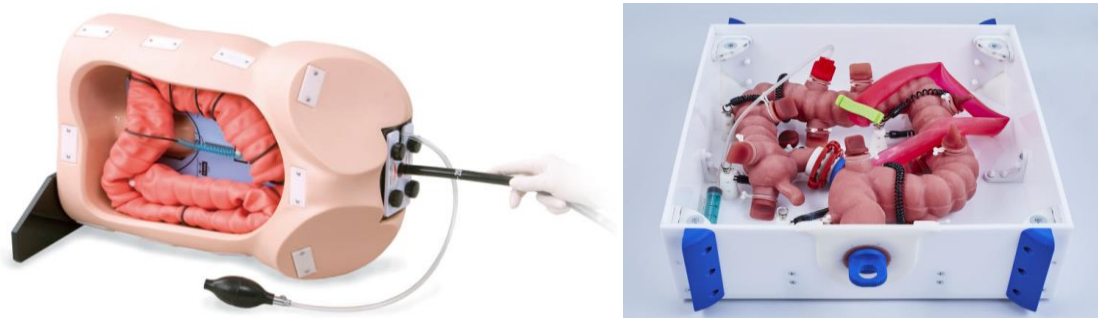


Figure 13. Colonoscope Training Model from Kyoto Kagaku (left) and Kroton Kolono Colonoscopy Trainer from Kroton Medical Technology (right). [45,46]

## 3.2. Historical evolution

### 3.2.1. Historical evolution of colonoscopy

The historical evolution of colonoscopy dates back to 1806 when Philipp Bozzini, often considered the father of endoscopy, designed the *Lichtleiter*, or "light conductor," with the goal of examining the inner cavities of the human body. His design not only enabled new procedures but also made

existing ones safer like the removal of rectal polyps by allowing for direct visualization. It was mainly utilized for urethra or larynx explorations. The first gastroscope was developed in the 1880s, the so-called Mikulicz esophagoscope, which enabled the assessment of esophageal conditions. In 1884, the first sigmoidoscopy was performed using a simple reflective lamp. This was followed by the development of a fiber-optic illumination system and flexible sigmoidoscopes for improved visualization. However, these rigid sigmoidoscopes had limitations and caused significant patient discomfort.

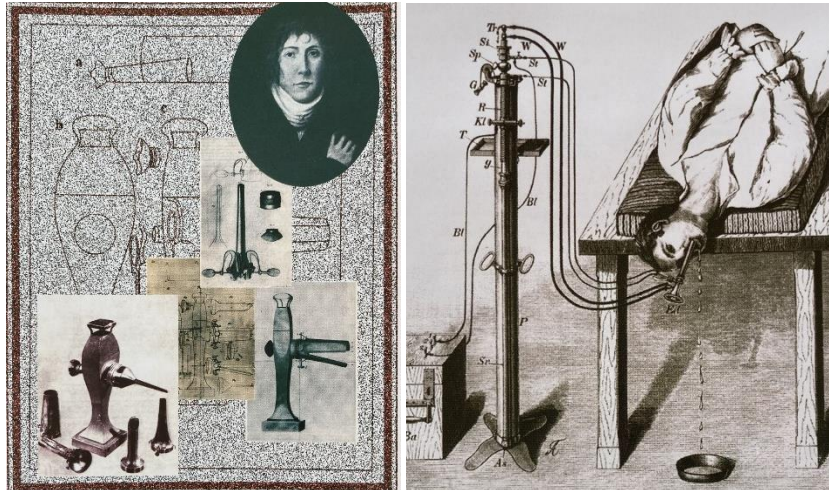


Figure 14. First successful endoscope, *Lichtleiter*, (left); first gastroscope (right). [47]

In the 1930s, Rudolf Schindler developed the first semi-rigid gastroscope, and the procedure consisted in the patient swallowing a piece of vinyl tubing, which exited the anus and subsequently passed the gastroscope through the tube that was pulled through to the colon. It was not until 1960 that Dr. Niwa and Dr. Yamagata at Tokyo University developed the first colonoscope. Shortly after, in 1969 the first modern colonoscopy as we know it today was performed at New York's Beth Israel Medical Center by Wolff and Shinya. [48,49]

The development of video endoscopy in 1983 revolutionized the field of colonoscopy. It provided real-time visualization of the colon on a monitor, as well as numerous benefits, including simultaneous viewing by the endoscopist and the team, and enhanced ergonomics for the operator. Additionally, it allowed easy capture of images and videos which was extremely useful for documentation and educational purposes. [48,50]

In 1999, capsule endoscopy was conceptualized by Israeli engineer, Gavriil Iddan and Israeli gastroenterologist Eitan Scapa. The first capsule endoscope was approved by the FDA in 2001, developed by Given Imaging. This non-invasive method allowed for the visualization of the digestive tract by swallowing a capsule equipped with a camera, avoiding the inconvenients and discomforts of conventional colonoscopy. [51]

During the early 2000s, significant progress was made in enhancing both the image quality and the examination capabilities of endoscopy. Numerous advancements, including high-definition imaging and the application of electronic image processing techniques for mucosal enhancement, like virtual chromoendoscopy, contributed to substantial improvements in the accuracy and quality of endoscopic examinations. These advancements focused on enhancing the visualization of the

mucosa and improving the detection of polyps, thereby enhancing the overall effectiveness of colonoscopy procedures.

Nowadays, advanced colonoscopy techniques continue to evolve, and new strategies based on artificial intelligence systems have been proposed to improve the performance and quality of the procedure. Other current trends in advanced colonoscopy consist in attaching accessories to the endoscope or using robotics with the principal aim of increasing the lesion detection rate. [41,52]

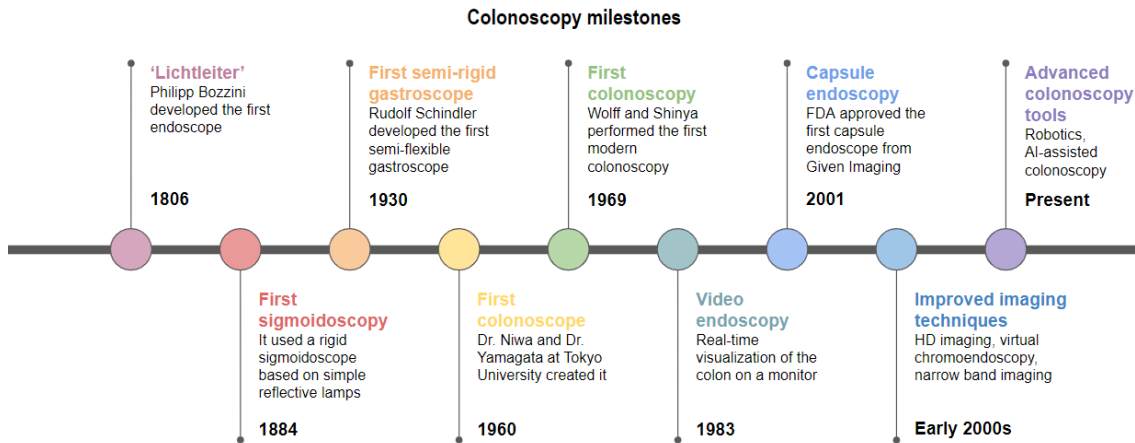


Figure 15. Colonoscopy historical milestones.

### 3.2.2. Historical evolution of imaging phantoms

From the early 1900s, researchers have had the urge to study the dosimetric effects within and around irradiated tissues. Since then, imaging phantoms have been widely employed in experimental radiation dosimetry. In the 1920s, the earliest imaging phantoms were developed, which consisted in simple, geometric objects made from materials like wax and water as muscle and soft tissue substitutes, and even plastic or metals. These phantoms were primarily employed for calibration and quality control in radiography.

During the 1950s, scientists illustrated the importance of realism in phantom body design. The so-called anthropomorphic phantoms began to be implemented which mimicked the shape, size, and anatomical features of specific human body parts or entire bodies. Anthropomorphic phantoms allowed simulating imaging operations more accurately and evaluating radiation dose distribution and imaging efficiency. The 'Temex' and the 'Rando', two adult-sized body phantoms, were introduced in the early 1960s, continuing the trend towards innovative body phantom design. These phantoms enabled the assessment of radiation dose distributions.

Tissue-Equivalent Phantoms first appeared in the 1970s. The materials used to create these phantoms closely matched the radiological characteristics (attenuation and scattering) of human tissues. Shortly after, due to the developments in imaging techniques such as computed tomography (CT), magnetic resonance imaging (MRI), and positron emission tomography (PET), there was an increasing demand for phantoms capable of reproducing dynamic and functional properties. Hence, during the 1980s-1990s, dynamic phantoms were developed to simulate blood

flow, tissue motion, and physiological processes. These phantoms allowed researchers to investigate perfusion, heart function, and other dynamic imaging applications.

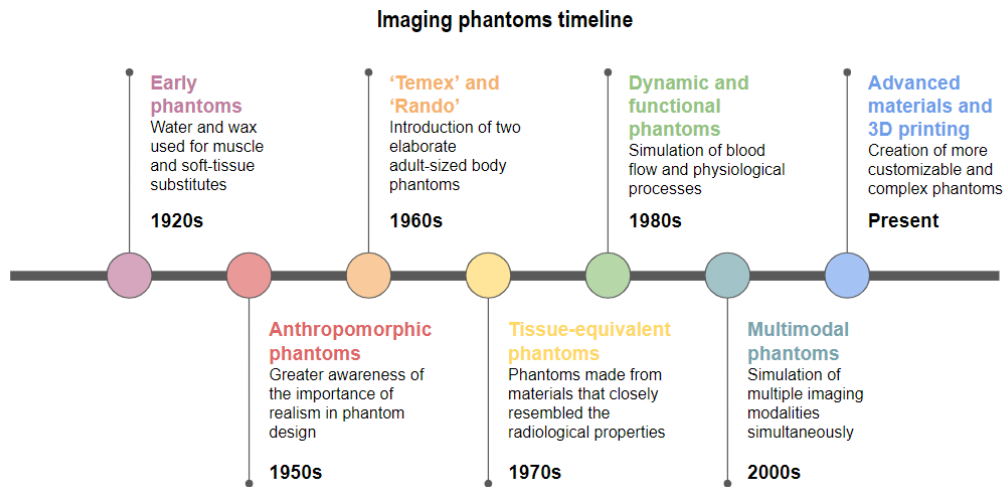


Figure 16. Imaging phantom's historical evolution.

Multimodal phantoms appeared in the early 2000s because of the evolution of imaging technologies and the increased necessity for precise comparisons between multiple imaging modalities. These phantoms were created to replicate numerous imaging modalities at the same time, enabling calibration, performance evaluation, and cross-modality validation.

Recent advances in materials science and 3D printing technology have resulted in more sophisticated and customized phantoms. Advanced materials, such as hydrogels, elastomers, and nanoparticle-based composites, enable phantoms to replicate tissue more accurately. 3D printing enables the exact production of patient-specific phantoms, which improves the realism and applicability of imaging simulations. [53]

### 3.3. Future perspectives

#### 3.3.1. Future perspectives of the colonoscopy market

According to Strategic Market Research, the global colonoscopy devices market will witness a robust Compound Annual Growth Rate (CAGR) of 5.1%, expected to reach \$2.14 billion by 2030 [38]. Additionally, the need for colonoscopy is expected to rise by 16% in the next decade [54]. In general, the colonoscopy market is expected to witness further technological advancements that will improve the accuracy, efficiency, and patient experience of the procedure. Some of the upcoming trends in the colonoscopy market are reviewed below.

AI-assisted image analysis is going to be implemented in routine colonoscopy procedures to assist in the real-time detection of abnormalities, lesion characterization, and aid in the identification of suspicious areas, potentially reducing the miss rate and improving diagnostic outcomes. [55]

Similarly as minimally invasive robot-assisted surgeries, in the field of endoscopy robotic applications may also be established. Robots in colonoscopy will be computer-integrated intelligent

machines that enhance interventional abilities of endoscopists and reduce daily workload while they improve the safety and the whole performance of the procedure providing precision and reliability. Besides, they might incorporate magnetic endoscopes and torque sensors which allow the control of the navigation of the endoscope from outside the patient, which will prevent harming the patient and reduce both discomfort and perforation risk. This all will eventually increase compliance rates. [54,56]

Finally, due to the Covid-19 pandemics, telemedicine and remote monitoring have become extremely popular. In the field of colonoscopy, wearable technologies and smartphone apps that track bowel preparation compliance, post-procedure recovery, and long-term surveillance can improve convenience and patient participation. [57]

### *3.3.2. Future perspectives of the imaging phantoms market*

Because of the sustained growth of imaging technology, materials science, and computational capabilities, the imaging phantoms market is expected to experience expansion and new developments. These advancements will result in more realistic and adjustable phantoms, which will be critical in calibration, quality assurance, research, training, and the evolution of medical imaging procedures. Some of the potential market developments are reviewed.

First, regarding phantom fabrication, it is interesting the development of phantoms with enhanced tissue-mimicking and conservation properties. Due to the constant development of new materials, more precise characteristics that provide larger resemblance to actual human tissues could be achieved. These enhanced features combined with materials that increase the lifespan of phantoms, could result in the ease of the validation stages in medical device development.

Another promising line of research for the imaging phantoms market are patient-specific phantoms. Advances in imaging technology and the reduction of costs in both 3D imaging and 3D printing, may enable the creation of phantoms that perfectly replicate individual patient anatomy and pathology for routine applications like radiotherapy. Patient-specific phantoms would allow more accurate and individualized medical imaging procedures for personalized treatment planning, simulation, and training. [53]

Lastly, the integration of imaging phantoms with Virtual and Augmented Reality (VR/AR) technologies is extremely promising. VR/AR can provide immersive and interactive experiences, allowing users to see and interact with virtual phantoms in real time. These technologies could significantly improve medical training, surgical planning, and procedural simulations by creating a realistic and dynamic environment. [58]

### *3.3.3. Future applications of the technology developed in this project*

Both the new phantom recipe and the automated measuring system that has been developed in this project may have further applications for future projects within MiWEndo Solutions company,



---

apart from MiWEndo device validation. Since MiWEndo's founders and personnel are specialized in the use of microwave technology for medical diagnosis, there are many other potential and affordable options for further developments and applications of this technology. Some of them are:

- Rheumatology, for the automatic detection of rheumatoid arthritis, arthrosis, and other rheumatologic disorders
- Odontology, for the automatic detection of periodontitis, gingivitis and other periodontal diseases
- Gynecology. A device for diagnosing the precise moment of in vitro fertilization or for the automatic diagnosis of gynecological cancers. [39]

Therefore, MWI phantoms with similar dielectric properties as all these tissues will have to be developed for the validation and test of these different applications, so that a newly conceived and more optimized phantom recipe would be useful. Besides, a similar conception of the automated measuring system developed in this project would also be of utmost utility to perform measurements and validation of these future projects.

## 4. CONCEPTION ENGINEERING

In this section, a description of the various aspects and potential solutions that have been examined for both MWI phantom production and the automated measuring system implementation will be provided. Additionally, an analysis and comparison of these proposals will be conducted to determine the most viable and suitable options in each case.

### 4.1. Phantom recipe

The new recipe for MWI colon phantoms developed in this project will be based on polyvinylpyrrolidone (PVP). PVP is a water-soluble polymer made from the monomer N-vinylpyrrolidone. It has numerous applications nowadays: in pharmacy as a binder in tablets, in cosmetics as a fixative or in industrial production. Furthermore, PVP does not require any special handling, storage precautions, or procedures, and it is generally recognized as safe. [59]

In the experimental phase of the project, PVP colon phantoms will be created to compare their lifespan and stability with the existing oil-based phantoms, currently used at MiWEndo Solutions for medical device validation. While the primary component of the new phantoms, PVP, has already been chosen, it is necessary to examine the physical features of the PVP phantoms themselves to develop the most appropriate ones for the comparative study.

In general, the main requirements for the developed phantoms are the capacity to mimic the physical and dielectric properties of the colon. Since several measurements will be conducted over an extended period of time, a phantom that is easy to handle, unmold, and exhibits an increased stability is preferred. Finally, in general, simplicity and reduced costs are both of interest.

Down below, the different options for consistency, geometry, and homogeneity of the PVP colon phantoms will be discussed.

#### 4.1.1. Consistency

The consistency of the developed PVP phantoms can either be liquid or gel. Liquid phantoms have low viscosity, similar to liquids such as water or oil, and they are usually fabricated to flow and spread easily. They do not require the usage of any jellifying agent. On the other hand, gel phantoms refer to those phantoms that exhibit a more solid-like behavior with higher viscosity, similar to gelatin or soft rubber. They require the introduction of a jellifying agent (like agar or gelatin) to the fabrication protocol.

In the table below, the main advantages and disadvantages of each consistency are assessed.

Table 3. Main advantages and disadvantages of liquid and gel phantom consistencies. [9]

	Advantages	Disadvantages
Liquid phantoms	- More realistic representation of bodily fluids or certain tissues due to their fluid nature.	- Limited shape retention. The container cannot be removed unlike gel phantoms, and it is made of plastics that have very small

	<ul style="list-style-type: none"> <li>- Simpler production. Phantoms do not require the usage of jellifying agents so the whole protocol of fabrication is easier.</li> <li>- More homogeneous. Due to the liquid consistency, it is easier to obtain homogeneous phantoms since there is no risk of separation during the jellifying process.</li> </ul>	<p>dielectric properties compared to tissues, which may affect the readings.</p> <ul style="list-style-type: none"> <li>- It is difficult to maintain specific phantom geometries.</li> <li>- Prone to instability. The components of the phantom may separate or settle, leading to changes in physical or dielectric properties.</li> <li>- Less accurate depiction of a solid-like organ.</li> </ul>
<b>Gel phantoms</b>	<ul style="list-style-type: none"> <li>- Fine-tuning of the physical properties. By changing the concentration of the jellifying agent, the final consistency of the phantom can be accurately tuned.</li> <li>- Less prone to separation or settling, ensuring more consistent and reliable results over extended periods.</li> <li>- Better shape retention. The obtained phantoms may be removed from the mold.</li> <li>- More realistic representation of solid-like organs and anatomical structures.</li> </ul>	<ul style="list-style-type: none"> <li>- More complex and time-consuming production. They require careful mixing and setting processes.</li> <li>- Less homogeneous. If the curing or settling processes are not correctly done, the obtained phantoms may have a non-homogeneous distribution of the dielectric properties.</li> <li>- Bubbles. During the fabrication process, if bubbles are not correctly removed, they may settle during the jellifying process and alter the final dielectric properties of the phantom.</li> <li>- More difficult conservation. They tend to incorporate organic components, which are prone to develop mold or degrade.</li> </ul>

#### 4.1.2. Geometry

Regarding the geometry, phantoms might be molded into simple structures like cylinders, spheres or cubes, or into more complex shapes, obtaining the so-called anthropomorphic phantoms, which are phantoms designed to replicate the shape and size of human organs or tissues to simulate realistic imaging scenarios. The main advantages and disadvantages regarding the production and the realism of the obtained phantoms for these geometries will be discussed below.

Table 4. Main advantages and disadvantages of simple-shaped and anthropomorphic phantom geometries. [23,29]

	<b>Advantages</b>	<b>Disadvantages</b>
<b>Simple-shaped phantoms</b>	<ul style="list-style-type: none"> <li>- Simple fabrication. It does not require a complex-shaped mold for their production, a simple container is used.</li> <li>- Cheaper. Fewer resources and materials to manufacture are required.</li> <li>- More suitable for preliminary and first-approach studies.</li> </ul>	<ul style="list-style-type: none"> <li>- Constrained representation accuracy. Limited realism when representing the complex anatomy and features of the human body.</li> <li>- Limited relevance and accuracy of experimental results.</li> </ul>

<b>Anthropomorphic phantoms</b>	<ul style="list-style-type: none"> <li>- Realistic representation. Phantoms closely mimic the anatomical structures, tissue properties, and spatial relationships found in the human body.</li> <li>- Further reliability and validity of experimental results.</li> <li>- Useful for tests in advanced stages of the validation process in medical devices.</li> </ul>	<ul style="list-style-type: none"> <li>- More expensive. The obtention of more realistic molds might require the usage of 3D printing or other shape-specific containers, which could increase the overall cost of the production.</li> <li>- Complex fabrication. More advanced fabrication techniques and materials are required. Their manufacture is more difficult and time-consuming.</li> </ul>
---------------------------------	---	--

#### 4.1.3. Homogeneity

Finally, in terms of homogeneity, imaging phantoms might be homogeneous, made of materials with uniform dielectric properties, or heterogeneous phantoms, incorporating different materials or compositions in order to mimic the dielectric properties of different tissues. Both compositions present different pros and cons regarding their fabrication process and accuracy in representing real tissues.

Table 5. Main advantages and disadvantages of homogeneous and heterogeneous phantoms. [60,61]

	<b>Advantages</b>	<b>Disadvantages</b>
<b>Homogeneous phantoms</b>	<ul style="list-style-type: none"> <li>- Ease of production. No need to use different compositions or materials within the phantom, resulting in reduced complexity and manufacturing time.</li> <li>- Cheaper. Less resources and materials for manufacturing are required.</li> <li>- Increased reproducibility in experiments or evaluation.</li> <li>- Most suitable for first approach studies.</li> </ul>	<ul style="list-style-type: none"> <li>- Limited accuracy. Variations in dielectric properties found in tissues are not fully captured.</li> <li>- Reduced tissue differentiation. Impossibility to represent and distinguish different tissues with distinct dielectric properties in the same phantom.</li> <li>- Limited significance of experimental results.</li> </ul>
<b>Heterogeneous phantoms</b>	<ul style="list-style-type: none"> <li>- Realistic tissue depiction. Accurate representation of the complicated dielectric characteristics of diverse tissues in the human body, enabling more realistic medical imaging simulations and assessments.</li> <li>- Customizability. Flexibility in tuning the dielectric properties of specific tissues or organs within the same phantom.</li> <li>- Higher medical relevance in the results obtained.</li> </ul>	<ul style="list-style-type: none"> <li>- Complex fabrication. Higher complexity and more time-consuming fabrication than homogeneous phantoms.</li> <li>- More expensive. Various materials required, which may increase the production costs.</li> <li>- Limited reproducibility due to the variable composition of heterogeneous phantoms.</li> </ul>

## 4.2. Automated measuring system

Prior to studying different options for the different components, the requirements of the automated measuring system that is aimed to be built must be reviewed.

As mentioned earlier, the goal of this project is to develop an automated measuring system to achieve more precise and repeatable measurements when performing phantom measurements for MiWEndo device validation. The first conception of the system was based on moving the phantom in the XYZ axes while leaving the MiWEndo device undisturbed. This approach was preferred to avoid potential interferences and noise in the readings caused by moving the device's cables during measurements. Nevertheless, this design had to be dismissed because the measured phantoms may reach weights of more than 5kg, and this elevated payload presented challenges in obtaining an XYZ motorized positioning system. Most of these systems utilize motors similar to those found in 3D printers, which are typically designed to handle much lower weights. Furthermore, the implementation of the system was also more complicated, since it required a stable platform on the Z axis to move the phantom.

Therefore, the final design of the automated measuring system consists in a motorized setup that moves the MiWEndo device in the three axes of the space to perform measurements of phantoms. Specifically, the system must incorporate an XYZ motorized positioning system with the following minimum linear travels in each axis:  $x=y=5\text{cm}$  and  $z=50\text{cm}$ . Additionally, since it just needs to carry the MiWEndo device, the payload required is 0.5 kg. To prevent interference, it is preferable to use a non-metallic material, such as wood or rigid plastic, for constructing the structural components of the system (e.g., the support where the motorized system will be fixed, and the adapter used to attach the MiWEndo to the moving system). Additionally, the motors' movement is controlled with a controller. Besides, the trajectories of the system should be managed using user-friendly software.

From this design conception, different options for the XYZ motorized positioning system, stepper motor drivers, the controller of the motors and the software used to direct the movement of the system, will be analyzed to find the most optimal solution in each case.

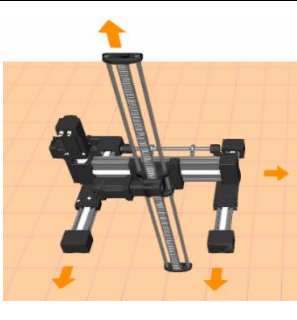


### 4.2.1. XYZ motorized positioning system

The central element of the automated measuring setup is the XYZ motorized positioning system. It needs to allow the movement of the MiWEndo device in the 3 axes with the aforementioned linear travels. XYZ motorized positioning systems are based on stepper motor-based linear actuators, a device that creates force and motion via a straight line and uses a stepping motor as the source of power. The rotational motion of the stepper motor is translated into linear motion using a mechanical mechanism. This mechanism often involves a lead screw, or a threaded rod attached to the rotor of the stepper motor. The threaded rod moves linearly as the motor turns, either expanding or retracting depending on the rotational direction. Using controllers and drivers, the position and movement of the motors can be precisely tuned. This allows for accurate and

repeatable positioning, making stepper motor-based linear actuators suitable for applications that require fine control and positioning. [62]

In the following table, the most important aspects of the XYZ motorized positioning systems considered are reviewed:

Table 6. Main characteristics of the Iigus, Fuyu and Toseastars XYZ motorized positioning systems. [63-65]

	IGUS Room gantry XYZ	FUYU FSK40 Gantry Linear Guide Stage	TOSEASTARS Gantry 3-Axis XYZ stage table
Image			
Linear travel (XxYxZ mm)	200x200x750	100x100x500	100x100x500
Motors	Nema24 x2 (XY axes) Nema23 x2 (Z axis)	Nema23 x4	Nema23 x4
Vertical payload	20 kg	10 kg	20 kg
Price	5382.98 €	810.52 €	1367.50 €
Implementation	Already implemented	Requires user implementation	Requires user implementation
Provider	Iigus	Amazon	AliExpress



#### 4.2.2. Stepper motor driver

Stepper motor drivers are electronic devices used to control and drive stepper motors. They serve as an interface between the control system (in this case the controller) and the stepper motor, providing the necessary signals and power to accurately control its movement.

When choosing the appropriate driver for the system, it must be done according to the current that must be delivered to the stepper motor to properly function. As it can be seen in Table 7 the stepper motors incorporated in the reviewed XYZ motorized positioning systems are Nema23 and Nema24, and these specific models require 2 and 2.8 A [66], respectively. Furthermore, the stepper motor driver allows to control the number of pulses required to perform a whole turn of the stepper motor, that is, it allows to fine-tune the precision of motion of the motor. The higher the number of pulses needed to perform a revolution, the larger the precision. This will translate in the minimum number of millimeters that the positioning system can move when performing a trajectory.

Thus, suitable stepper motor drivers will be studied:

Table 7. Main characteristics of the stepper motor drivers considered. [67,68]

	TB6600	DM542
Image		
Output current	1.0-4.0 A	1.0-4.2 A
Voltage supply	9-42 V	18-48 V
Max pulse/rev	6400	25000
Price	8.99 €	19.99 €

#### 4.2.3. Controller

Another fundamental element of the system is the controller. As its name indicates, this device is responsible for controlling the movement of the motors through the stepper motor drivers. Currently on the market there are several types of controllers for motors, like Arduino or even controllers from companies like Fuyu that have their own software to control their stepper motors.

The primary criteria for choice of the controller are the following: firstly, it must possess an adequate number of pins to accommodate all motor connections, and secondly, it should be compatible with user-friendly software for easy programming and control.

A brief review on the controllers considered in the project is displayed below.

- **Arduino UNO:** It is the standard Arduino board and is highly recommended for beginners in electronics due to its intuitive nature. Arduino UNO is based on the ATmega328P microcontroller, its dimensions are 69x53mm, and it has 6 analog and 14 digital pins. The voltage input ranges from 6 to 20 V, although it is advisable to use a maximum of 12 V. It counts with a USB connection and can be controlled with Arduino Software (IDE). The price of an Arduino UNO board is 24.00€. [69]

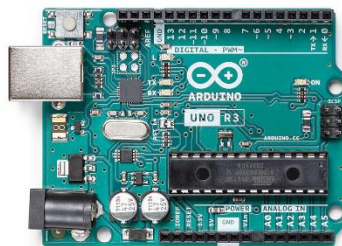


Figure 17. Arduino UNO board. [69]

- **Arduino Nano:** Despite its compact size, measuring only 18x45 mm, this Arduino board boasts a remarkable number of features. With 22 digital and 8 analog pins, it offers ample connectivity options. Additionally, it operates with input voltages of 7-12V and requires the usage of a protoboard for its implementation. It works with a mini-B USB cable and can be controlled with Arduino Software (IDE). The price of an Arduino Nano board is 21.60€. [70]

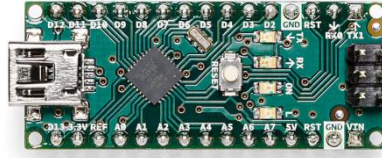


Figure 18. Arduino Nano board. [70]

- **Fuyu FMC4030:** The FMC4030 controller is a pulse controller that uses a 32-bit ARM chip as its primary control unit. It is intended for the control of Fuyu CNC systems. This chip manages various functions, including EtherNet and other communication functions, allowing seamless interaction with the host computer. The controller has 4 digital inputs and 4 digital outputs, providing flexibility when connecting external devices.

The FMC4030 controller operates at 24V voltage. To enhance usability, the controller comes with its own software called FMC4030 software, which eliminates the need for additional user programming and speeds up the setup process. The Fuyu FMC4030 controller is priced at 266.46 €. [71]



Figure 19. FMC4030 controller. [72]

#### 4.2.4. Firmware

The firmware used to control the motorized system depends on the selected control unit. The most important requirement is that it should be simple for users to implement and use, and it should have the capability to program simple trajectories by coordinating the movement of the different motors.

- **Arduino IDE:** It is a cross-platform freeware (for Windows, macOS, Linux) written in Java programming language. It is used to write and upload programs to Arduino-compatible boards. It requires the user's development of the code. Nevertheless, there are openly available codes for motion control of CNC stage equipment such as Grbl in Github [73], which allows the introduction of simple trajectories for the CNC equipment in a very intuitive way. It is compatible with both Arduino Nano and Arduino UNO, but it requires configuration, such as introducing the corresponding ports for each type of board.





Figure 20. Arduino IDE software layout. [74]

- FMC4030 Software:** It provides the host computer controller software, and it runs on Windows operating system. FMC4030 Software is a highly intuitive application that allows the introduction of the target position, speed, acceleration, deceleration and other parameters, to control the CNC system. Thus, it does not require any sort of programming skills, but it obviously requires the implementation of a Fuyu FMC4030 controller in the system. [71]

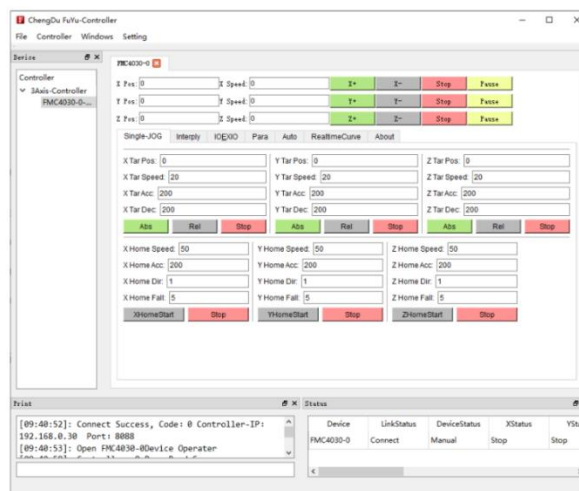


Figure 21. FMC4030 Software layout. [71]

### 4.3. Selected solution

After conducting a thorough analysis of all potential solutions, taking into account their respective features and drawbacks, a final decision has been reached considering the project's specific requirements and how well each option fits with them. Down below, the solutions chosen for both the phantom comparative study and the automated measuring system will be reviewed.

#### 4.3.1. Phantoms

Regarding the consistency, the developed phantoms must accurately simulate the physical properties of a solid-like organ such as the colon. Since several measurements will be conducted over an extended period of time, a phantom that is easier to handle, unmold, and exhibits an

increased stability is preferred. Thus, **gel phantoms** have been selected despite their larger complexity in fabrication.

Since the comparative study performed is a first-approach study in order to assess the lifespan and stability between the two phantom recipes, there is no need for important realism in terms of anatomical structure. The most important variable assessed during the comparative study will be the stability of the dielectric properties. Therefore, both simplicity and low cost have been prioritized by choosing a **simple-shaped phantom**.

Finally, the developed PVP phantom will be **homogeneous** because, as aforementioned, the conducted study will only focus on the assessment of the dielectric properties' conservation. Hence, there is no need for further realistic, complex or expensive approaches. Besides, only one type of tissue, healthy colon mucosa, will be mimicked with both recipes. Nevertheless, depending on the results obtained, a future study might consider including different tissues like cancerous or hyperplastic polyps. But, as for the scope of this project, the homogeneous phantoms will suffice adequately.

#### 4.3.2. Automated measuring system

In terms of the automated motorized measuring system, the selected components are the following. The XYZ motorized positioning system of choice is the **FUYU FSK40 Gantry Linear Guide Stage**. Despite its significantly lower price (over 500 €), its performance is comparable to that of the TOSEASTAR system, with the exception of a slight reduction in vertical payload capacity. Considering that the MiWEndo medical device is the only component being carried by the system and weighs less than 0.5kg, a 10 kg payload is more than sufficient. Moreover, the shipping and return terms of Amazon are better than those of Aliexpress. Furthermore, the IGUS Room Gantry has an exorbitant price and offers features that exceed the required specifications. Additionally, given the presence of a skilled team of engineers at MiWEndo Solutions, the implementation can be performed in-house, eliminating the need for external assistance.

Regarding the stepper motor driver, both options have very similar features, and fulfill the requirement of current and supply, considering that a standard Meanwell power supply of 24V will be utilized. Therefore, taking into account that DM542 is more expensive due to being slightly oversized for this particular application, the **TB6600** will be the stepper motor driver of choice for this project.

Following with the controller, an Arduino board has been selected because of the significant reduction in price and the previous knowledge of the author of using this component. Besides, since the Arduino board is highly versatile, it could be reused for other and future applications at MiWEndo Solutions, while the FMC4030 can just be utilized for the control of CNC systems. Between Arduino UNO and **Arduino Nano**, the selected board for the project is Arduino Nano, because it offers very similar features as Arduino UNO, and it has both a reduction in size and in price. Furthermore, at MiWEndo Solutions they already have an Arduino Nano kit.

Finally, with the Arduino Nano being selected as the system's controller, the firmware of choice will be **Arduino IDE**. Additionally, the Grbl software will be configured and implemented to suit the project's needs.

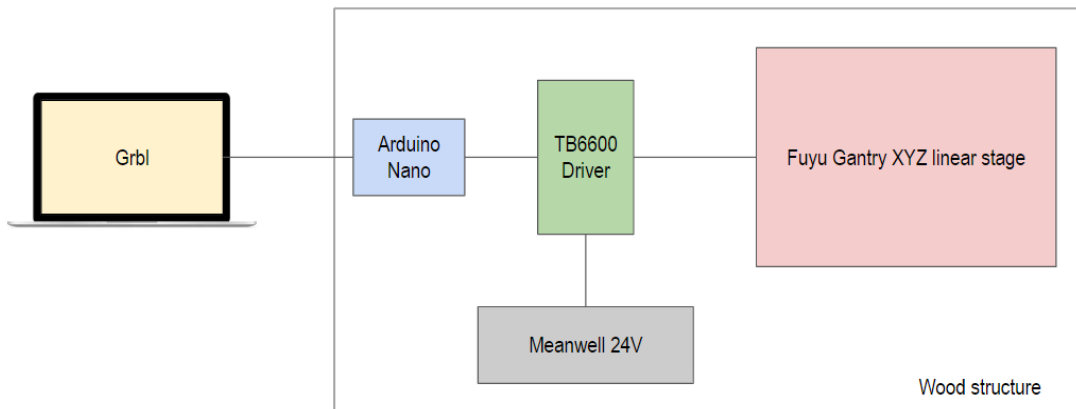


Figure 22. Simplified schematic of the implemented automated measuring system with the selected components.

Further details on the implementation of all these components is explained in the upcoming section.

## 5. DETAILED ENGINEERING

Once the project has been conceptualized, in this section the actual implementation of the proposed solutions for both the phantoms and the automated MWI measuring system will be discussed, and the methodology followed for their testing and validation will be detailed.

### 5.1. Phantoms

#### 5.1.1. Ingredient concentration assessment

Once establishing all the required materials for the new phantom recipe (water, PVP and agar), it must be determined the concentrations of each component in order to obtain the desired characteristics. Due to the lack of literature in the production of PVP with colon-like dielectric properties, a prior study of the concentration of PVP was required to obtain phantoms that met the established requirements.

PVP is the essential component in the recipe for creating the phantom. Its presence is crucial as it allows the fine-tuning of the phantom's dielectric properties. For the experimental work (the comparison study between the old and the new recipes), we will try to mimic colon healthy mucosa tissue. Since the developed phantoms are aimed for MiWEndo device validation, we will focus on the healthy colon dielectric properties at a frequency of 7.5 GHz. According to Figure 4 in subsection 2.1.2. *MiWEndo Solutions*, the developed phantoms should have a relative permittivity ranging from 41 to 44 and a conductivity between 6 and 8 S/m.

As initial reference, the PVP-phantom recipe for breast microwave imaging discussed in *Siyun Li et al (2021)* has been considered [24]. In order to fine-tune the required concentration of PVP to achieve these characteristics, a study was conducted in which increasing concentrations of PVP were mixed with 30 ml of deionized water in order to establish which one retrieved the most similar dielectric properties to the theoretical ones. Further information on this study is collected in *Annex 2. Assessment of PVP concentration*.

Following the protocol in *Annex 1. Dielectric properties measurements protocol*, the dielectric properties of each mixture were retrieved using the VNA. The results for a frequency of 7.5GHz are displayed in Table 8.

Table 8. Dielectric properties of water and PVP mixtures for increasing PVP concentrations.

PVP (%)	Relative permittivity $\epsilon'$	Conductivity $\sigma$ (S/m)
20	50.23 $\pm$ 0.13	10.30 $\pm$ 0.06
25	46.23 $\pm$ 0.06	9.63 $\pm$ 0.04
30	42.85 $\pm$ 0.15	9.72 $\pm$ 0.12
35	39.78 $\pm$ 0.01	9.24 $\pm$ 0.03
40	36.74 $\pm$ 0.20	8.73 $\pm$ 0.05

From this study, it was first determined that increasing concentrations of PVP caused a decrease in the dielectric properties of the phantom obtained. Additionally, the standard deviation of the measurements was very low in general, showing the homogeneity of the liquid phantoms.

Furthermore, it was seen that this PVP recipe provided accurate relative permittivity values that resembled those of healthy colon tissue, but it retrieved slightly high conductivity ones. Nonetheless, considering the simplicity of the recipe, it is the mixture of two components, it was considered a reasonable and valid approximation.

The PVP concentrations that provided the most similar dielectric properties to those of healthy colon tissue were 25%, 30% and 35%. Among these, the concentration of 30% with a relative permittivity of 42.85 and a conductivity of 9.72 S/m was found to be the most accurate one. Subsequently, a follow-up study was conducted using these three PVP concentrations (25%, 30%, and 35%) to investigate whether their dielectric properties changed after the addition of agar and solidification of the phantoms. This study played a crucial role in selecting the optimal PVP concentration for phantom development.

In accordance with the reference by *Siyun Li et al. (2021) [24]*, a concentration of 5.5% agar was selected due to its ability to produce a solid-like phantom that was both easy to handle and kept its shape. After mixing the PVP with the deionized water, the mixture was heated, and agar was added. After letting the phantom solidify and cool down, the dielectric properties were assessed, similarly as before. The obtained values are displayed in Table 9.

Table 9. Dielectric properties of water, PVP and agar mixtures for increasing 25, 30 and 35% PVP concentrations.

PVP (%)	Agar (%)	Relative permittivity $\epsilon'$	Conductivity $\sigma$ (S/m)
25	5.5	46.35 $\pm$ 0.94	9.58 $\pm$ 0.28
30	5.5	41.64 $\pm$ 1.17	9.38 $\pm$ 0.46
35	5.5	38.87 $\pm$ 0.72	9.05 $\pm$ 0.15

First, it can be seen that in comparison to those results from Table 8, the measurements after adding agar show a higher standard deviation meaning that the gel phantoms obtained are less homogeneous than the liquid ones. This might be caused by the settling process. Moreover, it is observed that the dielectric properties values remain relatively stable before and after the addition of agar, indicating that the incorporation of the jellifying agent does not have a significant impact on this particular feature of the phantoms.

After conducting this second experiment, it is clear that the dielectric properties of the healthy colon tissue are best-mimicked by PVP phantoms that contain 30% of PVP. Specifically, these phantoms exhibit the most similar dielectric to the actual healthy colon tissue:  $\epsilon' = 41.64$  and  $\sigma = 9.38$  S/m.

To sum up, thanks to the PVP concentration studies, the final concentrations for the PVP phantom production have been established: **30% of PVP and 5.5% of agar** (weights in grams computed applying the percentage to the volume in milliliters of deionized water). Thus, for the comparative study, this will be the concentration used.

### 5.1.2. New developed phantom recipe

In this subsection, the developed recipe to produce PVP phantoms that has been used to perform the comparative study is explained. The aim of this study is to assess the lifespan between the oil-based phantoms and the new PVP-based ones. To do so, homogeneous, cylindrical gel phantoms mimicking colon healthy mucosa dielectric properties will be fabricated using the ingredient concentrations found in the previous section.

Several trials were required to obtain the final phantom, because a major problem was encountered when developing it: bubbles appeared in the mixture when the PVP and the agar were added to the boiling hot deionized water. Due to the fast jellification process, when the mixture cooled down, bubbles remained in the final product causing a severe decrease in the dielectric properties of the phantom. To overcome this problem, PVP and water were mixed and allowed to settle to eliminate any bubbles prior to the gelation process. Subsequently, the agar was added.

The materials needed for approximately 120 ml phantom, are the following: (for other volumes, the recipe might be adapted using the ingredient percentages)

- Polyvinylpyrrolidone (PVP-40): 36 g
- Deionized water (Eroski): 120 ml
- Agar (Químics Dalmau E-406): 6.6 g
- 2x 500 ml Glass Beaker
- 100 ml urine container
- Plastic film
- Glass stirring rod
- Hot plate
- Thermometer
- Rigid plastic support

The procedure to fabricate the PVP phantoms is the following:

1. Cover the urine container with plastic film, so that the final phantom can be easily retrieved from the container after polymerization.
2. Pour 60 ml (50%) of deionized water in the 500 ml glass beaker and heat it up to 50°C.
3. Remove the water from the hot plate and add the PVP. Stir the mixture using the glass stirring rod till the polymer is completely dissolved.
4. Let the mixture cool down and sit until no bubbles are observed.
5. Then, mix the other 60 ml of deionized water with the agar in the glass beaker and heat it up to 85°C, so that the gelling agent is completely dissolved.
6. Next, pour the agar-water mixture into the PVP-water solution and pour the resulting solution into the urine container.
7. Let the phantom cool down and jellify in the refrigerator for 24 hours.
8. After polymerization, remove the phantom from the urine container using the plastic film cover, and put the rigid plastic support at the bottom part of the urine container with the phantom on top. This will be useful to monitor degradation, by studying the water formation.
9. Finally, phantoms are preserved hermetically in the fridge, covering them with film to prevent any contact with air, in order to avoid water condensation and dehydration.

### 5.1.3. Phantom experimental work

PVP phantoms, which are based on non-organic materials, are proposed as a new recipe to prolong the lifespan of phantoms for MiWEndo device validation. To prove this theoretical increased lifespan of PVP phantoms, a comparative study on the conservation and stability of PVP phantoms and the currently-used oil-based phantoms is conducted [75]. Furthermore, the most-suitable conservation protocol (low or room temperature) for PVP-based phantoms is also assessed.

In this study, three samples of phantoms are produced: an oil-based phantom (look for the recipe in Annex 3. *Oil-based phantom recipe*), and two PVP phantoms (following the recipe 5.1.2. *New developed phantom recipe*). Both PVP phantoms have the same concentrations of each component and are fabricated under the same conditions.

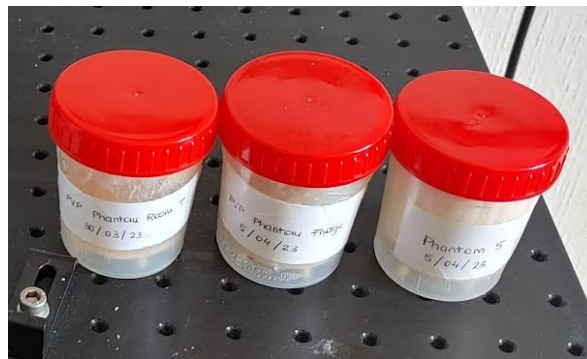


Figure 23. The 3 produced phantoms, from left to right: PVP phantom left at room T, PVP phantom preserved at the fridge and oil-based phantom.

For the stability and conservation study, the oil-based phantom and one of the PVP phantoms are stored in the fridge, at 7°C, and the other PVP phantom is preserved at room temperature. With this approach it is aimed to assess whether PVP phantoms are best conserved at 7°C, at room temperature (~20°C), or if no significant changes are observed between both conditions. In terms of oil-based phantoms, since the preservation protocol is well-known for this old recipe, this variable will not be assessed.

Thus, according to these different conservation strategies, from now on, the 3 phantoms will be known as:

- *Oil-based phantom*, produced with the old recipe.
- *Room T PVP phantom*, for the PVP-based phantom stored at room temperature.
- *Fridge PVP phantom*, for the PVP-based phantom stored at the fridge.

During a two-month period, all phantoms are stored under the mentioned conditions and measured on a weekly basis. The initial measurement is conducted on the day the sample is prepared (first day), and subsequent measurements are taken every seven days thereafter. From all the measurements performed over the span of two months, data has been retrieved and stored in an Excel sheet for posterior analysis in the 5.3. *Results and discussion* section.

The set of variables that are measured and monitored in the phantoms over the course of two months are the following:

- **Temperature** is measured before and after the dielectric properties' measurement, because both relative permittivity and conductivity may vary with temperature.
- **Dielectric properties**, with the intention of assessing whether they are conserved and stable over time, so that phantoms can be used to perform MiWEndo device validation measurements over long periods of time with no need for producing more phantoms.
- **Hardness** to study whether the degradation has an effect on the consistency and toughness of the phantom.
- **Water formation** to evaluate the presence of water drops underneath the phantom, as the result of its degradation.
- Finally, **visual homogeneity** is also studied with the aim of assessing whether the appearance of the phantom changes over time due to the presence of mold, bubbles...

Measurements and conservation protocols of the phantoms have both been specified and further explained in the *Annex 4. Phantom measurements and conservation protocol*.

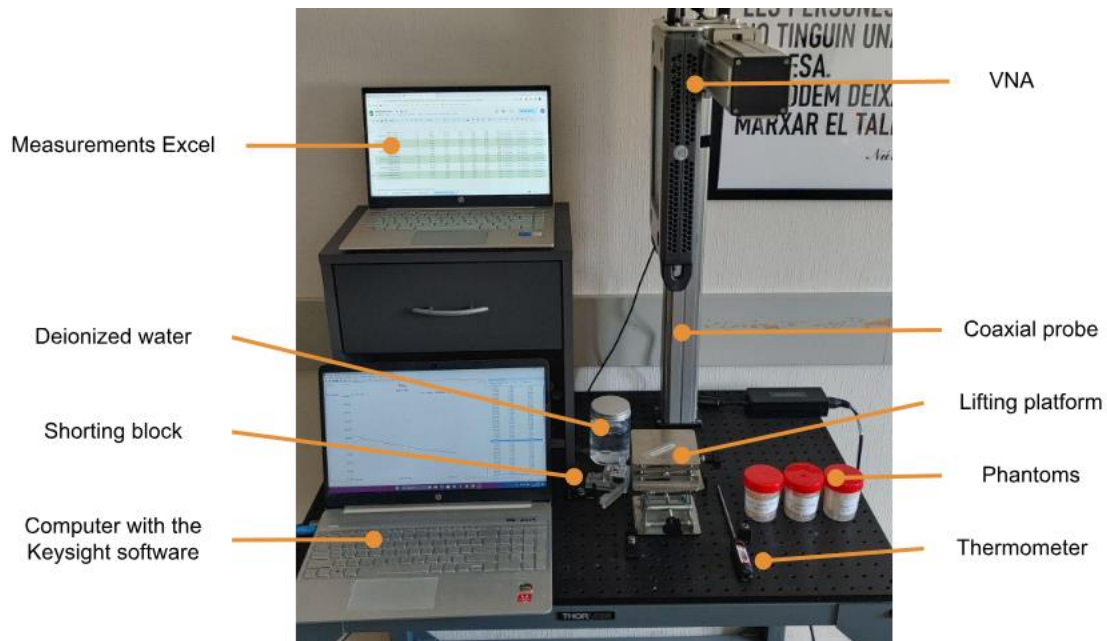


Figure 24. Setup for dielectric properties measurements.

## 5.2. Automated measuring system

The conceived automated measuring system is composed of the structure, the electronics and firmware. Each of these components will be explained in detail throughout this section.

### 5.2.1. CAD design

The design of the automated measuring system's hardware has been generated using AutoCAD. The wood-based structure of the system aims to assemble and provide support to the different electronic components. Regarding all the requirements explained in subsection 4.2. *Automated measuring system*, the final design of the system is displayed down below:



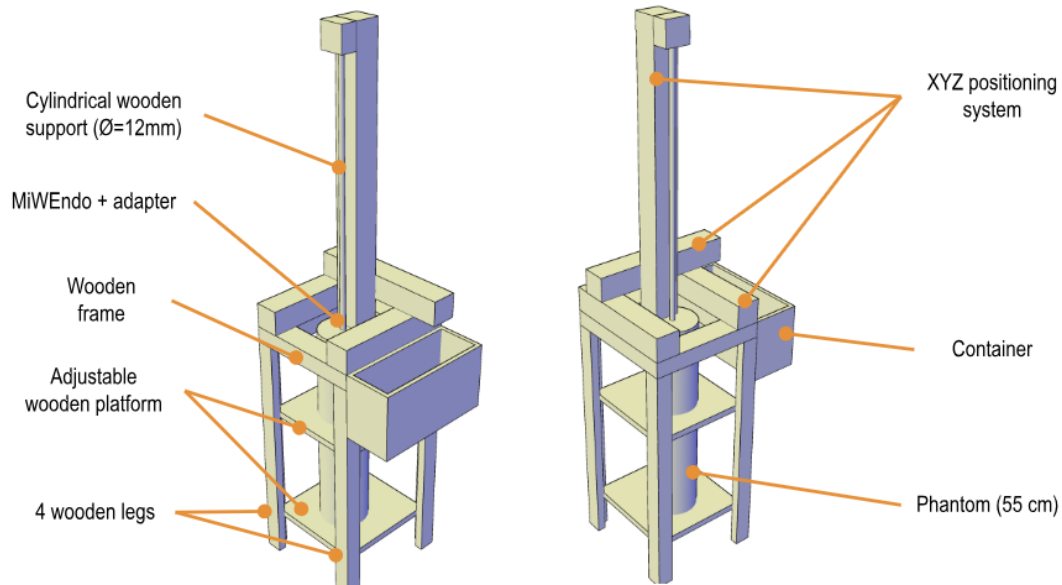


Figure 25. Automated measuring system design with AutoCAD.

The final proposed design of the automated measuring system consists of a wooden frame where the XYZ Fuyu positioning system is securely attached using screws. To correct potential unevenness, a threaded rod is incorporated to perform adjustments. This frame is supported by 4 wooden legs, each equipped at the inner part with two supports at two different heights: 20 cm and 55 cm from the wood frame's surface ( $z=0$ ). These supports are specifically designed to accommodate a wooden platform, which serves as the placement surface for the measured phantom. These two levels of the platform are intended to accommodate the different phantoms that will be measured with this automated system, which can either be 20 or 55 cm tall. Furthermore, it is crucial to ensure that the planes of both the positioning system and the platform where the phantoms are placed are parallel, in order to ensure reliable measurements.

At the z-axis slide block of the motorized positioning system, there is a cylindrical wooden support that measures 12 mm in diameter and 600 mm in length to attach the MiWEndo device. This support must be totally straight in order to avoid deviations during measurements. Furthermore, at the distal end of the cylindrical wooden support there is a 3D printed plastic adapter to accommodate the MiWEndo device.

Finally, at one side of the wooden frame there is a wooden container to store all the electronic components (drivers, Arduino Nano, power supply...) of the system.

### 5.2.2. Electronics

In terms of the electronics of the system, all the components mentioned at section 4. *Conception Engineering* have been implemented as shown in the schematics:

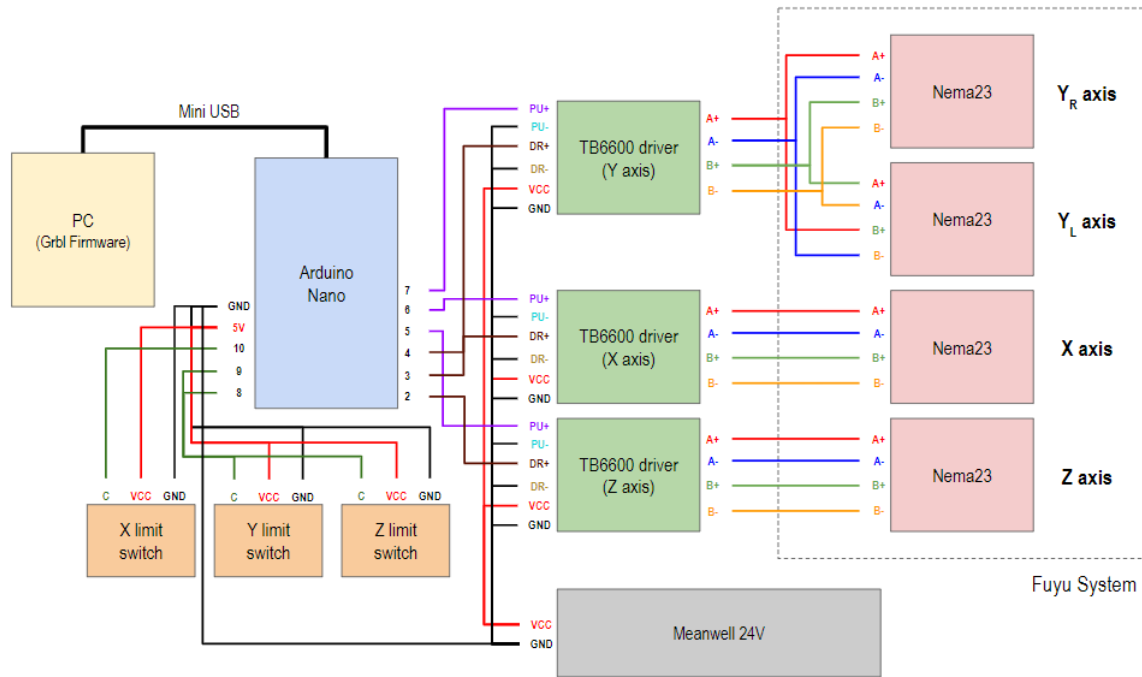


Figure 26. Electronics schematics of the automated measuring system.

First, the computer that controls the automated system with the Grbl Firmware is connected to the Arduino Nano through a mini-USB port. Three digital pins (10, 9, 8) of the Arduino Nano are connected to the XYZ axes limit switches, which limit the stroke of the motor of each axis to avoid undesired movements. If needed, more limit switches could be implemented.

Then, there are three TB6600 stepper motor drivers, one for each axis. They establish connections with the following pins:

- A+, A-, B+, B- are the stepper motor connections. Depending on the direction of rotation of the stepper motor, the order to connect the wires will change.
- PU+ and DR+ are connected to different digital pins (2-7) of the Arduino Nano board and control the administration of pulses to the stepper motors, and the direction of rotation, respectively.
- VCC is connected to the Meanwell power supply.
- PU-, DR- and GND are wired to the ground of the power source.

Furthermore, each TB6600 driver is connected to one Nema23 stepper motor that corresponds to one axis of movement of the Fuyu positioning system. Nevertheless, this positioning system has two Nema23 motors in the Y axis, and they need to rotate in opposite directions to perform a movement in the same sense. Thus, their connections with the TB6600 are inverted, and the two motors are both connected to the same driver. Since the intensity required to power these particular Nema23 is 2A, seeing that TB6600 drivers can provide up to 4A, the system will work fine.

### 5.2.3. Firmware

Grbl is an open-source software or firmware which enables motion control for CNC machines. The Grbl software uses G-code as input, and the output is the motion control signals via the Arduino, in other words, the function of the Grbl firmware is to translate the G-code into motor movement. The required steps for the configuration and implementation of the firmware will be now discussed. [73]

First, the Grbl software needs to be installed in the computer, from the Github repository [73]. Using the Arduino IDE, the Grbl library can be imported. It is vital to first check the configuration of the Arduino Nano connections because, by default, these are the pinouts for the Arduino Nano board when using Grbl v0.8 firmware:

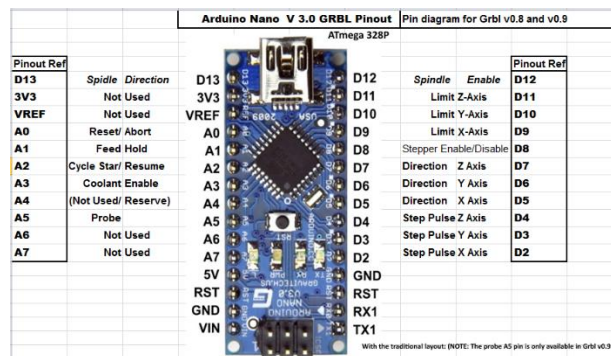


Figure 27. Pinout configuration of Arduino Nano for Grbl firmware. [76]

Thus, if the configuration of the connections implemented in the system are different from those in Figure 28, the pin assignment may be changed in the header file (*cpu\_map.h*).

```
// Define step pulse output pins. NOTE: All step bit pins must be on the same port.
#define STEP_DDR      DDRD
#define STEP_PORT     PORTD
#define X_STEP_BIT    2 // Uno Digital Pin 2
#define Y_STEP_BIT    3 // Uno Digital Pin 3
#define Z_STEP_BIT    4 // Uno Digital Pin 4
#define STEP_MASK     ((1<<X_STEP_BIT)|(1<<Y_STEP_BIT)|(1<<Z_STEP_BIT)) // All step bits

// Define step direction output pins. NOTE: All direction pins must be on the same port.
#define DIRECTION_DDR  DDRD
#define DIRECTION_PORT PORTD
#define X_DIRECTION_BIT 5 // Uno Digital Pin 5
#define Y_DIRECTION_BIT 6 // Uno Digital Pin 6
#define Z_DIRECTION_BIT 7 // Uno Digital Pin 7
#define DIRECTION_MASK ((1<<X_DIRECTION_BIT)|(1<<Y_DIRECTION_BIT)|(1<<Z_DIRECTION_BIT)) // All direction bits
```

Figure 28. Header file to tune pinout configuration in the Arduino Nano. [76]

After ensuring everything is working properly and all the pins are correctly connected, by typing “\$\$” at the Command Window of Arduino IDE, the current settings of the Arduino system are displayed. Parameters such as the step/mm, the speed of motion in mm/min or the maximum travel for each axis can be established according to the characteristics of the system. Thus, when implementing the system, it will be needed to compute how many steps of the stepper motor are required to perform a linear displacement of 1mm, which depends on the distance the nut travels when the lead-screw turns one revolution. This might be tuned with the drivers, since it allows to divide the step of the stepper motor (1.8°) to obtain the desired motion precision, so that more steps are required to perform one revolution. Furthermore, in the implemented system of this project, the maximum travels should be 100 mm for the XY axes, and 500 mm for the Z axis. [76]

```

$100=250.000 (x, step/mm)
$101=250.000 (y, step/mm)
$102=250.000 (z, step/mm)
$110=500.000 (x max rate, mm/min)
$111=500.000 (y max rate, mm/min)
$112=500.000 (z max rate, mm/min)
$120=10.000 (x accel, mm/sec^2)
$121=10.000 (y accel, mm/sec^2)
$122=10.000 (z accel, mm/sec^2)
$130=100.000 (x max travel, mm)
$131=100.000 (y max travel, mm)
$132=500.000 (z max travel, mm)
    
```

Figure 29. Example of some of the parameters that may be used to configure Grbl for the proposed system. [76]

Once completing the configuration of the Grbl firmware, it is time to establish the GCode Sender, in the computer.

As aforementioned, Grbl works in the following way: it receives G-code commands from computer-aided design (CAD) or computer-aided manufacturing (CAM) software, and it translates it into low-level signals, which are then used to control the stepper motors. G-code is a standardized programming language for CNC machines, encompassing instructions related to toolpaths, speeds, feeds, and various operations. For this purpose, the installation of a G-code compatible software such as Universal G-code Sender (UGS) is needed in the computer. [76]

For further understanding of the system, a diagram in Figure X is displayed. With the computer, G-code instructions are sent to the Grbl firmware using the Universal G-code Sender program. Then, Grbl calculates the trajectory for each axis based on the G-code commands and the machine's configuration parameters. The calculated trajectories are converted into step and direction signals for each motor. Grbl sends these signals to the motor driver, which converts them to the appropriate current and power required to drive the stepper motor. [76]

Furthermore, Grbl continuously checks the status of the CNC machine, providing real-time feedback. This feedback includes information such as the machine's position, motors speed, and any error conditions that may arise.

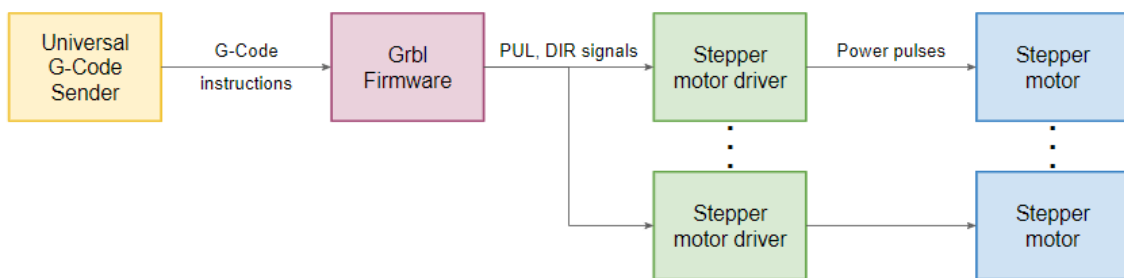


Figure 30. Diagram of the sent signals between the firmware and the hardware of the automated measuring system. [73]

### 5.3. Results and discussion

In this section, the results of the comparative study on the lifespan of each phantom recipe will be reviewed and discussed, along with the proof of concept of the measuring system.

5.3.1. Phantoms comparative study

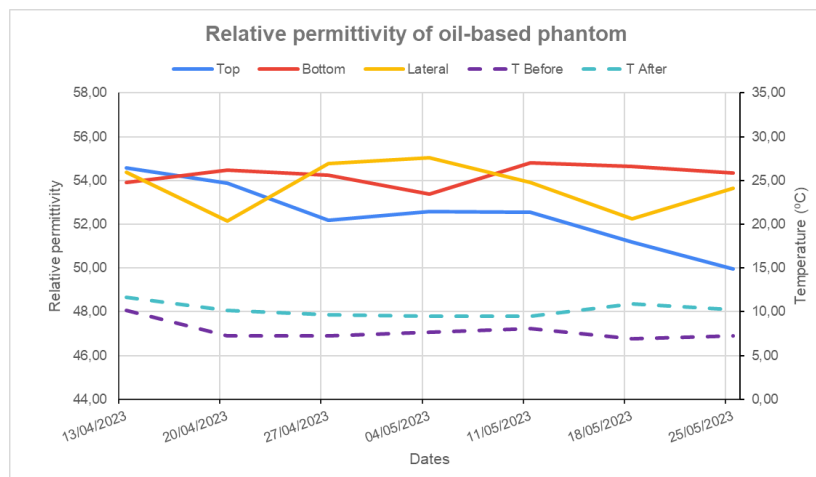
The comparative study to assess the stability and conservation of the dielectric properties, among other variables, of the two phantom recipes has been successfully conducted throughout two months, obtaining seven measurements, one per week. The results obtained will be now discussed.

First, in terms of the dielectric properties assessment, every measuring-day measurement at the top, bottom and lateral parts of each phantom were performed. Each position was measured three times, for each phantom. Furthermore, before and after conducting such measurements, the temperature of the phantoms was assessed. The evolution with time of the relative permittivity, was computed as the mean of the three measurements for each phantom and position, which is displayed in Table 10. Also, the mean temperature before and after the measurement has also been computed and represented in the secondary (right) axis of the plots in order to ensure that it is constant so that the variations in the dielectric properties' readings are not caused by it:

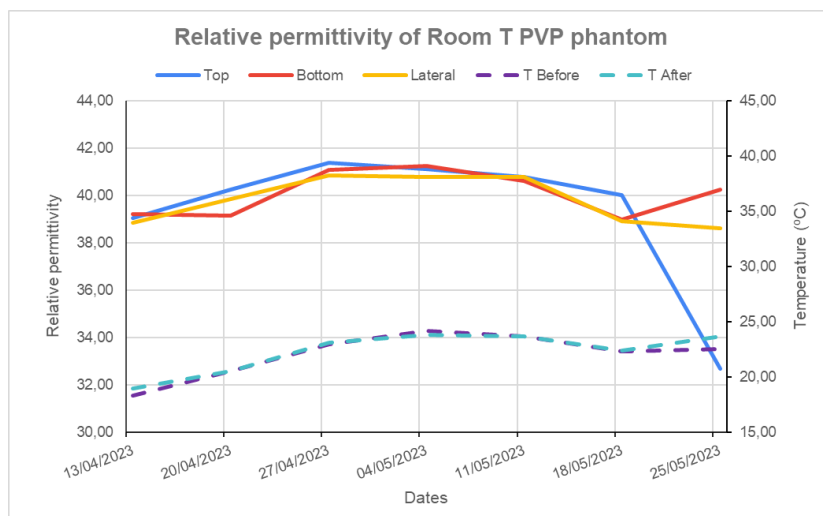
Table 10. Plots of the relative permittivity measurements (left axis) and temperature (right axis) throughout time of the oil-based phantom (top), room T-conserved PVP phantom (middle), and fridge-conserved PVP phantom (bottom).

RELATIVE PERMITTIVITY

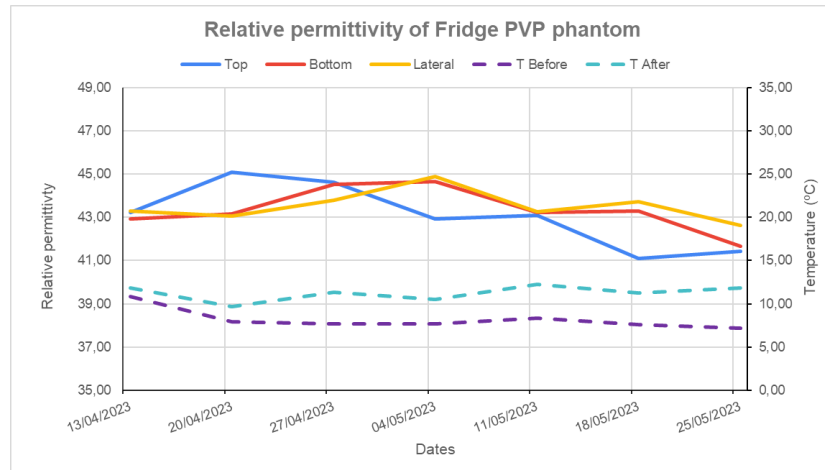
Oil-based phantom



Room T PVP phantom



Fridge PVP phantom



As it can be seen, the oil-based phantom shows the highest values of relative permittivity, with values around 52-55. At the beginning, the variation in the values between the different parts is small, but throughout the weeks, it becomes more significant, showing heterogeneity in the phantom. The top part seems to experience the most noticeable decrease in the dielectric properties. This might be related to the degradation and water evaporation of the phantom, which seems consistent considering that it is the part most prone to dry out.

When it comes to the Room T PVP phantom, it shows a relative permittivity around 39-41, with small variations between the different positions, showing large homogeneity of the phantom. Nevertheless, in week 7 measurements, the top part of the phantom shows a major decrease in the relative permittivity: it falls down to 32. This might indicate a significant degradation of the phantom, which will be discussed shortly after.

In the third place, the Fridge PVP phantom shows relative permittivity values reasonably stable, among 42-46. Different parts show similar relative permittivity values indicating homogeneity. Additionally, values tend to slightly decrease throughout, which might be a sign of degradation.

All these variations in the dielectric properties are not caused by temperature fluctuations since the temperature before and after the measurements for each phantom is almost constant throughout the two months. Thus, the changes observed among the measurements of the same phantom are most likely due to degradation processes or other factors, rather than temperature.

It can be seen a variation between the dielectric properties' values of the two PVP phantoms. Considering that both were made utilizing the same concentrations and with the same procedure, this variation might be due to the temperature difference of the phantom per se when it is being measured, that for the Fridge PVP phantom is around 10°C, and for the Room T PVP phantom is 20°C. Besides, a potential human error when elaborating the phantoms might be considered.

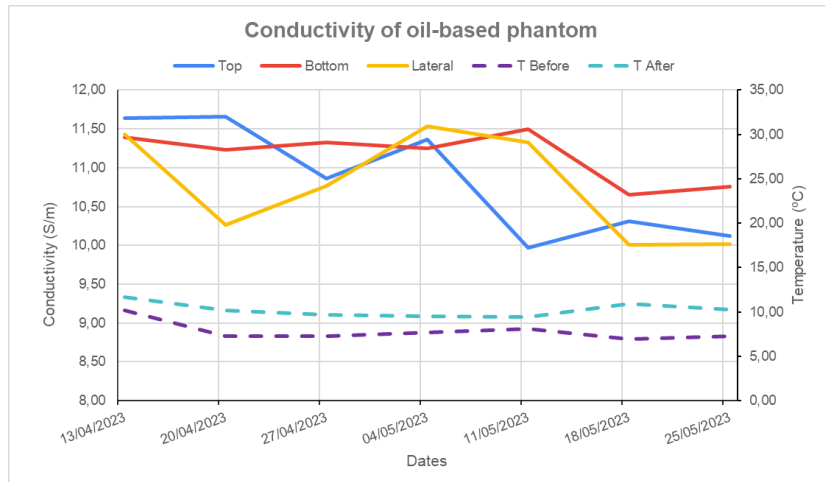
It is worth mentioning that, since this study was only performed to assess the stability of the two different phantom production protocols, although the obtained dielectric properties of the oil-based phantom are larger than those of healthy colon mucosa, it is not relevant nor problematic. The focus of interest lies in examining the variation of the particular dielectric properties established for each phantom throughout time.

Furthermore, the conductivity was also assessed using the vector network analyzer (VNA) and, similarly as before, the evolution of the obtained readings is displayed below:

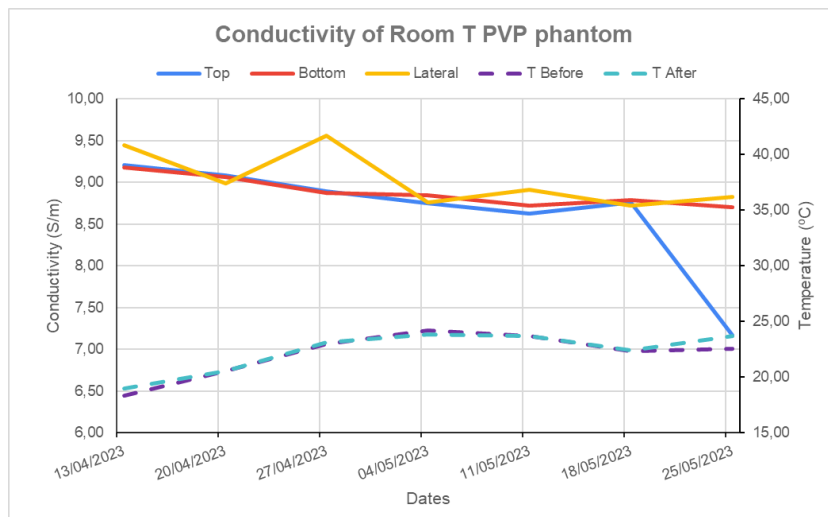
Table 11. Plots of the conductivity measurements (left axis) and temperature (right axis) throughout time of the oil-based phantom (top), room T-conserved PVP phantom (middle), and fridge-conserved PVP phantom (bottom).

**CONDUCTIVITY**

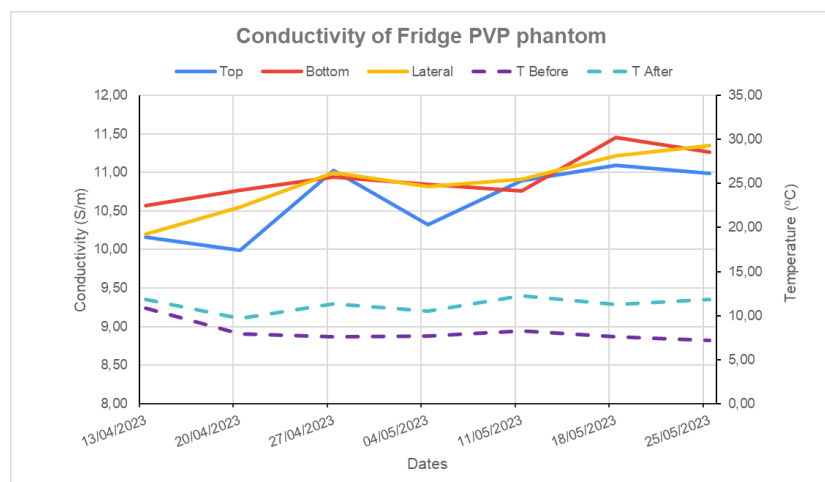
Oil-based phantom



Room T PVP phantom



Fridge PVP phantom



The largest conductivity values are shown by the oil-based phantom (10-11.5 S/m), followed by the Fridge PVP phantom (10-11 S/m). The oil-based phantom also has the largest variation in the values from different parts, indicating heterogeneity. Besides, the Room T PVP phantom also experiences a significant decrease in the conductivity on the 7th-week measurement.

By performing the mean of the measurements of top, bottom and lateral parts of each phantom, plots showing both the relative permittivity and the conductivity evolution of the three phantoms have been obtained:

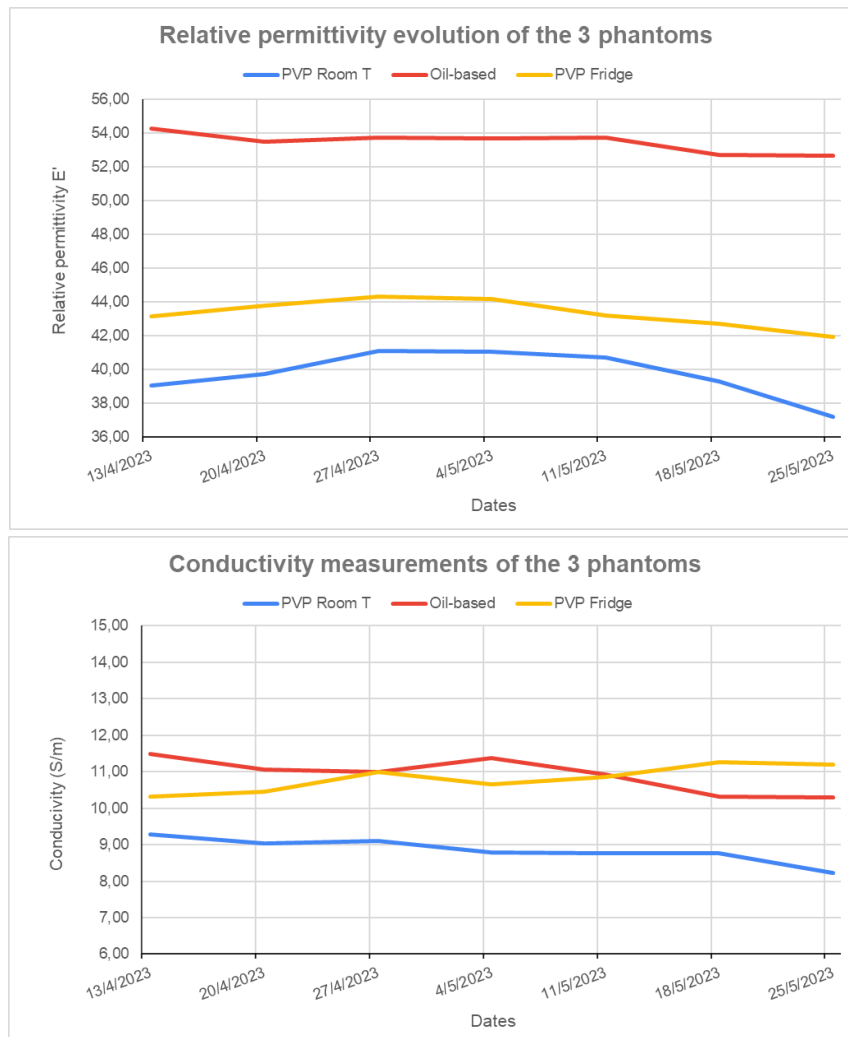


Figure 31. Plots of the relative permittivity (top) and conductivity (bottom) measurements throughout time of the three phantoms.

Figure 31 shows that, in general, the conductivity and relative permittivity values are reasonably stable for all the phantoms throughout the duration of the study. Nevertheless, it can be seen that since the 5th-week measurement, all phantoms seem to experience a decrease in the relative permittivity, indicating possible degradation of the phantoms. But due to the limited span and number of samples of the study, this conjecture is not conclusive. Finally, as aforementioned, Room T PVP phantom has a significant decrease in the dielectric properties in the 7th-week measurement.



In terms of the hardness assessment, the mean values of force measured throughout the seven-week study are displayed below. First, it can be seen that the oil-based recipe generates harder phantoms, since the force required to perform the same displacement is 12 and 20 N larger than the force required to deform the Room T PVP phantom and Fridge PVP phantom, respectively.

Between the Room T PVP-based phantom and the Fridge PVP phantom, it is clearly seen that the Room temperature one is harder with values of 10-15 N. This might be due to alterations in the jellification process or the overall fabrication process (changes in temperature, mixing...), since the concentration of agar was the same in both phantoms.

Furthermore, it can be seen that, in general, the mechanical properties of all phantoms seem reasonably stable, nevertheless, the Room T PVP phantom experiences a large increase (over 5N) in the force needed to perform the same deformation on the last day, meaning that it became harder.

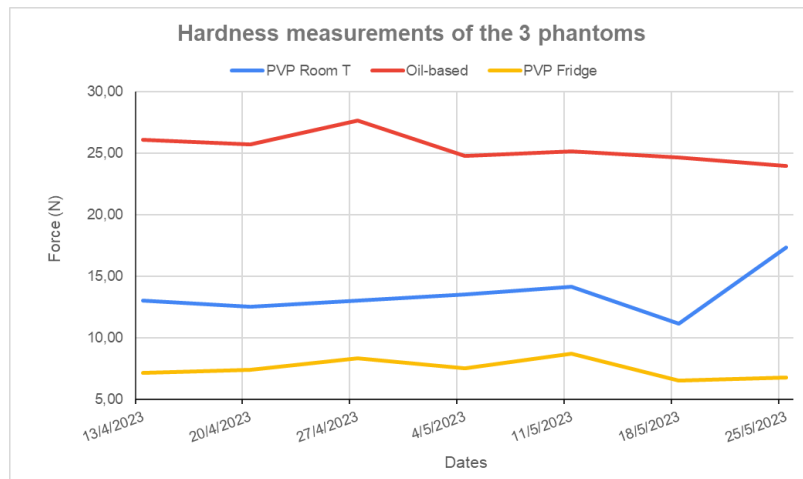


Figure 32. Plot of the hardness measurements evolution for the 3 phantoms

In terms of visual homogeneity, down below, an image of the three phantoms after the first measurement is displayed:



Figure 33. Images of the oil-based phantom (left), Room T PVP phantom (middle) and Fridge PVP phantom (right), after the first measurement.

And after the last measurement:

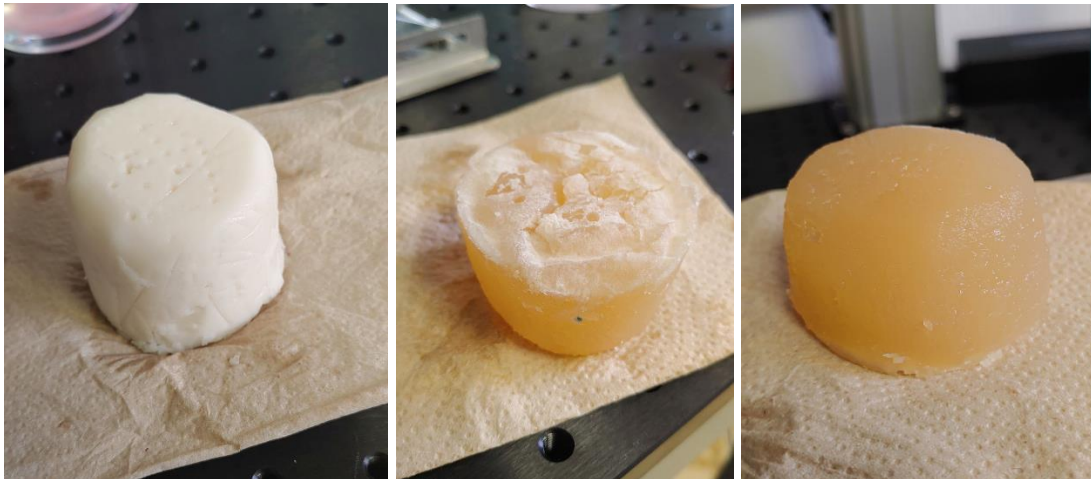


Figure 34. Images of the oil-based phantom (left), Room T PVP phantom (middle) and Fridge PVP phantom (right), after the last measurement.

It is worth noticing that both oil-based phantom and Fridge PVP-based phantom did not experience notorious changes in their visual appearance throughout the study. Nonetheless, on the 6th-week measurement day, the Room T PVP phantom showed a small colony of mold at the lateral part. By the time the seventh measurement was conducted, the mold had covered all the top surface of the phantom. The places where the mold was growing appeared drier and stiffer, which is consistent with the decreased dielectric properties measured on the 25/05/2023, especially on the top part of the Room T PVP phantom. Besides, the mechanical properties also appeared altered since the phantom became harder.

In terms of water formation, the phantom that showed more drops at the bottom of the container was the oil-based phantom.

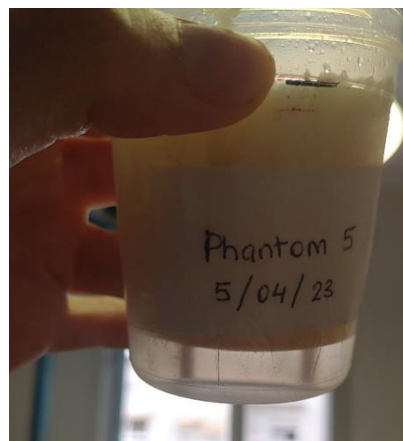


Figure 35. Water formation under oil-based phantom on day 25/05/2023.

From this study it can be concluded that the conservation protocol for the PVP phantoms should be their preservation in the fridge to avoid the growth of mold that ultimately modifies the properties of the phantom.

In terms of the best fabrication recipe, since no significant variations of the dielectric and mechanical properties have been noticed during the duration of the study in both the oil-based and the Fridge PVP phantoms, it cannot be concluded whether the PVP phantom recipe provides an increased lifespan in the production of MWI phantoms with respect to the old oil-based recipe. Further studies that include measurements over longer periods of time should be conducted in order to obtain more significant and conclusive results.

For further information, check the tables with all the measured values displayed in Annex 5.

### 5.3.2. Proof of concept of the automated measuring system

In order to have a preliminary assessment of the validity of the system, a proof of concept of the automated measuring system has been carried out. The aim of this trial is to verify that the controller-driver-motor assembly works correctly and determine whether further implementation of the system seems viable.

The proof of concept consists in the implementation of a single motor Nema17, simulating one of the axes of the positioning system. The stepper motor is controlled with its corresponding TB6600 driver and an Arduino Nano. The driver is connected to the digital pins 2 and 3 of the Arduino board. The whole system is powered using a Meanwell 24V power supply. As firmware, a simple code with Arduino IDE has been written in order to perform rotations of the motor in both directions, clockwise and anticlockwise simulating the movement of the MiWEndo device in the two senses of one axis. The used code is displayed in Annex 6.

A further schematic of the implemented system is displayed below:

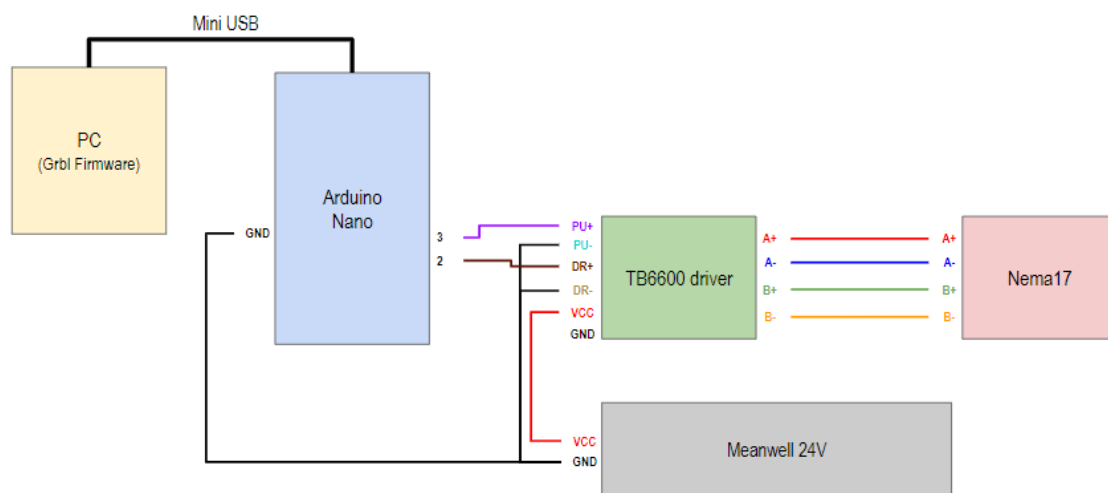


Figure 36. Schematic of the proof of concept.

The actual implemented circuit system is shown:

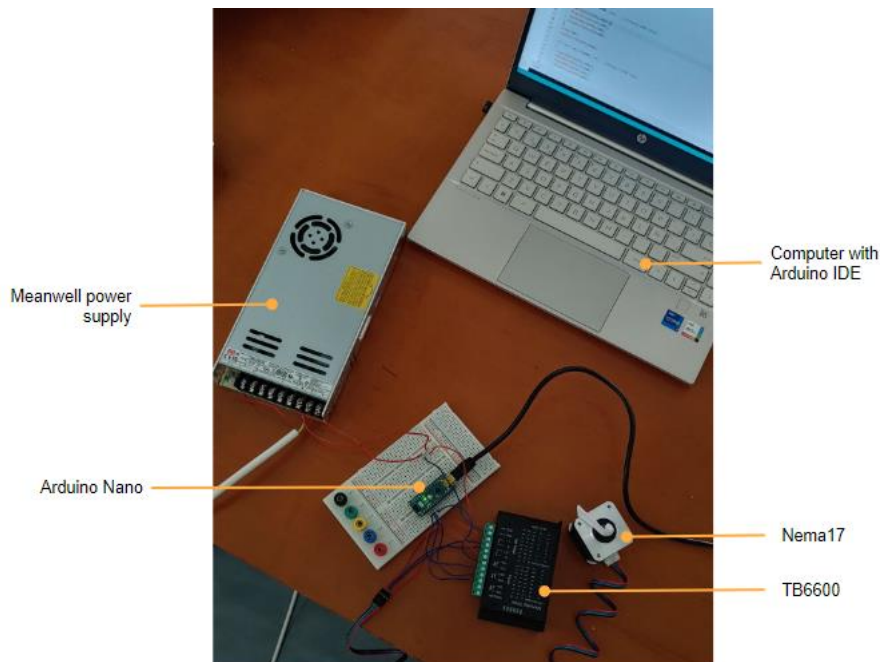


Figure 37. Proof of concept setup.

The proof of concept has been successful, since the motor could be both rotated in clock and anticlockwise, as desired, which in the actual system would translate into movement in both senses of one axis. This simple experimentation has shown a preliminary validity of the automated measuring system, making reasonable to further implement it. Once having the rest of the components, applying the methods described in section 5.2. *Automated measuring system*, this proof of concept could be extrapolated to build the actual complete system: the same connections can be established between the motors and the drivers, each driver is connected to two digital ports of the Arduino Nano, and Grbl is configured according to the connections and properties of the motors. Finally, when all the components are integrated, further validation stages would be required in order to test the repeatability of the measurement that the system provides.

## 6. TECHNICAL VIABILITY: SWOT ANALYSIS

Taking into account the proposed solution, in this section a SWOT analysis has been carried out to study the strengths, weaknesses, opportunities and threats of the implementation of the project, and thus analyze its technical viability.

Table 12. SWOT analysis of the project

STRENGTHS	WEAKNESSES
<ul style="list-style-type: none"> <li>○ High motivation of the author.</li> <li>○ Clear definition of the project and its global objectives.</li> <li>○ Guidance and support of the MiWEndo team and especially of my mentor.</li> <li>○ Resources for dielectric properties assessment (VNA...).</li> <li>○ New and simple phantom recipe that just requires 3 ingredients.</li> </ul>	<ul style="list-style-type: none"> <li>○ Limited time.</li> <li>○ Small number of samples in the MWI phantoms comparison study.</li> <li>○ Lack of experience of the author in the field.</li> <li>○ Room for design improvements of the measuring system.</li> <li>○ Until its implementation, the performance of the automated system cannot be validated.</li> </ul>
OPPORTUNITIES	THREATS
<ul style="list-style-type: none"> <li>○ Both the colonoscopy and the imaging phantoms markets are in constant growth.</li> <li>○ Alternative to animal testing.</li> <li>○ Necessity of improved repeatability of the measurements.</li> <li>○ New phantom recipe for MWI endoscopic applications.</li> <li>○ Evidence that PVP might produce a more-stable-in-time phantom recipe because it is inorganic.</li> <li>○ Both the phantom recipe and the measuring system could be adapted for the validation of other projects of MiWEndo Solutions.</li> </ul>	<ul style="list-style-type: none"> <li>○ New phantom recipe for colon MWI, never done before.</li> <li>○ Lack of standardized protocols for PVP phantom fabrication.</li> <li>○ Limited bibliographic information on the topic.</li> <li>○ High cost of the motorized positioning systems.</li> <li>○ Delays on electronic providers as a result of microchip crisis.</li> </ul>

The first row of Table 12 shows the strengths and weaknesses of the proposed solutions that allow an internal analysis of the project.

To start with, this final degree project has several strengths that contribute to its success. The author's high motivation towards the project, combined with the guidance and support from the

MiWEndo team, especially the author's mentor, play a crucial role. Besides, from a very early stage, the definition of the project and its global objectives were clearly defined. The entire project has been conducted at the MiWEndo Solutions office, which provides access to all the necessary resources for measuring dielectric properties, including a new vector network analyzer (VNA) setup. Additionally, the development of the new phantom recipe in this project is characterized by its simplicity, as it only requires three ingredients and basic tools for implementation.

Nevertheless, the project does have several notable weaknesses that need to be addressed. Firstly, the most significant weakness is the limited timeframe, which has impacted various aspects of the project. It has constrained the monitoring of the phantoms to only 7 weeks, making it difficult to draw conclusive findings that could be derived from longer-term studies. Secondly, the phantom comparison study has been conducted with just three phantoms, for more consistent results it should be repeated more times with a larger sample size. Additionally, the author presents a limited expertise in the field, i.e. in phantom fabrication and automated measuring systems' conception. Thus, there is certainly room for design improvements of the measuring system, but until the actual implementation of the system, its performance cannot be evaluated nor enhanced.

On the other hand, the second row of the table shows the external opportunities and threats that may affect the proposed project. In terms of opportunities, this project is framed within two rapidly expanding markets: colonoscopy and imaging phantoms markets. Besides, the techniques developed in the project offer an alternative to animal testing during the medical device validation stage, while also improving the repeatability of the measurements, which is vital during this evaluation phase. Although it might be challenging, the innovative nature of the phantom recipe for MWI endoscopic applications developed in the project opens up numerous opportunities in an unexplored field. Additionally, there is scientific evidence that PVP might produce a more stable phantom recipe with an increased life span because it is inorganic. In the near future, both the phantom recipe and the measuring system could be adapted for validating upcoming projects at MiWEndo Solutions, such as the automatic diagnosis of gynecological cancer.

Finally, there are several significant challenges and potential risks associated with this project, which are summarized in the table as 'Threats'. One major concern is the novelty of this new phantom recipe since it has never been used before for colon MWI. Besides, there is a considerable lack of standardized protocols for PVP phantom fabrication in the MWI field, even for non-endoscopic applications. Additionally, there is limited bibliographic information on the development of such phantoms or the conception of automated measuring systems, due to the highly specific and novelty nature of the entire project. Lastly, the high cost of motorized XYZ-positioning systems poses another significant obstacle to the conception and selection of components for the measuring system.

## 7. ECONOMIC VIABILITY

In this section, the total economic costs of the project are reviewed. The total cost of the project includes the cost of producing phantoms with the oil and PVP recipes, purchasing all the components for the automated measuring system implementation, and the salary of the workers.

In Table 13 all the material resources used in the project have been separated between those needed for the phantoms development and for the automated measuring system implementation. Multiplying the cost of each unit, by the number of units needed of each item, the total approximate price has been computed. Furthermore, in terms of human resources, it has been considered that this project is majorly conducted by a biomedical engineering student that has a salary of 15€/h, and a supervisor that assists the student throughout the project, who gets paid 30€/h. With these salaries and knowing the hours worked, the total cost of human resources has been calculated.

Table 13. Direct costs of the project.

Concept: Material resources	Units	Unit price	Total price
<i>Phantoms</i>			
Polyvinylpyrrolidone (PVP-40) 500g	1	29.99 €	29.99 €
Agar E-406 (Quimics Dalmau) 250g	1	20.00 €	20.00 €
Deionized water 2L	1	1.20 €	1.20 €
Sunflower oil 1L	1	1.95 €	1.95 €
Dishwashing liquid (Mistol) 650 ml	1	2.55 €	2.55 €
Glass beaker 500 ml	2	4.99 €	9.98 €
Urine container 100 ml	3	0.50 €	1.50 €
Cardboard cups	10	0.20 €	2.00 €
Thermometer (Digital Cooking Food Probe)	1	4.09 €	4.09 €
Hot plate	1	23.90 €	23.90 €
Glass stirring rod	1	1.12 €	1.12 €
Aluminum foil	1	3.79 €	3.79 €
<i>Automated measuring setup</i>			
FUYU FSK40 Gantry Linear Guide Stage 100x100x500	1	810.52 €	810.52 €
TB6600 Stepper motor driver	4	8.99 €	35.96 €
Arduino Nano	1	21.60 €	21.60 €
Meanwell Power supply 24V	1	36.14 €	36.14 €
Nema17 Stepper motor	1	11.54 €	11.54 €
Arduino IDE	1	0 €	0 €
Grbl Software	1	0 €	0 €
AutoCAD Software	1	0 €	0 €
Wood structural support	1	150.00 €	150.00 €
MiWEndo adaptor	1	3.50 €	3.50 €
<b>TOTAL MATERIAL RESOURCES</b>			<b>1171.33 €</b>

Concept: Human resources	Hours	Price/hour	Total price
Biomedical engineering student	300 h	15.00 €/h	4500.00 €
Supervisor	20 h	30.00 €/h	1000.00 €
<b>TOTAL HUMAN RESOURCES</b>			<b>5500.00 €</b>

Indirect costs of the project have also been considered, which stand for the usage of the facilities and equipment at MiWEndo Solutions office, such as the VNA setup, computers or the 3D printer. Furthermore, it also considers the usage of electricity and other employees' salaries. It is computed as 12% of the total direct costs. Thus, by adding the indirect and the direct costs, the total cost of the project is obtained:

Table 14. Approximation of the total cost of the project.

Type of cost	Concept	Cost
Direct costs	Material resources	5500.00 €
	Human resources	1171.33 €
Indirect costs	Structural costs (12%)	800.56 €
<b>TOTAL COST OF THE PROJECT</b>		<b>7471.89 €</b>

The total cost of the project is **7471.89 €**. Note that this final calculation includes the components to implement the automated measuring system, in order to obtain a first approximation of the economic feasibility of the actual implementation and integration of the system, along with the new phantom production.



## 8. EXECUTION SCHEDULE

This section focuses on the techniques that have been implemented to organize the project and to accomplish productivity. Hence, the Work Breakdown Structure (WBS) has been elaborated in order to establish and detail each one the tasks that need to be fulfilled with the aim of achieving the final goal of the project. Besides, the Program Evaluation and Review Technique with its Critical Path Method (PERT-CPM) and GANTT diagrams have been developed with the aim of studying the work schedule and ensuring proper time and resources management.

### 8.1. Work Breakdown Structure (WBS)

The Work Breakdown Structure (WBS) is a project management tool based on the hierarchic decomposition of the final project scope into simpler and more manageable tasks. The WBS eases the planification, execution, and monitoring of the project activities by giving a clear and structured perspective of the project scope, timeline, and budget. The final project is typically shown at the top of a tree structure, with the tasks and subtasks underneath. Each task is defined by a deliverable that has quantifiable results that may be used to track progress.

The WBS of the project is presented in Figure 38:

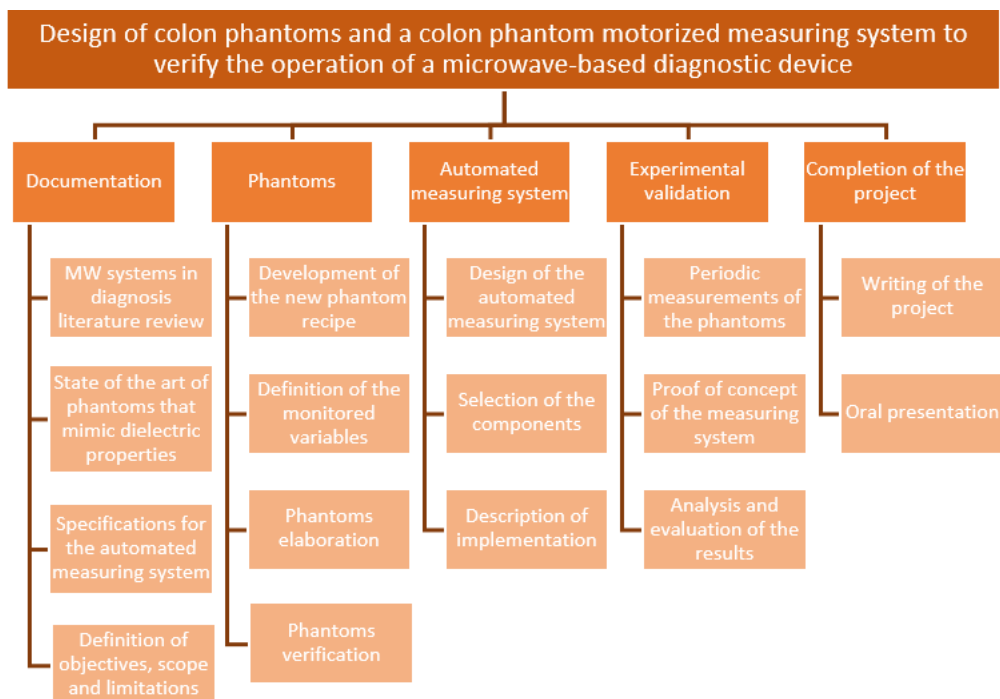


Figure 38. WBS of the project.

As it is portrayed in Figure 38, the project is split into five basic levels, each of which is then divided into several simpler work packages. Each of these packages will be now presented in the WBS dictionary with a brief explanation that will include the description of the package, the deliverables, and the estimated duration.

Table 15. WBS dictionary of the task *1.Documentation*.

<b>1. Documentation</b>	
<b>1.1. Microwave systems in diagnosis literature review</b>	
<b>Package description</b>	Extensive research on microwave systems in diagnosis, as well as the dielectric properties of biological tissues.
<b>Deliverables</b>	Obtention of a bibliographic references list.
<b>Estimated duration</b>	2 weeks
<b>Predecessors</b>	-
<b>Antecessors</b>	1.2. State of the art of phantoms that mimic dielectric properties 1.3. Specifications for the automated measuring system
<b>1.2. State of the art of phantoms that mimic dielectric properties</b>	
<b>Package description</b>	In depth review on the currently-used phantoms for mimicking dielectric properties of tissues for MWI in order to find a new recipe for phantom elaboration.
<b>Deliverables</b>	Obtention of bibliographic references for posterior writing of the section: 2.2. <i>State of the art</i> .
<b>Estimated duration</b>	2 weeks
<b>Predecessors</b>	1.1. Microwave systems in diagnosis literature review
<b>Antecessors</b>	1.4. Definition of objectives, scope and limitations
<b>1.3. Specifications for the automated measuring system</b>	
<b>Package description</b>	After a market analysis, establish the required characteristics of the automated measuring system so that it allows the performance of accurate and repeatable measurements of phantoms.
<b>Deliverables</b>	List of specifications of the automated measuring system.
<b>Estimated duration</b>	2 weeks
<b>Predecessors</b>	1.1. Microwave systems in diagnosis literature review
<b>Antecessors</b>	1.4. Definition of objectives, scope and limitations
<b>1.4. Definition of objectives, scope and limitations</b>	
<b>Package description</b>	Determine the aim of the work, what it intends to solve and how. Specify the scope of the topic that will be covered and be aware of the limitations of the project.
<b>Deliverables</b>	Writing of the sections: 1.2. <i>Objectives</i> and 1.4. <i>Limitations and scope</i> .
<b>Estimated duration</b>	1 week

<b>Predecessors</b>	1.2. State of the art of phantoms that mimic dielectric properties 1.3. Specifications for the automated measuring system
<b>Antecessors</b>	2.1. Development of the new phantom recipe 3.1. Design of the automated measuring system 5.1. Writing of the project

 Table 16. WBS dictionary of the task *2.Phantoms*.

<b>2. Phantoms</b>	
<b>2.1. Development of the new phantom recipe</b>	
<b>Package description</b>	Elaborate a new procedure in order to obtain PVP-based colon phantoms with the desired dielectric properties and consistency.
<b>Deliverables</b>	Writing of the new PVP phantom recipe.
<b>Estimated duration</b>	3 weeks
<b>Predecessors</b>	1.4. Definition of objectives, scope and limitations
<b>Antecessors</b>	2.2. Definition of the monitored variables 2.3. Phantoms elaboration
<b>2.2. Definition of the monitored variables</b>	
<b>Package description</b>	Determine the variables that will be monitored during the duration of the project in order to assess the stability and conservation of the elaborated phantoms. Besides, define how they are going to be measured.
<b>Deliverables</b>	Phantom measurements protocol.
<b>Estimated duration</b>	1 week
<b>Predecessors</b>	2.1. Development of the new phantom recipe
<b>Antecessors</b>	2.4. Phantoms verification
<b>2.3. Phantoms elaboration</b>	
<b>Package description</b>	Prepare three phantoms: two PVP-based phantoms with the new recipe and one made with the currently-used recipe (oil- based).
<b>Deliverables</b>	Obtention of the three phantoms.
<b>Estimated duration</b>	1 week
<b>Predecessors</b>	2.1. Development of the new phantom recipe
<b>Antecessors</b>	2.4. Phantoms verification

<b>2.4. Phantoms verification</b>	
<b>Package description</b>	Ensure that the elaborated phantoms have the desired dielectric properties and consistency. Repeat the elaboration of the phantoms if they do not meet the requirements.
<b>Deliverables</b>	Measurements of the elaborated phantoms and obtention of verified phantoms.
<b>Estimated duration</b>	1 week
<b>Predecessors</b>	2.2. Definition of the monitored variables 2.3. Phantoms elaboration
<b>Antecessors</b>	4.1. Periodic measurements of the phantoms

Table 17. WBS dictionary of the task 3. Automated measuring system.

<b>3. Automated measuring system</b>	
<b>3.1. Design of the automated measuring system</b>	
<b>Package description</b>	After exhaustive research, develop a design of the automated measuring system that fulfills the established requirements.
<b>Deliverables</b>	Draft of the conceived automated measuring system.
<b>Estimated duration</b>	3 weeks
<b>Predecessors</b>	1.4. Definition of objectives, scope and limitations
<b>Antecessors</b>	3.2. Selection of the components
<b>3.2. Selection of the components</b>	
<b>Package description</b>	Look for the specific hardware components needed for the automated measuring system, purchase them and wait for the acquisition.
<b>Deliverables</b>	List of the components with their respective providers.
<b>Estimated duration</b>	3 weeks
<b>Predecessors</b>	3.1. Design of the automated measuring system
<b>Antecessors</b>	3.3. Description of implementation
<b>3.3. Description of implementation</b>	
<b>Package description</b>	Properly describe the different components (hardware and software) to ensure correct functioning of the system.
<b>Deliverables</b>	Writing of the implementation of the system

<b>Estimated duration</b>	3 weeks
<b>Predecessors</b>	3.2. Selection of the components
<b>Antecessors</b>	4.2. Proof of concept of the measuring system

 Table 18. WBS dictionary of the task 4. *Experimental validation*.

<b>4. Experimental validation</b>	
<b>4.1. Periodic measurements of the phantoms</b>	
<b>Package description</b>	Perform weekly measurements of the different phantoms following the previously written <i>Phantom measurements protocol</i> in order to monitor their stability and conservation.
<b>Deliverables</b>	An Excel sheet that contains the periodic measured variables of the different phantoms.
<b>Estimated duration</b>	8 weeks
<b>Predecessors</b>	2.4. Phantoms verification
<b>Antecessors</b>	4.2. Analysis and evaluation of the results
<b>4.2. Proof of concept of the measuring system</b>	
<b>Package description</b>	Perform a proof of concept of the designed automated measuring system to study its preliminary viability.
<b>Deliverables</b>	Implementation of the proof of concept.
<b>Estimated duration</b>	3 weeks
<b>Predecessors</b>	3.3. Description of implementation
<b>Antecessors</b>	4.2. Analysis and evaluation of the results
<b>4.3. Analysis and evaluation of the results</b>	
<b>Package description</b>	Examine and interpret the obtained results of the measurements from the phantoms and evaluate the proof of concept of the automated measuring system.
<b>Deliverables</b>	Analysis of the measurements, evaluation of the proof of concept and writing of the main derived conclusions.
<b>Estimated duration</b>	2 weeks
<b>Predecessors</b>	4.1. Periodic measurements of the phantoms 4.2. Proof of concept of the measuring system

<b>Antecessors</b>	5.2. Oral presentation
--------------------	------------------------

 Table 19. WBS dictionary of the task 5. *Completion of the project*

<b>5. Completion of the project</b>	
<b>5.1. Writing of the project</b>	
<b>Package description</b>	Development of the written project that will be submitted in June 2023.
<b>Deliverables</b>	Written final bachelor thesis.
<b>Estimated duration</b>	16 weeks
<b>Predecessors</b>	1.4. Definition of objectives, scope and limitations
<b>Antecessors</b>	5.2. Oral presentation
<b>5.2. Oral presentation</b>	
<b>Package description</b>	Elaboration of the PowerPoint presentation and preparation of the explanation to be done during the oral exposition of the final project.
<b>Deliverables</b>	PowerPoint that summarizes the work done and written explanation that will be presented.
<b>Estimated duration</b>	1 week
<b>Predecessors</b>	4.2. Analysis and evaluation of the results 5.1. Writing of the project
<b>Antecessors</b>	-

## 8.2. PERT-CPM diagram

A PERT-CPM diagram has been created in order to efficiently coordinate all of the necessary tasks and meet the project's deadline. In this diagram, all the tasks that need to be completed, their time, and their relationship are visually displayed. It indicates which tasks must be completed first and which must come later.

Firstly, all the activities described in the WBS have been included in Table 20, indicating the chronological dependence that exists between them and their duration.

Table 20. Collection of the chronological dependencies of the activities with their respective ID and duration

WBS code	ID PERT	Previous tasks	Posterior tasks	Time (in weeks)
1.1.	A	-	B, C	2
1.2.	B	A	D	2

1.3.	C	A	D	2
1.4.	D	B, C	E, I, N	1
2.1.	E	D	F, G	3
2.2.	F	E	H	1
2.3.	G	E	H	1
2.4.	H	F, G	L	1
3.1.	I	D	J	3
3.2.	J	I	K	3
3.3.	K	J	M	3
4.1.	L	H	N	8
4.2.	M	K	N	3
4.3.	N	L, M	P	2
5.1.	O	D	P	16
5.2.	P	N, O	-	1

From these precedences, the chronological order of the tasks is set, so that the PERT diagram with all the activities and nodes can be drawn. In each node of the diagram, two times are displayed: on the left, the *early time* which is the minimum time necessary in order to perform a task; and on the right, the *last time* that indicates the latest time in which a task can be completed. From these definitions, the critical path of the project can be found. The critical path is the trajectory composed of all the activities that, in case of a delay, would modify the final timing of the project, in other words, it indicates the minimum time needed to complete the entire project.

Using the method Activity-on-arc (AOC), the PERT diagram of the project has been elaborated and it is displayed in Figure 39.

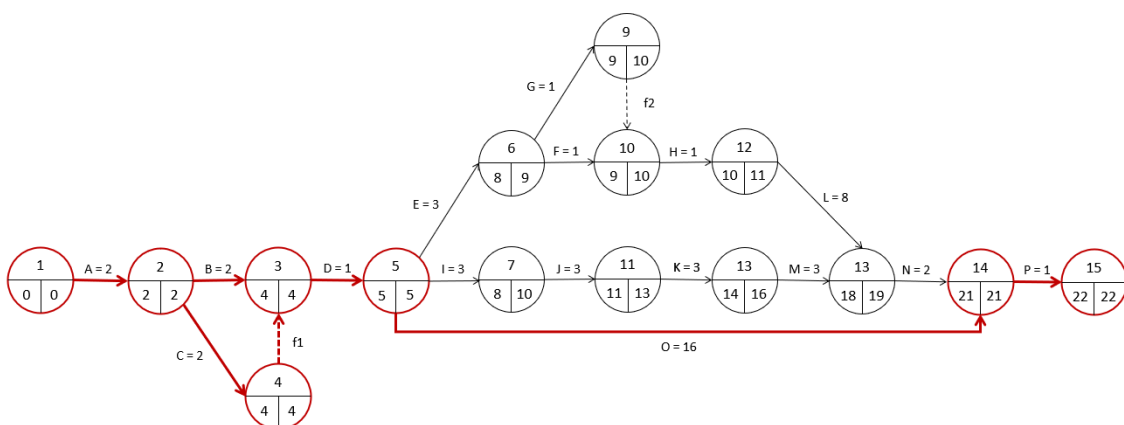


Figure 39. PERT-CPM diagram.

In this diagram, it can be observed that the estimated duration of the project is of 22 weeks, that is, from mid-January to early June. Furthermore, this project has 18 activities: 16 real activities (from

A to P) and 2 fictitious ones (f1 and f2). In this PERT, the critical path of the project has been indicated in red and it consists of the events A, B, C, D, O and P.

### 8.3. GANTT diagram

A GANTT chart is a horizontal bar chart used in project management to display all the tasks of a project against time. Each activity is represented by a bar: the position and length of the bar reflects the start date, duration and end date of the activity. Hence, in this last part of the 8. *Execution schedule* section, the GANTT diagram of the project has been developed in order to study and manage the temporal evolution of all the activities described in previous sections.

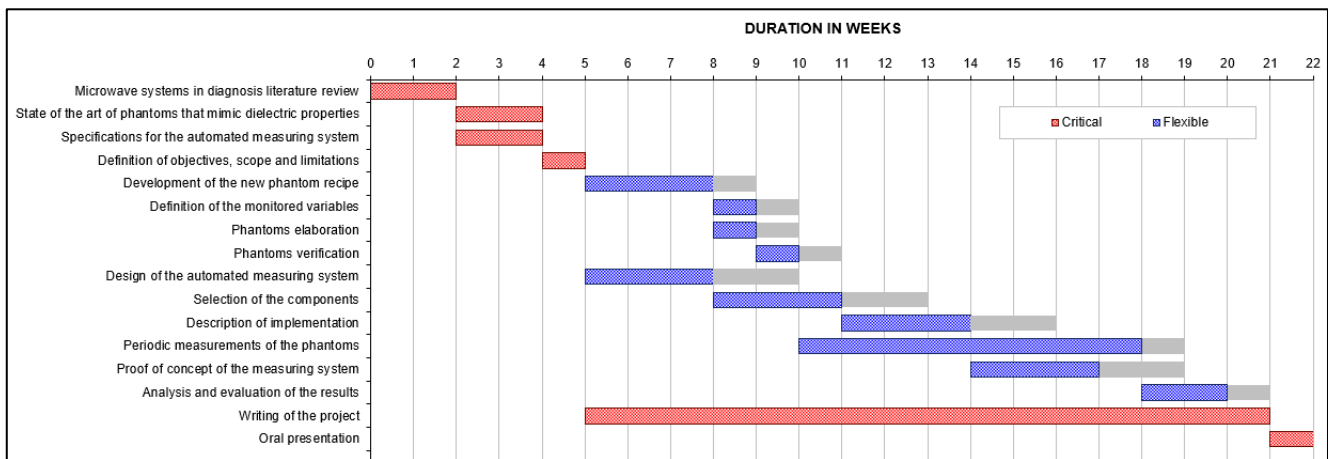


Figure 40. GANTT diagram. Template from: [77]

It has been considered that the project was initiated on the 9th of January 2023, and since it lasts over 22 weeks, it will be finished on the 12th of June 2023 with the oral presentation. In the diagram, all those tasks that compose the critical path are colored in red, those that are flexible are shown in blue, and their slack is indicated in gray. The whole experimental part, both the elaboration and measurement of the phantoms and the development of the automated measuring system, will be carried out in parallel for further efficiency. Finally, it can be observed that the measuring system subproject has a slack of 2 weeks, hence, its development might be adapted to other stages of the project that may be more time constrained.



## 9. LEGISLATION AND REGULATION

MiWEndo Solutions is a spinoff based in Barcelona devoted to the development of a MWI endoscopic probe for CRC diagnosis. The market of such a medical device is global, thus MiWEndo Solutions, as a manufacturer of medical devices, must obtain the marketing authorization in all the target countries. The target countries of MiWEndo Solutions are Europe, United States and Japan because they concentrate the vast majority of the market share of colonoscopic devices. This project is focused on the European framework. In The European Union, the current legislation for medical devices is the Medical Devices Regulation (MDR) 2017/745. The MDR compliance is mandatory to be able to place Medical Devices on the European market. The MDR is designed to ensure a high level of safety and performance for medical devices and aims to improve transparency and accountability throughout the entire supply chain. It sets out the requirements for the design, manufacture, labeling, and packaging of medical devices, as well as the clinical evaluation and post-market surveillance of these devices. [78]

Nonetheless, considering that the development and execution of this project has been focused on developing a system for the validation process of a medical device the MDR does not apply. Figure X shows the medical device lifecycle where the different development phases of a MD are depicted. As it can be seen, the verification and validation stage are under the umbrella of the Quality Management System defined by the ISO 13485.

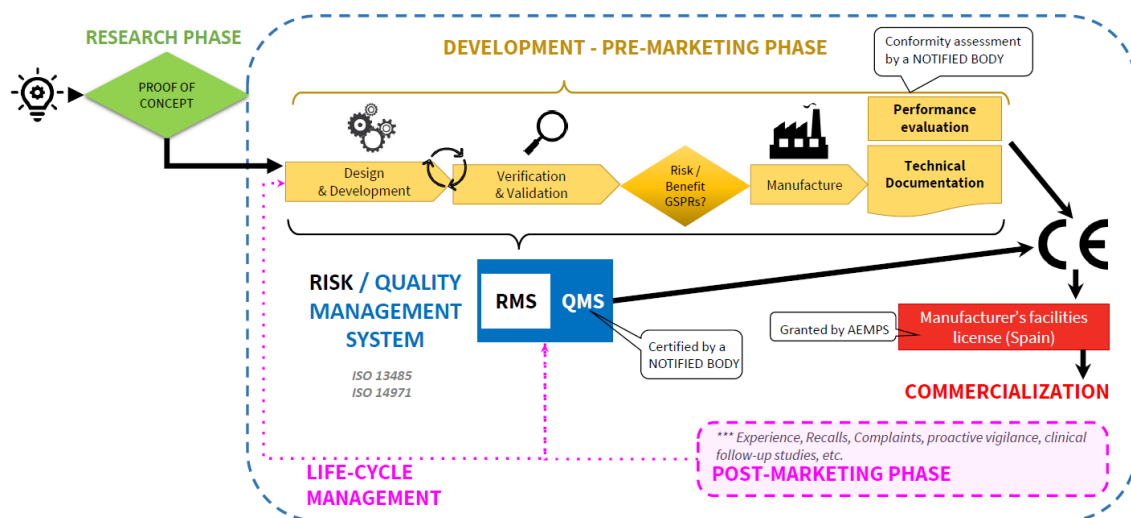


Figure 41. Schematic of a medical device's lifecycle.[39]

The ISO 13485 provides requirements for the development, implementation, and maintenance of the quality management system (QMS) for medical devices, which covers all aspects of the medical device lifecycle, including design, development, validation, production, storage and distribution. ISO 13485 assures a commitment to quality and increasing efficiency within the organization, reduces entry barriers to foreign markets, and facilitates the attainment of ISO 9001 certification. [79]

According to EMA (European Medicines Agency), *validation* is the process of providing proof that a method works and satisfies the specified requirements and is suitable for its intended application. Specifically, *medical device validation* refers to the process of ensuring that the device operates as

meant to guarantee that every gadget is safe to use and will function properly for all patients, with no room for error or harm. Furthermore, ISO 13485 establishes several aspects that must be considered in validation: preparation of a validation protocol, execution of the validation, drafting of the validation reports and their conclusions on whether the system is valid for its use in the production process. [80,81]

Compliance with ISO 13485 in the validation and preclinical trials of a medical device involves ensuring that the QMS includes appropriate procedures for these activities, that the procedures are followed, and that the documentation is maintained. This helps to ensure that the medical device is safe and effective for its intended use, and that it meets regulatory requirements. It is important to note that compliance with ISO 13485 is not a guarantee of regulatory approval or market access, but it is an important step in demonstrating that a medical device meets the required quality and safety standards. [81,82]

Hence, both colon phantoms and the automated measuring system that have been developed and tested in this project will be included in the regulatory documentation of MiWEndo Solutions, as part of the validation and verification plan and in the preclinical trials protocols. All these documents will be part of the Technical File that is sent to the Notified Body, an organization designated by an EU country to assess the conformity of medical products before being placed on the market, when requesting authorization to commercialize MiWEndo in Europe (CE Marking). [83]

---

## 10. CONCLUSIONS

In this project a validation setup for a novel microwave imaging colonoscopy system called MiWEndo has been developed. The setup consists of two parts: a motorized system for moving the device automatically and a new phantom recipe to mimic the dielectric properties of colon tissues. This new setup may allow more precise and controllable measurements that can be used to verify and optimize both hardware and software of the microwave imaging device.

To develop such project, first a market analysis and a review of the current trends in microwave imaging both motorized systems and phantoms has been conducted. After reviewing the state of the art on imaging phantoms, it has become clear that there are no commercially available microwave imaging phantoms, and there is no literature on microwave imaging phantoms for colonoscopy applications. Thus, there is a clear need for further research in this field, and new recipes might be developed adapting protocols from other tissue mimicking applications.

Regarding the development of PVP phantoms, it has been obtained a PVP phantom fabrication protocol that allows the production of phantoms that mimic the dielectric properties of the healthy colon mucosa. By using 30% of PVP and 5.5% of agar, phantoms that show both relative permittivity of 42 and a conductivity of 9 S/m are obtained. Besides, the developed protocol is simple, highly reproducible and just requires the mixture of three ingredients.

Then, a comparative study has been carried out to assess the lifespan and the conservation of the dielectric properties of PVP phantoms versus the currently used oil-based phantoms, which has drawn several conclusions. First of all, it has become clear that PVP-phantoms must be stored at the fridge as part of the conservation protocol. If not, it has been observed that after a span of 6-7 weeks, the phantoms become moldy, and their dielectric properties are totally altered, along with their mechanical ones. Nevertheless, it is suggested to perform further studies with more samples in order to draw up more robust conclusions.

The study also revealed that oil-based phantoms are harder than PVP-phantoms for similar concentrations of agar. Besides, no significant differences in the stability and conservation of mechanical and dielectric properties between the PVP phantom kept in the fridge and the oil-based phantom have been observed. Further studies during longer periods of time should be conducted.

Regarding the motorized measuring system, a design that fulfills all the established requirements has been conceived. It is based on a wood structure in which a XYZ motorized positioning system is secured. An adaptor is used to attach the MiWEndo device in the moving part of the positioning system so that the following maximum linear travels are achieved:  $x=y=10\text{cm}$  and  $z=50\text{cm}$ . This will allow the realization of reproducible measurements in all different-sized phantoms.

After performing a thorough study of the different options for each component of the system, it has been determined that the most suitable choices for this project are as follows: the FUYU FSK40 Gantry Linear Guide Stage as the positioning system, the TB6600 motor drivers, and an Arduino Nano as the controller. The whole system and trajectories are commanded using the Grbl freeware from Arduino IDE and a G-Code sender installed in the computer. The integration of all these parts

has been meticulously detailed, so that once the components are purchased and acquired, the system may be easily implemented by MiWEndo's Solutions team.

Furthermore, a proof of concept of the conceived motorized system has been implemented to preliminary test the feasibility of the system. It consisted in a demonstrator system using a single a motor, a driver, a power source, and a controller. A simple code to move the motor in both directions (clockwise and anticlockwise) has also been developed using Arduino IDE. This proof of concept has been successfully conducted and has allowed to verify that the controller-driver-motor assembly works correctly.

To sum up, this thesis has allowed the development of a new fabrication and conservation protocol for PVP phantom production and has shown the potential of this new recipe to perform dielectric properties assessments with the MiWEndo device during prolonged lifespans. Moreover, a first conception of an automated measuring system has been conceived, which is of reasonable-cost and simple-implementation. Hence, a further implementation of the measuring system has been concluded as viable.

With all these results, this project has provided a new and very useful validation setup that may be utilized by MiWEndo Solutions for further testing and validation of their MWI colonoscopy medical device and might be adapted for validating upcoming projects.

### 10.1. Future work

To conclude, some future work along this project line might be discussed.

First of all, the comparative study between PVP and oil-based phantoms should be repeated over a longer period of time, 5 to 6 months, in order to achieve more conclusive and significant results regarding the most stable phantom recipe. It must be mentioned that PVP phantoms should be stored in the fridge. Furthermore, it would also be interesting to have more samples for each recipe, 4 or 5 phantoms for each fabrication strategy, in order to provide repeatability data and more robust results and omit non-significant variations.

Furthermore, the same comparative study could be repeated for different tissue-mimicking phantoms, that is, for phantoms that mimic adenomas with low grade dysplasia and hyperplastic polyps, to assess the capacity of the PVP phantom recipe to mimic these tissues and assess whether the properties are also conserved in these conditions.

As for the automated measuring system, it would be interesting to implement all the components and integrate all the electronics with the firmware, in order to verify the correct operability of the system. Prior to performing measurements with the system, a calibration stage would be needed, in order to ensure the proper coordination and functioning of all the components. Finally, measurements for the experimental validation of the system should be conducted using the MiWEndo medical device, to test the capacity of the system to perform repeatable and reliable measurements of the dielectric properties of the phantoms. Thus, the calculation of the standard deviation throughout the measurements might be interesting as an indicator of repeatability.

---

## 11. BIBLIOGRAPHY

- [1] Xi Y, Xu P. Global colorectal cancer burden in 2020 and projections to 2040. *Transl Oncol.* 2021 Oct;14(10):101174.
- [2] Macrae, F. (2018) Colorectal cancer: Epidemiology, risk factors, and protective factors
- [3] Gonzalez-Pons M, Cruz-Correa M. Colorectal Cancer Biomarkers: Where Are We Now? *Biomed Res Int.* 2015 May 27. 2015;2015:149014.
- [4] Samadder NJ, Curtin K, et al. Characteristics of missed or interval colorectal cancer and patient survival: a population-based study. *Gastroenterology.* 2014 Apr;146(4):950-60.
- [5] van Rijn JC, Reitsma JB, Stoker J, Bossuyt PM, van Deventer SJ, Dekker E. Polyp miss rate determined by tandem colonoscopy: a systematic review. *Am J Gastroenterol.* 2006 Feb;101(2):343-50.
- [6] Bolomey JC, Jofre L. Three Decades of Active Microwave Imaging Achievements, Difficulties and Future Challenges. Honolulu, HI: IEEE ICWITS. 2010;2010:1–4.
- [7] Lazebnik M, Popovic D, McCartney L, et al. A large-scale study of the ultrawideband microwave dielectric properties of normal, benign and malignant breast tissues obtained from cancer surgeries. *Phys Med Biol.* 2007;52:6093–6115.
- [8] MiWendo Solutions - UPC Spin offs. Accessed on April 2022. Retrieved from: <https://www.upc.edu/innovacio/ca/p-innova/empreses-creades/miwendo-solutions>
- [9] Di Meo S, Pasotti L, Iliopoulos I, Pasian M, Ettorre M, Zhadobov M, Matrone G. Tissue-mimicking materials for breast phantoms up to 50 GHz. *Phys Med Biol.* 2019 Feb 20;64(5):055006.
- [10] Dekker E, Tanis PJ, et al. Colorectal cancer. *The Lancet.* 2019. 394(10207): 1467-1480.
- [11] Lotfollahzadeh S, Recio-Boiles A, Cagir B. Colon Cancer. 2022. In: StatPearls [Internet]. Treasure Island (FL): StatPearls Publishing; 2023 Jan.
- [12] Sawicki T, Ruszkowska M, Danielewicz A, et al. A Review of Colorectal Cancer in Terms of Epidemiology, Risk Factors, Development, Symptoms and Diagnosis. *Cancers (Basel).* 2021 Apr 22;13(9):2025.
- [13] Agüero F, Andreu-García M, et al. (2012). Colorectal cancer survival: Results from a hospital-based cancer registry. *Revista española de enfermedades digestivas: órgano oficial de la Sociedad Española de Patología Digestiva.* 104. 572-577.
- [14] Guardiola M, Buitrago S, Fernández-Esparrach G, et al. Dielectric properties of colon polyps, cancer, and normal mucosa: Ex vivo measurements from 0.5 to 20 GHz. *Med Phys.* 2018.
- [15] Guardiola, M.; Dghoughi, W.; Sont, R., et al. MiWEndo: Evaluation of a Microwave Colonoscopy Algorithm for Early Colorectal Cancer Detection in Ex Vivo Human Colon Models. *Sensors* 2022, 22.
- [16] La Gioia, A.; Porter, E.; Merunka, I.; et al. Open-Ended Coaxial Probe Technique for Dielectric Measurement of Biological Tissues: Challenges and Common Practices. *Diagnostics* 2018, 8, 40.

- 
- [17] Cheng Y, Fu M. Dielectric properties for non-invasive detection of normal, benign, and malignant breast tissues using microwave theories. *Thorac Cancer*. 2018 Apr;9(4):459-465.
- [18] Imaging phantom - Wikipedia, The Free Encyclopedia. Accessed on May 2023. Retrieved from: [https://en.wikipedia.org/wiki/Imaging\\_phantom](https://en.wikipedia.org/wiki/Imaging_phantom)
- [19] What are Imaging Phantoms? - National Institute of Standards and Technology. Accessed on May 2023. Retrieved from: <https://www.nist.gov/physics/what-are-imaging-phantoms>
- [20] Grudzinski, J. J., et al. (2021). The Role of Imaging Phantoms in the Development of Medical Imaging Technologies. *Physics in Medicine & Biology*, 66(14), 14TR01.
- [21] Li L., et al. (2019). Fabrication and Characterization of Phantom Materials for Ultrasound and Photoacoustic Imaging. *Diagnostics*, 8(4), 85.
- [22] Madsen, M. T., & Hobson, M. A. (2015). Imaging phantoms: the importance of material selection in a multidisciplinary approach. *Journal of Medical Imaging*, 2(4), 043502.
- [23] A. Garrido, J. Romeu, M. Guardiola, L. Jofre (2018). Rapid Progress in Early Detection of Colorectal Cancer Using Microwaves. *Iskander*. (pp. 1-47)
- [24] Li S, Fear E, Curiel L. Breast tissue mimicking phantoms for combined ultrasound and microwave imaging. *Phys Med Biol*. 2021 Dec 13;66(24).
- [25] M. Lazebnik, E. L. Madsen, et al. Tissue mimicking phantom materials for narrowband and ultrawideband microwave applications. *Phys. Med. Biol.*, vol. 50, no. 18, p. 4245, 2005.
- [26] Joachimowicz, N. & Conessa, Christophe et al. (2014). Breast Phantoms for Microwave Imaging. *Antennas and Wireless Propagation Letters, IEEE*. 13. 1333-1336.
- [27] Villa, E., Arteaga-Marrero, N., González-Fernández, J. et al. Bimodal microwave and ultrasound phantoms for non-invasive clinical imaging. *Sci Rep* 10, 20401 (2020).
- [28] Joachimowicz, N. & Duchêne, Bernard & Conessa, et al. (2017). Reference phantoms for microwave imaging. 2719-2722.
- [29] Joachimowicz N, Duchêne B, Conessa C, Meyer O. Anthropomorphic Breast and Head Phantoms for Microwave Imaging. *Diagnostics (Basel)*. 2018 Dec 18;8(4):85.
- [30] Mohammed, Beadaa & Abbosh, Amin et al. (2012). Head phantom for testing microwave systems for head imaging. 2012 Cairo International Biomedical Engineering Conference, CIBEC 2012. 191-193.
- [31] O'Loughlin D, O'Halloran M, Moloney BM, Glavin M, Jones E, Elahi MA. Microwave breast imaging: Clinical advances and remaining challenges. *IEEE Trans Biomed Eng*. 2018;65(11); pp.2580–90.
- [32] S. Kibria, M. Samsuzzaman, M. T. Islam, M. Z. Mahmud, N. Misran and M. T. Islam, "Breast Phantom Imaging Using Iteratively Corrected Coherence Factor Delay and Sum,". *IEEE Access*, (2019). Vol. 7, pp. 40822-40832.
- [33] Guardiola M, Sont R, Marcoval S. Phantom 3 Study Protocol. MiWendo Solutions (2021).
- [34] Guardiola M, Sont R, Marcoval S. Phantom 4 Study Protocol. MiWendo Solutions (2021).
-

- 
- [35] Guardiola M, Sont R, Marcoval S. Phantom 5 Study Protocol. MiWendo Solutions (2022).
- [36] Guardiola M, Moliner A, Benavides M, Garrido A. Phantom 8 Study Protocol. MiWendo Solutions (2022).
- [37] Colonoscopy Market Size, Share & Trends Analysis Report By Product (Colonoscope, Visualization Systems, Others), By Application, By End-Use (Hospitals, Clinics, Ambulatory Surgery Centers, Others), By Region, And by Segment Forecasts, 2023-2031. InsightAce Analytic (2023).
- [38] Colonoscopy Devices Market By Component (Colonoscope, Visualization Systems, Others), Applications (Ulcerative Colitis, Lynch Syndrome, Colorectal Cancer, Crohns Disease, Others) End-user (Hospitals And Ambulatory Surgery Centers, Diagnostic Centers, Clinics), By Geography, Segment revenue Estimation, Forecast: 2021-2030. Strategic Market Research (2021).
- [39] Business plan. MiWendo Solutions (Feb 2023).
- [40] Colonoscopy devices market size and share analysis, growth trends & forecasts (2023-2028). - Mordor Intelligence. Accessed on May 2023. Retrieved from: <https://www.mordorintelligence.com/industry-reports/colonoscopy-devices-market>
- [41] Mark A. Gromski, Charles J. Kahi. Advanced colonoscopy techniques and technologies. *Techniques in Gastrointestinal Endoscopy*. (2015). 17(4):192-198.
- [42] Medical Imaging Phantoms Market Size, Share & Trends Analysis Report By Device Type (X-ray, Ultrasound, CT, MRI), By End Use, By Material (Simulating Organs, False Organs), By Region, And Segment Forecasts, 2020 - 2027. Grand View Research (2018).
- [43] McGarry, C. K., Grattan, L. J., Ivory, A. M., Leek, F., Liney, G. P., et al. (2020). Tissue mimicking materials for imaging and therapy phantoms: A Review. *Physics in Medicine & Biology*.
- [44] Medical Imaging Phantoms Market - Fact. Accessed on May 2023. Retrieved from: <https://www.factmr.com/report/5119/medical-imaging-phantoms-market>
- [45] Colonoscope Training Simulator - Kyoto Kagaku. Accessed on May 2023. Retrieved from: [http://www.kyotokagaku.com/en/products\\_data/m40/](http://www.kyotokagaku.com/en/products_data/m40/)
- [46] Kroton Kolon Colonoscopy Trainer (END001) - Kroton Medical Technology. Accessed on May 2023. Retrieved from: <https://kroton.info/en/endoscopic/138-kroton-kolono-colonoscopy-trainer-end001>
- [47] Modlin, I M. (2000) A brief history of endoscopy. MultiMed, Milano.
- [48] Gangwani, Manesh Kumar & Aziz, Abeer & Dahiya, Dushyant & Nawras, Mohamad & Aziz, Muhammad & Inamdar, Sumant. (2023). History of colonoscopy and technological advances: a narrative review. *Translational Gastroenterology and Hepatology*.
- [49] Zhang, J., Ross, H.M. (2017). History of Colonoscopy. In: Lee, S., Ross, H., Rivadeneira, D., Steele, S., Feingold, D. (eds) *Advanced Colonoscopy and Endoluminal Surgery*. Springer, Cham.
- [50] Gangwani MK, Aziz A, Dahiya DS, Nawras M, Aziz M, Inamdar S. History of colonoscopy and technological advances: a narrative review. *Transl Gastroenterol Hepatol*. 2023 Apr 20;8:18.
- [51] Capsule endoscopy - Wikipedia. Accessed on May 2023. Retrieved from: [https://en.wikipedia.org/wiki/Capsule\\_endoscopy](https://en.wikipedia.org/wiki/Capsule_endoscopy)
-

- 
- [52] Seward E. Recent advances in colonoscopy. *F1000Res*. 2019 Jul 9;8:F1000 Faculty Rev-1028.
- [53] Oliveira, Susie & Thomas, Sylvia & Torres Berdeguez, Mirta & Sá, Lidia & Souza, Sergio. (2017). Anthropomorphic Phantoms - Potential for More Studies and Training in Radiology. *International journal of radiology and radiation therapy*.
- [54] Martin, J.W., Scaglioni, B., Norton, J.C. et al. Enabling the future of colonoscopy with intelligent and autonomous magnetic manipulation. *Nat Mach Intell* 2, 595–606 (2020).
- [55] Kudo S, Mori Y, et al. Artificial intelligence and colonoscopy: Current status and future perspectives. *Digestive Endoscopy*, 2019. 31: 363–371
- [56] Ciuti G, Skonieczna-Żydecka K, et al. Frontiers of Robotic Colonoscopy: A Comprehensive Review of Robotic Colonoscopes and Technologies. *J Clin Med*. 2020 May 31;9(6):1648.
- [57] Umar, S, et al. Utilization of Telemedicine for Colorectal Cancer Outreach During the COVID-19 Pandemic: COLOVID-19. *The American Journal of Gastroenterology*, 2020. 115: 142.
- [58] Vassantachart AY, Yeo E, Chau B. Virtual and Augmented Reality-based Treatments for Phantom Limb Pain: A Systematic Review. *Innov Clin Neurosci*. 2022 Oct-Dec;19(10-12):48-57.
- [59] Mahadevappa Y. Kariduraganavar, Arjumand A. Kittur, Ravindra R. Kamble. Chapter 1 - Polymer Synthesis and Processing. *Natural and Synthetic Biomedical Polymers*. Elsevier, 2014. Pages 1-31.
- [60] S. Senthilkumar. Design of homogeneous and heterogeneous human equivalent thorax phantom for tissue inhomogeneity dose correction using TLD and TPS measurements. *International Journal of Radiation Research*, April 2014. 12(2).
- [61] Saleh A, Sabira K, et al. Homogeneous and heterogeneous breast phantoms for UWB imaging. *Association for Computing Machinery*, 2011. Article 1, 1–5.
- [62] Stepper Actuator Guide – Anaheim Automation. Accessed on May 2023. Retrieved from: <https://www.anaheimautomation.com/manuals/forms/stepper-actuator-guide.php>
- [63] Número de oferta 23-063852-BRG-ES-PGO – Igus S.L. (2023).
- [64] Cartesian Robot XYZ Stage Positioning Rail Guide Linear Gantry System - Fuyu Motion. Accessed on May 2023. Retrieved from: <https://www.fuyumotion.com/cartesian-robot-xyz-stage-positioning-rail-guide-linear-gantry-system-product/>
- [65] TOSEASTARS Gantry 3-Axis XYZ stage table – Aliexpress. Accessed on May 2023. Retrieved from: <https://es.aliexpress.com>
- [66] Nema 23 stepper motor datasheet – Components 101. Accessed on May 2023. Retrieved from: <https://components101.com/motors/nema-23-stepper-motor-datasheet-specs>
- [67] DM542 Motor driver – Amazon. Accessed on May 2023. Retrieved from: <https://www.amazon.es/DM542-Controlador-motor-fases-18-48/dp/B07MC8FGQ2>
- [68] TB660 Motor driver – Amazon. Accessed on May 2023. Retrieved from: <https://www.amazon.es/controladores-motor-paso-TB6600>
-



- 
- [69] Arduino UNO Rev3 - Arduino Store. Accessed on May 2023. Retrieved from: <https://store.arduino.cc/products/arduino-uno-rev3>
- [70] Arduino Nano - Arduino Store. Accessed on May 2023. Retrieved from: <https://store.arduino.cc/products/arduino-nano>
- [71] FMC4030 Three-axis motion controller: instructions for use - R&D Department Fuyu Technology Co. (2021).
- [72] FMC4030 controller - Aliexpress. Accessed on May 2023. Retrieved from: <https://es.aliexpress.com/i/32870127198.html>
- [73] Grbl - Github. Accessed on May 2023. Retrieved from: <https://github.com/grbl/grbl>
- [74] Arduino IDE - Wikipedia. Accessed on May 2023. Retrieved from: [https://es.wikipedia.org/wiki/Arduino\\_IDE](https://es.wikipedia.org/wiki/Arduino_IDE)
- [75] Said M. S, Seman N. Preservation of gelatin-based phantom material using vinegar and its life-span study for application in microwave imaging. Feb. 2017. IEEE, Transactions on Dielectrics and Electrical Insulation, vol. 24, no. 1, pp. 528-534.
- [76] How to setup Grbl and control CNC machine with Arduino – How to mechatronics. Accessed on June 2023. Retrieved from: <https://howtomechatronics.com/tutorials/how-to-setup-grbl-control-cnc-machine-with-arduino/>
- [77] Excel Templates – Vertex 42. Accessed on March 2023. Retrieved from: <https://www.vertex42.com/ExcelTemplates/critical-path-method.html>
- [78] European Union. (2017). Regulation (EU) 2017/745 of the European Parliament and of the Council of 5 April 2017 on medical devices. Official Journal of the European Union. Accessed on 19/04/2023. Retrieved from: <https://eur-lex.europa.eu/legal-content/ES/ALL/?uri=celex:32017R0745>
- [79] Asociación Española de Normalización. (2017). UNE-EN ISO 13485:2016. Dispositivos médicos. Sistemas de gestión de la calidad. Requisitos para fines reglamentarios. Accessed on 19/04/2023. Retrieved from: <https://www.une.org/encuentra-tu-norma/busca-tu-norma/norma?c=N0060449>
- [80] European Medicines Agency. (n.d.). Medical devices. Accessed on 20/04/2023. Retrieved from <https://www.ema.europa.eu/en/human-regulatory/overview/medical-devices>
- [81] Universidad Santo Tomás. (2019). Guía metodológica para buenas prácticas de manufactura - ISO 13485. Bogotá, Colombia: USTA.
- [82] NQA Certification Ltd. (2015). Guía de introducción a ISO 13485. Alcobendas, Spain: NQA.
- [83] European Union. (n.d.). Mercado CE - Productos. Accessed on 20/04/2023. Retrieved from [https://europa.eu/youreurope/business/product-requirements/labels-markings/ce-marking/index\\_es.htm](https://europa.eu/youreurope/business/product-requirements/labels-markings/ce-marking/index_es.htm)

## ANNEXES

### ANNEX 1. Dielectric properties measurements protocol

#### Materials:

- N1501A Dielectric Probe Kit
- Vector Network Analyzer (N9918A FieldFox Microwave Analyzer or VNA Agilent Technologies E5071C)
- Coaxial probe
- Keysight Materials Measurement Suite 2018 Program
- Support for the probe
- Lifting platform 100x100mm
- Thermometer (ThermoPro TP02S)
- Deionized water (Lubrisolve)
- 80 ml Glass Beaker

#### Procedure:

1. Turn on the VNA and insert the coaxial probe in its corresponding port.
2. After 30 minutes, verify the correct connection of the different components.
3. Fill the glass beaker with distilled water and measure its temperature.
4. Open the Keysight Materials Measurement Suite program
5. Set the calibration parameters:
  1. Calibration type: *Air/short/water*
  2. Probe type: *Slim form*.
  3. Refresh standard type: *Air*.
  4. Water temperature (°C): introduce the previously measured water temperature.
6. Define frequency range (from 5GHz to 15 GHz) and set -6 dBm of Power, the Intermediate Frequency Band Width in 300 Hz, 101 points, and no average in the measures (average=1)
7. Calibrate following program instructions. Watch out for air bubbles that may be between the probe and the water
8. Perform a measurement of the air to make sure that the calibration has been done correctly ( $\epsilon'_{\text{air}} = 1$ ,  $\epsilon''_{\text{air}} = \sim 0$ ).
9. Place the lifting platform under the probe
10. Place the specimen that is aimed to measure on the lifting platform.
11. Raise the platform until the coaxial probe is inserted into the material, exerting sufficient pressure to avoid any interference from air bubbles
12. Measure the dielectric properties of the specimen. Three measurements for each specimen/orientation of the specimen are recommended.
13. Save the measurements.
14. Clean the tip of the probe when a different specimen is measured.
15. Refresh the calibration periodically (e.g. each hour). [33]

## ANNEX 2. Assessment of PVP concentration

With the aim of assessing which is the concentration of PVP that will generate phantoms that best mimic the dielectric properties of healthy colon tissue, the following study will be conducted. Increasing concentrations of PVP will be dissolved in deionized water, and the dielectric properties of the mixtures will be assessed in order to find the percentage of PVP that allows to obtain relative permittivity ranging from 41 to 44 and a conductivity between 6 and 8 S/m.

The materials utilized to perform the study are the following:

- Polyvinylpyrrolidone, PVP-40
- Deionized water (Eroski)
- 500 ml Glass Beaker
- Cardboard cups
- Glass stirring rod
- Hot plate
- Thermometer

And all the required materials to perform the dielectric properties measurements specified in the *Annex 1. Dielectric properties measurements protocol*.

As initial reference, the PVP-phantom recipe for breast microwave imaging discussed in *Siyun et al (2021)* has been considered [24]. Thus, PVP concentrations of 20, 25, 30, 35 and 40% will be assessed. In the following table, the exact amounts of PVP and deionized water for each case are indicated:

Deionized water (ml)	PVP (%)	PVP (g)
30	20	6.00
30	25	7.5
30	30	9
30	35	10.5
30	40	12

Table 2.1. Volume of deionized water, % of PVP and grams of PVP for each PVP-water mixture.

The followed procedure:

1. Cover the urine container with plastic film, so that the final phantom can be easily retrieved from the container after polymerization.
2. Pour 30 ml of deionized water in the 500 ml glass beaker and heat it up to 50°C.
3. Remove the water from the hot plate and add the corresponding amount of PVP. Stir the mixture using the glass stirring rod till the polymer is completely dissolved.
4. Pour the mixture into a cardboard cup, and let the mixture cool down until no bubbles are observed.

5. Repeat the procedure for all the PVP concentrations.
6. Once all the mixtures have cooled down and are at room temperature, assess the dielectric properties following the steps indicated in *Annex 1. Dielectric properties measurements protocol*.

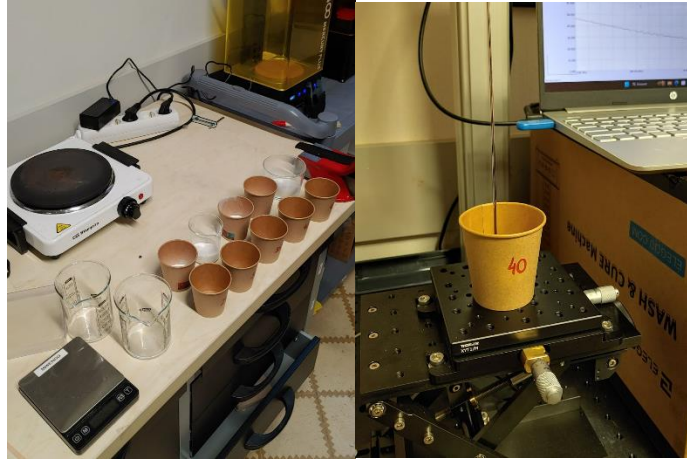


Figure 2.1. Materials used to perform the ingredient concentration assessment (left); dielectric properties measurement of the 40% PVP mixture (right).

---

### ANNEX 3. Oil-based phantom recipe

**Materials:** (to produce approximately 120 ml of phantom)

- 100 ml urine container
- Deionized water (Eroski): 83.84 ml = 83.84 g
- Agar (Químics Dalmau E-406): 3.88 g
- Sunflower Oil (Eroski): 31.44 ml = 28.92 g
- Dishwashing liquid (Mistol): 4.71 ml = 4.85 g
- 2x 500 ml Glass Beaker
- Aluminum Foil
- Hot Plate
- Glass stirring rod
- Thermometer

**Procedure:**

1. Put the agar in the room-temperature deionized water using the 500 ml glass beaker.
2. Dissolve the agar in the deionized water by rapidly heating the mixture up to 85°, using the hot plate, and continuously stirring the solution using the glass stirring rod, cover the solution with aluminum foil to not lose water by evaporation.
3. Switch off heating when the solution starts to boil. Then, allow the temperature to reduce to about 65°C.
4. Heat the sunflower oil to about 65°C using the 500 ml glass beaker. Be aware that sunflower oil heats up fast. Therefore, this step must be carried out when the water-agar solution temperature is approximately at 67 °C.
5. Add the sunflower oil to the water-agar mixture with the dishwashing liquid, covering the solution with aluminum foil to form an emulsion, appearing as a uniform, dense, pale liquid.
6. Stir continuously until temperature falls to approximately 52 °C.
7. Pour the mixture in the urine container and cover it hermetically.
8. Allow the mixture to jellify in the fridge for 24h.
9. After polymerization, phantoms are preserved hermetically in the fridge, covering them with film to prevent any contact with air, in order to avoid water condensation and dehydration.

## ANNEX 4. Phantom measurements and conservation protocol

### 1. Phantom conservation

All phantoms are conserved inside a 100 ml urine container which is closed. Besides, top surfaces of all phantoms are covered with film to avoid water evaporation.

#### 1.1. Oil-based phantom

- The phantom is kept in the fridge.
- If the phantom is kept outside of the fridge (room temperature), it loses its consistency (the phantom melts as the temperature increases above 24 °C). If the phantom reaches this temperature, store it again back in the fridge.

#### 1.2. PVP phantom stored in the fridge

- The phantom is kept in the fridge.

#### 1.3. PVP phantom at room T

- The phantom is kept outside the fridge, at room T.

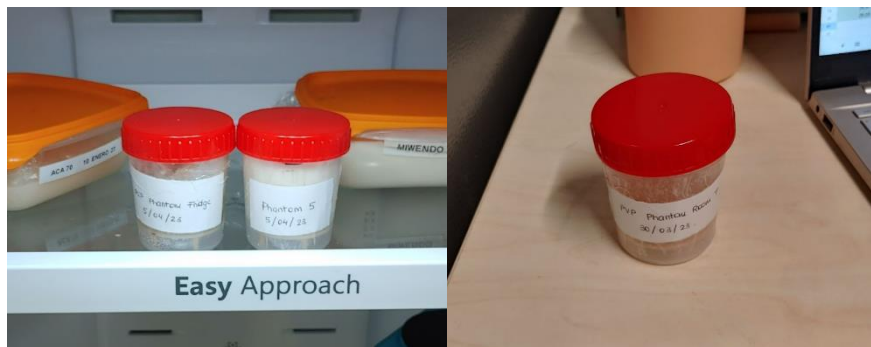


Figure 4.1. Phantoms kept in the fridge (left) and phantom preserved at room temperature (right).

## 2. Temperature measurements

### 2.1. Temperature measurements setup

- Thermometer (ThermoPro TP02S)

### 2.2. Temperature measurements protocol

Phantoms are retrieved from their conservation condition (fridge or outside) and before conducting the other measurements, their temperature is assessed following this measurement procedure:

1. Turn on the thermometer and open the urine containers.
2. Introduce the thermometer at the top part of the phantom making sure that the tip of the thermometer is well inserted in the material, and wait until the value of temperature is fixed.
3. Perform three measurements at different points of the surface to evaluate the mean and standard deviation, and annotate them in the *Temperature B* column of the Excel sheet.

This temperature measurement protocol must be repeated right after conducting the dielectric properties measurement and annotate it in the *Temperature A* column in the Excel sheet.

### 3. Dielectric properties measurements

#### 3.1. Dielectric properties measurements setup

- N1501A Dielectric Probe Kit
- Vector Network Analyzer (N9918A FieldFox Microwave Analyzer or VNA Agilent Technologies E5071C)
- Coaxial probe
- Keysight Materials Measurement Suite 2018 Program
- Support for the probe
- Lifting platform 100x100mm
- Thermometer (ThermoPro TP02S)
- Deionized water (Eroski)

#### 3.2. Dielectric properties measurements protocol

Once the tissue-mimicking materials have been polymerizing for at least 24h, their dielectric properties will be measured. The measurement procedure is the following:

1. Turn on the VNA
2. Assemble the coaxial probe support
3. Insert the coaxial probe into the support and connect it to the VNA with a semi-rigid cable
4. Fill the glass beaker with distilled water and measure its temperature
5. Open the Keysight Materials Measurement Suite program
6. Set the calibration parameters:
  1. Calibration type: *Air/short/water*.
  2. Probe type: *Slim form*.
  3. Refresh standard type: *Air*.
  4. Water temperature (°C): introduce the previously measured water temperature.
7. Define frequency range (from 5GHz to 15 GHz) and set -6 dBm of Power, the Intermediate Frequency Band Width in 300 Hz, 101 points, and no average in the measures (average=1)
8. Calibrate following program instructions. Watch out for air bubbles that may be between the probe and the water
9. Perform a measurement of the air to make sure that the calibration has been done correctly ( $\epsilon'_{\text{air}} = 1$ ,  $\epsilon''_{\text{air}} = \sim 0$ ).
10. Place the lifting platform under the probe
11. Place the tissue-mimicking material on the lifting platform
12. Raise the platform until the coaxial probe is inserted into the material, exerting sufficient pressure to avoid any interference from air bubbles
13. Perform three measurements to evaluate their mean and standard deviation. After each measurement, lower the platform, move the material slightly. Repeat step 12 to take another measure.

14. Once the dielectric properties of the top of the phantom have been measured, repeat steps 12 and 13 for the bottom and lateral parts. [33]

Once this protocol has been completed, measure the temperature again following the protocol called 2.2. *Temperature measurements*.

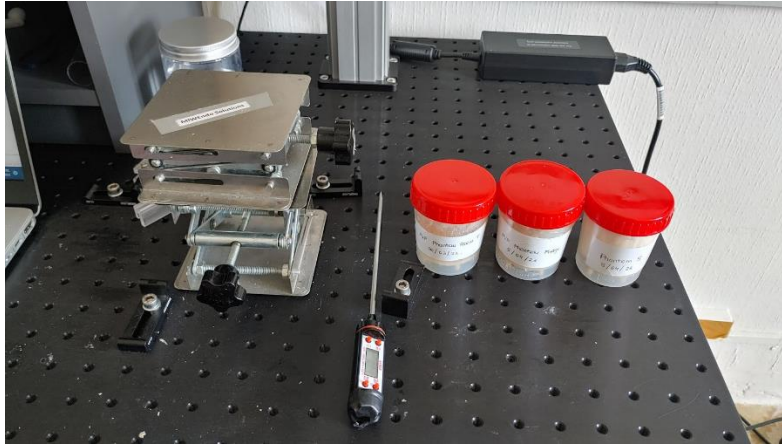


Figure 4.2. Close look to the dielectric properties measurements setup.

#### 4. Hardness measurements

To perform the study of the hardness of the phantom a vertical compressive force is applied at the top of the phantom with a dynamometer. The force required to cause a vertical displacement of 3 mm is measured. With the aim of distributing the force evenly over the entire surface of the phantom and avoiding breakage, the pressure is applied to a circular piece of rigid plastic that is placed on top of the material and that has the same diameter as the phantom.

##### 4.1. Hardness measurements setup

- Dynamometer (AMF-500 Digital Force Gauge)
- Circular piece of rigid plastic ( $\varnothing = 4.5$  cm)

##### 4.2. Hardness measurements protocol

To assess the hardness of the phantom, this protocol must be followed:

1. Place the circular plastic piece at the top of the phantom.
2. (This step only needs to be conducted the first time that the hardness is assessed). Draw two reference marks at the urine container: a top line at the height of the plastic piece and a second one, 3 mm below the first one.
3. Apply the required force with the dynamometer to achieve the displacement that has been set with the reference marks, so that the circular plastic piece goes from the top line to the bottom one.
4. Perform three measurements of the force to evaluate the mean and standard deviation.



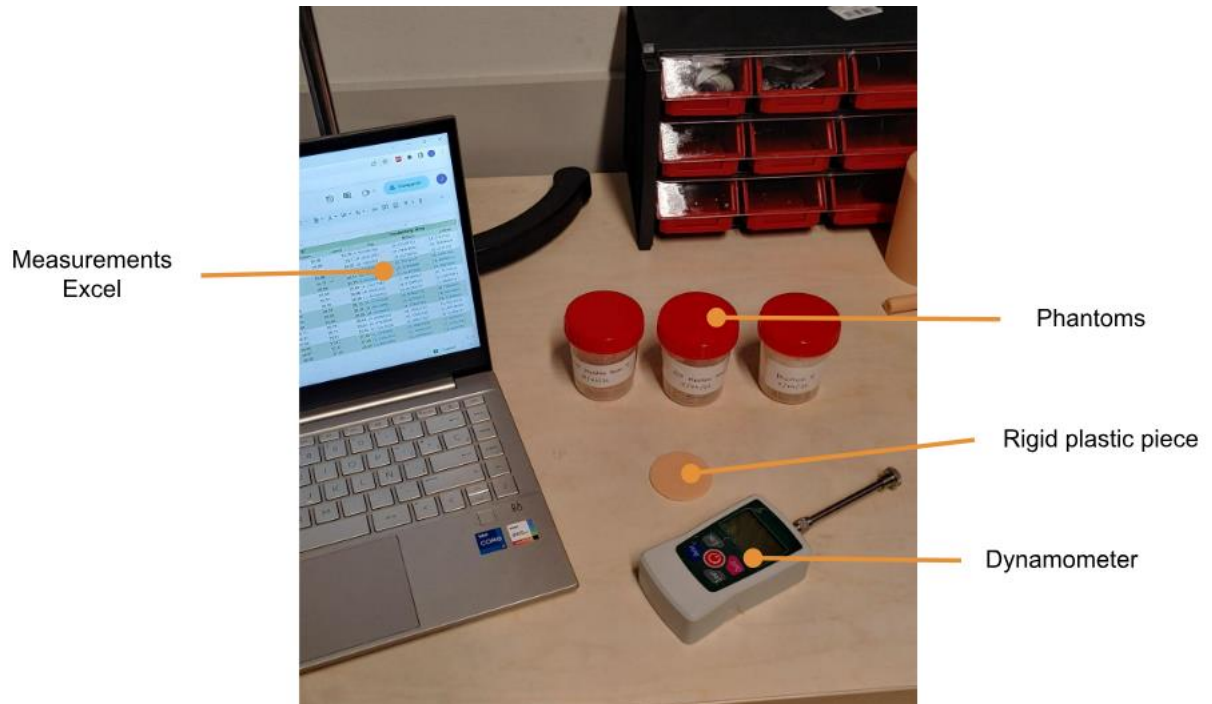


Figure 4.3. Hardness measurements setup.

## 5. Water formation measurements

In order to study the degradation process of the different phantoms, the formation of water underneath the phantom is monitored periodically. To do so, all phantoms have been placed on top of a rigid plastic piece that is placed at the bottom of the urine container (see Figure \_). This plastic piece has 4 short support structures and presents small holes, so that the generated water is kept at the bottom part of the urine container, underneath the phantom, and it can be visually assessed and measured.

### 5.1. Water formation measurements protocol

1. Observe the bottom part of the urine container and look for water drops.
2. Indicate in the Excel sheet of measurements the water presence in the corresponding cell with the following code:
  1. A: absence of water.
  2. P: presence of water.
3. In the particular case that there is presence of water (P), indicate the number of drops inside brackets. For instance: P (6), indicating that there is water formation and there are 6 drops.

## 6. Visual homogeneity measurements

Another variable to monitor the degradation of phantoms is the visual homogeneity of the material, that is, if the appearance of the phantom presents any changes with respect to the previous measurement.

### 6.1. Visual homogeneity measurements protocol

1. Observe carefully the phantom.
2. In the Excel sheet, write the homogeneity that presents the material, indicating the existence of bubbles, the presence of different phases (different color or composition), the appearance of mold, the smell or if the phantom has shrunk due to the loss of water.

## ANNEX 5. Phantom measurements

Excel tables showing the values obtained of the measurements performed to the three phantoms during the comparative study:

### Oil-based phantom:

		Temperature B (°C)	Relative permittivity (E')			E''			Conductivity (S/m)		
			Top	Bottom	Lateral	Top	Bottom	Lateral	Top	Bottom	Lateral
13/04/2023	Measurement 1	10,30	53,99	54,89	53,52	27,16	27,17	26,93	11,33	11,33	11,23
	Measurement 2	10,20	55,21	52,05	54,65	28,43	25,95	27,79	11,86	10,82	11,59
	Measurement 3	10,00	54,49	54,76	54,97	28,13	28,84	27,50	11,73	12,03	11,47
20/04/2023	Measurement 1	7,50	53,85	56,14	50,99	28,17	27,19	23,96	11,75	11,34	9,95
	Measurement 2	7,20	52,37	55,06	51,42	26,58	27,73	24,30	11,09	11,56	10,13
	Measurement 3	7,00	55,44	52,26	54,02	29,08	25,89	25,58	12,13	10,80	10,67
27/04/2023	Measurement 1	7,40	51,67	53,38	54,79	24,82	26,10	25,66	10,35	10,88	10,70
	Measurement 2	7,20	51,77	55,85	54,40	26,15	28,32	26,03	10,91	11,81	10,86
	Measurement 3	7,20	53,09	53,52	55,14	27,14	27,03	25,76	11,32	11,27	10,74
04/05/2023	Measurement 1	7,80	53,97	55,18	54,02	26,76	28,42	27,18	11,16	11,85	11,34
	Measurement 2	7,60	48,89	53,08	54,20	26,09	26,48	27,49	10,88	11,04	11,46
	Measurement 3	7,70	54,87	51,89	56,87	28,90	26,01	28,29	12,05	10,85	11,80
11/05/2023	Measurement 1	8,20	50,72	55,23	55,63	25,01	27,53	28,67	10,43	11,48	11,96
	Measurement 2	8,00	51,44	53,97	54,09	26,41	27,14	27,18	11,01	11,32	11,34
	Measurement 3	8,00	55,53	55,17	51,97	20,27	28,01	25,61	8,45	11,68	10,68
18/05/2023	Measurement 1	6,80	49,78	55,39	51,92	23,39	25,36	23,50	9,75	10,58	9,80
	Measurement 2	7,10	50,51	54,28	49,83	25,37	25,48	22,48	10,58	10,63	9,38
	Measurement 3	6,80	53,26	54,22	55,00	25,44	25,78	25,98	10,61	10,75	10,83
25/05/2023	Measurement 1	7,30	50,06	54,94	55,97	23,83	25,22	24,67	9,94	10,52	10,29
	Measurement 2	7,30	47,17	53,79	53,91	23,16	26,28	24,43	9,66	10,96	10,18
	Measurement 3	7,30	52,68	54,33	51,05	25,81	25,89	22,97	10,76	10,80	9,58

Temperature A (°C)	Force (N)	Water formation	Visual homogeneity
11,50	27,10	A	Homogeneous, no bubbles, absence of stink or mold.
11,50	27,40		
11,90	23,80		
10,60	25,10	P(5)	Homogeneous, no bubbles, absence of stink or mold. Water below the plastic piece
9,80	26,20		
10,10	25,80		
9,90	26,70	P(6)	Homogeneous, no bubbles, absence of stink or mold. Water below the plastic piece
9,40	27,20		
9,80	29,00		
9,50	26,50	P(6)	Homogeneous, no bubbles, absence of stink or mold. Water below the plastic piece
9,50	23,10		
9,50	24,70		
9,80	22,50	P(12)	Homogeneous, no bubbles, absence of stink or mold. A significant increase in the amount of water
9,30	24,10		
9,30	28,80		
10,70	24,80	P(18)	Homogeneous, no bubbles, absence of stink or mold. Increase in the amount of water.
11,10	24,00		
10,90	25,20		
10,20	24,00	P(22)	Homogeneous, some bubbles, absence of stink or mold. Holes from the other day measurements are still present. It appears a little bit more dry on the top part
10,30	21,40		
10,30	26,50		

Figure 5.1. Measurements of the oil-based phantom.

### Room T PVP phantom:

		Temperature B (°C)	Relative permittivity (E')			E''			Conductivity (S/m)		
			Top	Bottom	Lateral	Top	Bottom	Lateral	Top	Bottom	Lateral
13/04/2023	Measurement 1	18,5	39,18	39,26	39,26	22,17	22,08	21,87	9,24519237	9,206385059	9,120805031
	Measurement 2	18,1	39,06	39,32	38,84	21,8	22,1	23,09	9,09161206	9,216725987	9,629601948
	Measurement 3	18,4	38,93	39,12	38,47	22,28	21,88	23	9,283453415	9,124375714	9,53206777
20/04/2023	Measurement 1	20,7	40,52	37,47	39,36	21,95	21,75	20,88	9,154169024	9,070759739	8,749633992
	Measurement 2	20,7	40,08	39,45	39,89	21,7	21,71	21,79	9,043907417	9,054078882	9,087441596
	Measurement 3	20,3	40,12	40,55	39,75	21,68	21,75	21,89	9,041566483	9,070759739	9,129146238
27/04/2023	Measurement 1	22,9	41,38	40,57	40,43	21,27	21,19	23	8,870577455	8,837213741	8,53206777
	Measurement 2	23,1	41,3	41,38	41,26	21,33	21,29	22,9	8,89560024	8,878918383	9,550363127
	Measurement 3	22,9	41,47	41,35	40,83	21,4	21,39	22,9	8,82479349	8,920623026	9,550363127
04/05/2023	Measurement 1	24,2	40,91	40,81	40,62	20,84	21,16	20,89	8,691241432	8,824102348	8,712093913
	Measurement 2	24,2	41,24	41,32	40,78	20,99	21,07	20,99	8,753804456	8,78716817	8,753804456
	Measurement 3	24,2	41,17	41,65	40,97	21,1	21,41	21,16	8,799679563	8,828363954	8,824702348
11/05/2023	Measurement 1	23,6	41,06	40,92	40,85	20,83	20,83	21,34	8,687077028	8,687077028	8,893770704
	Measurement 2	23,7	40,54	39,76	40,78	20,49	20,62	21,37	8,545281243	8,59497279	8,312828097
	Measurement 3	23,7	40,78	41,14	40,76	20,74	21,28	21,43	8,64954285	8,874747919	8,337304883
18/05/2023	Measurement 1	22,3	39,52	37,95	39,07	20,62	20,8	20,95	8,599497279	8,674556535	8,737122599
	Measurement 2	22,3	40,36	39,71	39,22	21,35	21,07	20,84	8,903941169	8,78716817	8,792895135
	Measurement 3	22,4	40,16	39,28	38,49	21,03	21,32	20,88	8,770486313	8,891428776	8,707929349
25/05/2023	Measurement 1	22,6	30,74	39,76	40,47	16,21	20,74	22,17	6,760322545	8,64954285	9,24519237
	Measurement 2	22,5	31,05	40,31	38,85	16,17	21,05	21,23	6,743640668	8,778827241	8,853355598
	Measurement 3	22,8	36,31	40,65	36,54	19,19	20,83	20,09	8,003120891	8,687077028	8,378462674

Temperature A (°C)	Force (N)	Water formation	Visual homogeneity
19,2	13,4	A	Homogeneous, some bubbles, absence of stink or mold.
19,1	13,1		
18,7	12,5		
20,8	14,8	P(2)	Homogeneous, some bubbles, absence of stink or mold. Some water under the phantom when removing it from the container. Holes from the other day measurements are still present.
20,7	9,2		
20,3	13,5		
23,2	12,5	P(4)	Homogeneous, some bubbles, absence of stink or mold. More water under the phantom when removing it from the container. Holes from the other day measurements are still present.
23,1	12,7		
23	13,9		
23,8	12,8	P(5)	Homogeneous, some bubbles, absence of stink or mold. More drops of water under the phantom when removing the phantom, all the bottom part is covered with water.
23,9	14,2		
23,9	13,5		
23,7	13,5	P(5)	Homogeneous, some bubbles, absence of stink or mold. More water under the phantom when removing it from the container. Holes from the other day measurements are still present.
23,7	16,3		
23,7	12,7		
22,4	13,3	P(8)	Homogeneous, some bubbles, absence of stink. It seems that there is an initial presence of mold (white, lateral). More drops of water under the phantom.
22,4	10,9		
22,4	9,3		
23,7	16,7	P(4)	The top part of the phantoms is all covered in white mold, and in the lateral part there are some colonies too. It appears dry on the top. Small amount of water under the phantom.
23,7	19,5		
23,7	15,7		

Figure 5.2. Measurements of the Room T PVP phantom.

Fridge PVP phantom:

		Temperature B (°C)	Relative permittivity (E')			E''			Conductivity (S/m)		
			Top	Bottom	Lateral	Top	Bottom	Lateral	Top	Bottom	Lateral
13/04/2023	Measurement 1	11,30	42,72	42,89	43,36	23,84	25,36	24,39	9,94	10,58	10,17
	Measurement 2	10,80	44,13	43,11	43,07	24,61	25,38	24,70	10,26	10,58	10,30
	Measurement 3	10,40	42,79	42,79	43,42	24,67	25,33	24,25	10,29	10,56	10,11
20/04/2023	Measurement 1	7,90	45,54	43,61	44,33	23,58	25,88	25,03	9,83	10,79	10,44
	Measurement 2	8,10	45,85	42,20	42,66	24,37	24,73	26,11	10,16	10,31	10,89
	Measurement 3	7,70	43,85	43,67	42,18	23,93	26,89	24,79	9,98	11,21	10,34
27/04/2023	Measurement 1	7,60	44,58	46,11	46,09	26,62	26,38	25,89	11,10	11,00	10,80
	Measurement 2	7,70	45,43	45,56	46,12	26,20	26,31	26,68	10,93	10,97	11,13
	Measurement 3	7,60	45,88	45,88	46,21	26,48	26,02	26,58	11,04	10,85	11,09
04/05/2023	Measurement 1	7,80	42,09	44,04	45,17	24,26	26,23	25,73	10,12	10,94	10,73
	Measurement 2	7,60	42,23	44,85	45,72	24,18	25,95	26,29	10,08	10,82	10,96
	Measurement 3	7,70	44,48	45,08	43,79	25,81	25,84	25,83	10,76	10,78	10,77
11/05/2023	Measurement 1	8,30	42,67	43,69	42,87	26,11	25,79	26,44	10,89	10,76	11,03
	Measurement 2	8,30	43,13	43,81	43,03	26,31	25,71	26,61	10,97	10,72	11,10
	Measurement 3	8,30	43,47	42,23	43,86	25,94	25,91	25,46	10,82	10,81	10,62
19/05/2023	Measurement 1	7,70	40,66	42,99	43,69	26,85	27,47	27,63	11,20	11,46	11,52
	Measurement 2	7,50	41,52	43,25	44,28	26,67	27,47	27,99	11,12	11,46	11,67
	Measurement 3	7,50	41,09	43,67	43,26	26,29	27,43	25,09	10,96	11,44	10,46
25/05/2023	Measurement 1	7,30	39,96	41,55	42,21	26,00	27,11	27,25	10,84	11,31	11,36
	Measurement 2	7,20	41,83	42,37	43,21	26,70	26,47	26,89	11,14	11,04	11,21
	Measurement 3	7,10	42,53	41,08	42,43	26,34	27,45	27,53	10,99	11,45	11,48

Temperature A (°C)	Force (N)	Water formation	Visual homogeneity
12,10	7,40	A	Homogeneous, some bubbles, absence of stink
11,90	7,10		
11,40	6,90		
9,60	8,20	A	Homogeneous, some bubbles, absence of stink
9,80	7,20		
9,50	6,80		
11,30	7,20	A	Homogeneous, some bubbles, absence of stink
11,30	6,30		
11,50	11,50		
10,60	6,20	P(2)	Homogeneous, some bubbles, absence of stink
10,50	7,50		
10,30	8,90		
12,30	9,70	P(2)	Homogeneous, some bubbles, absence of stink
12,30	9,10		
12,20	7,40		
11,30	5,90	P(5)	Homogeneous, some bubbles, absence of stink
11,30	6,40		
11,10	7,30		
11,80	6,20	P(7)	Homogeneous, some bubbles, absence of stink
11,90	6,80		
11,80	7,40		

Figure 5.3. Measurements of the Fridge PVP phantom.

## ANNEX 6. Proof of concept code

Code to perform continuous rotations in both senses (clockwise and anticlockwise) of a Nema17 using a motor driver, an Arduino Nano and a power source:

```
int PUL=3; // Pin to define the PULSE signal
int DIR=2; // Pin to define the DIRECTION signal
void setup() {
  pinMode (PUL, OUTPUT);
  pinMode (DIR, OUTPUT);
}

// TB6600 is set so that one revolution is performed with 800 steps.

void loop() {

  digitalWrite(DIR,LOW);
  for (int i=0; i<1600; i++) // Rotates forward 1600 steps
  {
    digitalWrite(PUL,HIGH);
    delayMicroseconds(400);
    digitalWrite(PUL,LOW);
    delayMicroseconds(400);
  }
  delay(100);
  digitalWrite(DIR,HIGH);

  for (int i=0; i<1600; i++) // Rotates backwards 1600 steps
  {
    digitalWrite(PUL,HIGH);
    delayMicroseconds(400);
    digitalWrite(PUL,LOW);
    delayMicroseconds(400);
  }
}
```

